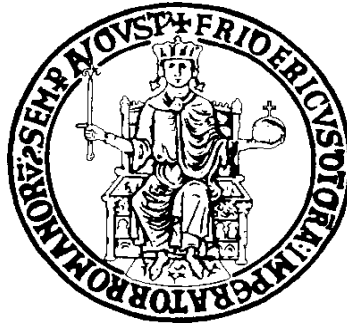


UNIVERSITÀ DEGLI STUDI DI NAPOLI “FEDERICO II”



DOCTORATE SCHOOL IN BIOLOGY

Cycle XXXIV

***Emerging concerns on Rare Earth Elements (REEs):  
new impacts?***

The potential environmental implications on an integrated multimatrix basis

Coordinator

Prof. Sergio Esposito

Supervisor

Prof. Giovanni Libralato

PhD student

Antonietta Siciliano

Academic Year 2020 – 2021



## Contents

|  |       |
|--|-------|
| List of Figures .....  | - 7 - |
| List of Tables.....  | 8     |
| Publications .....   | 10    |
| Introduction .....   | 13    |
| Chapter 1 .....  | 17    |
| 1.1 Discovery and Occurrence of REEs .....   | 17    |
| 1.2 Properties and Uses of REE .....   | 19    |
| 1.3 Anthropogenic sources and environmental occurrence.....  | 23    |
| 1.4 REE-associated adverse effects.....  | 25    |
| 1.5 REE-associated hormetic trends .....   | 28    |
| Chapter 2 .....  | 31    |
| 2.1 Topsoil pollution and toxicity in industrial areas of Taranto, Augusta, Priolo<br>(southern Italy) and Gardanne (southern France)..... | 31    |
| 2.1.1 Taranto case study .....   | 32    |
| 2.1.2 Gardanne case study .....  | 33    |
| 2.1.3 Augusta- Priolo case study .....   | 34    |
| 2.2 Methods .....  | 35    |
| 2.2.1 Soil sample collection and processing.....   | 35    |
| 2.2.2 Metal analysis .....   | 35    |
| 2.2.3 PAH and total organic analysis.....  | 36    |
| 2.2.4 <i>Caenorhabditis elegans</i> bioassays.....   | 36    |
| 2.2.5 Statistical analysis.....  | 37    |
| 2.3 Results and discussions .....  | 38    |
| 2.3.1 Taranto area .....   | 38    |

|  |    |
|--|----|
| 2.3.2 Gardanne area .....  | 42 |
| 2.3.3 Augusta-Priolo areas.....  | 47 |
| 2.4 Conclusions .....  | 51 |
| Chapter 3 .....  | 52 |
| 3.1 Sediment pollution and toxicity in a formerly industrialized bay in central Mediterranean (Pozzuoli, Italy)..... | 52 |
| 3.1.1.Pozzuoli case study .....  | 53 |
| 3.2 Methods .....  | 54 |
| 3.2.1 Sediment sampling and handling.....  | 54 |
| 3.2.2 Metal analysis .....   | 54 |
| 3.2.3 PAH and total hydrocarbon analysis .....   | 55 |
| 3.2.4 Sea urchin bioassays .....   | 55 |
| 3.2.5 Algal bioassays .....  | 56 |
| 3.2.6 Statistical Analysis.....  | 56 |
| 3.3 Results and discussions .....  | 57 |
| 3.4 Conclusions .....  | 67 |
| Chapter 4 .....  | 68 |
| 4.1 The effects of cerium, gadolinium, lanthanum, and neodymium in simplified acid mine discharges .....             | 68 |
| 4.2 Materials and methods.....   | 69 |
| 4.2.1 Analytical methods .....   | 69 |
| 4.2.2 Algal growth inhibition test.....  | 70 |
| 4.2.3 Phytotoxicity test .....   | 70 |
| 4.2.4 Micronucleus test.....   | 70 |
| 2.5. Data analyses .....   | 71 |
| 4.3 Results and discussion.....  | 71 |

|  |     |
|--|-----|
| 4.4 Conclusions .....  | 79  |
| Chapter 5 .....  | 80  |
| 5.1 Cerium and erbium effects on <i>Daphnia magna</i> generations .....  | 80  |
| 5.2 Material and methods .....   | 81  |
| 5.2.1 Chemicals, testing solutions, and analytical characterization.....   | 81  |
| 5.2.2 A multi-endpoint experimental approach with <i>D. magna</i> (organisms' size,<br>parental reproduction, organisms' survival) ..... | 82  |
| 5.2.3 Reactive oxygen species and enzymatic activity.....  | 83  |
| 5.2.4 Gene expression.....   | 83  |
| 5.2.5 Uptake of Ce and Er.....   | 84  |
| 5.2.6 Statistical analysis.....  | 85  |
| 5.3 Results and discussion.....  | 85  |
| 5.3.1 Chemical characterization of testing solutions .....   | 85  |
| 5.3.2 Acute effects (48 h) of Ce and Er on <i>D. magna</i> .....   | 86  |
| 5.3.3 Growth rate, first brood appearance and offsprings production .....  | 87  |
| 5.3.4 Reactive oxygen species and enzymatic activity.....  | 89  |
| 5.3.5 Gene expression.....   | 92  |
| 5.3.6 Uptake.....  | 96  |
| 5.4 Conclusions .....  | 99  |
| Chapter 6 .....  | 100 |
| 6.1 Cerium and lanthanum effects on <i>Raphidocelis supcapitata</i> long-term multi-<br>endpoint exposure.....                           | 100 |
| 6.2 Material and methods .....   | 101 |
| 6.2.1 Chemicals, testing solutions, and analytical characterization.....   | 101 |
| 6.2.2 Cell culture conditions and <i>R. subcapitata</i> growth inhibition (GI) test<br>.....   | 102 |
| 6.2.3 A multi-endpoint experimental approach with <i>R. subcapitata</i> .....  | 102 |

|  |     |
|--|-----|
| 6.2.4 Statistical analysis.....  | 103 |
| 6.3 Results and discussion.....  | 104 |
| 6.3.1 72 h GI test.....  | 104 |
| 6.3.2 Long-term exposure effects .....   | 105 |
| 6.4 Conclusions .....  | 110 |
| Chapter 7 .....  | 111 |
| 7.1 Comparative toxicity of rare earth elements in marine <i>diatoms</i> and <i>luminescent bacteria</i> ..... | 111 |
| 7.2 Material and methods .....   | 112 |
| 7.2.1 Chemicals, testing solutions, and analytical characterization.....                                       | 112 |
| 7.2.2 <i>P. tricorutum</i> bioassay .....  | 112 |
| 7.2.3 <i>A. fischeri</i> bioassay .....  | 112 |
| 7.2.4 Statistical analysis.....  | 113 |
| 7.3 Results and discussion.....  | 113 |
| 7.4 Conclusions .....  | 121 |
| General conclusions .....  | 122 |
| References .....   | 124 |

## List of Figures

|   |    |
|---|----|
| Figure 1 REE history The complex compositions of the two starting minerals cerite and gadolinite (ytterbite) are revealed in the flow chart of discoveries of the elements. ....  | 18 |
| Figure 2 REEs (%) consumption in various application. Adapted from Roskill (2015) [45]. ....  | 20 |
| Figure 3 Outline of the Taranto industrial area and location of sampling sites. ...   | 32 |
| Figure 4 Map of Gardanne and of soil sampling points. Abbreviations: BPP – Bauxite Processing Plant; PP – Power Plant. ....   | 33 |
| Figure 5 An overview map and localization of sampling sites in Augusta and Priolo. ....   | 34 |
| Figure 6 Principal component analysis (PCA) of metal levels identifying the most affected sites (5 and 6) (a), and the relative levels of individual metals (b)..   | 40 |
| Figure 7 Measured levels of total hydrocarbons (C10–C40) and of PAHs .....  | 41 |
| Figure 8 Twenty-four-hour mortality of <i>C. elegans</i> exposed to Taranto soil samples. ....  | 42 |
| Figure 9 Principal component analysis (PCA) of metal levels identifying the most affected sites (8, 9 and 13) (a), and the relative levels of individual metals (b). ....   | 43 |
| Figure 10 Concentrations of PAH sums in soil samples following organic extraction. Triplicate determinations; data ( $\mu\text{g/l}$ ) are expressed as means $\pm$ SEM (a); concentrations of total hydrocarbons (C10–C40) in soil samples following organic extraction (b). LOD and LOQ were 1.7 and 5.1 mg/kg . Data with different letters (a–c) are significantly different ( $p < 0.05$ ). .... | 45 |
| Figure 11 24-h % Mortality of <i>Caenorhabditis elegans</i> exposed to $\cong 40\%$ (dry wt/vol) of soil samples. ....  | 46 |
| Figure 12 Principal component analysis (PCA) of metal levels identifying the most affected sites of Augusta-Priolo(a), and the relative levels of individual metals (b). ....   | 49 |

|  |    |
|--|----|
| Figure 13 Concentrations of PAH sums in soil samples following organic extraction(a); concentrations of total hydrocarbons (C10–C40) in soil samples following organic extraction (b); data ( $\mu\text{g}/\text{Kg}$ ).....   | 50 |
| Figure 14 24-h % Mortality of <i>C. elegans</i> exposed to $\cong$ 40% (dry wt/ vol) of Augusta- Priolo soil samples. ....   | 51 |
| Figure 15 Sediment sampling sites along five transects in the present study: Monte di Procida (MdP) and four transects (T1-T4) in the Bay of Pozzuoli.....   | 53 |
| Figure 16 Metal levels in sediment samples showed highest levels in T3 and T4 as consistently observed in total metal levels (a) [excepted Al(III) and Fe(III)] and in Fe(III) (b) and Al(III) (c) levels. Data with different letters (a–n) are significantly different (Tukey’s, $p < 0$ .....   | 57 |
| Figure 17 Logarithmic expression of total PAH levels showed dramatic differences between two sites (MdP and T2) showing PAH levels in the order of 4,000 mg/kg and sites T3 and T4 displaying PAH levels in the order of 2- to 500,000 mg/kg. Data with different letters (a–d) are significantly different (Tukey’s, $p < 0.05$ ). ....   | 62 |
| Figure 18 Levels of total hydrocarbons (C10 – C40) showing highest levels at sites T3-3 T3-4 and T4-3. Data with different letters (a–d) are significantly different (Tukey’s, $p < 0.05$ ). ....  | 63 |
| Figure 19 Percent developmental defects in sediment (WS)-exposed sea urchin (s-u) larvae showing bell-shaped rates in the five sites of the T3 transect and highest rates at sites T4-2 and T4-3. Asterisks indicate the results of two-tailed Student t-tests: $p < 0.05$ ; $**p < 0.01$ ; $***p < 0.001$ .....   | 64 |
| Figure 20 The offspring of sediment-exposed sperm displayed significant damage in terms of developmental defects and mortality at several sites across all transects. Asterisks indicate the results of two-tailed Student t-tests: $*p < 0.05$ ; $**p < 0.01$ ; $***p < 0.001$ .....  | 64 |
| Figure 21 Exposure of <i>P. tricornutum</i> to sediment EL resulted in significant growth rate inhibition vs. controls (growth rate $\mu = 1.9$ ). The data are normalized with control. Again sites from transect 3 displayed a bell-shaped trend with T3-3 and T3-4 resulting in highest growth rate inhibition. Asterisks indicate the results of two-tailed Student t-tests: $*p < 0.05$ ; $**p < 0.01$ ; $***p < 0.001$ ..... | 65 |

|  |    |
|--|----|
| Figure 22 Concentration-response relationship at pH 4 and 6 of Ce (A and B), Gd (C and D), La (E and F), and Nd (G and H) exposed to <i>R. subcapitata</i> ; concentrations in the x-axis are expressed as mg/L; IG = inhibition of growth. ....   | 72 |
| Figure 23 Concentration-response relationship at pH 4 and 6 of Ce (A and B), Gd (C and D), La (E and F), and Nd (G and H) exposed to <i>L. sativum</i> ; concentrations in the x-axis are expressed as mg/L; GI = germination index. ....  | 76 |
| Figure 24 Frequency of micronuclei (MC) in <i>V. faba</i> root exposed to Ce (0.010 mg/L), Gd (0.012 mg/L), La (0.012 mg/L), and Nd (0.005 mg/L) at pH = 4 and 6; letters (a-c) correspond to significantly different data (Tukey's test, $p < 0.05$ ); ctr = negative control; error bars indicate standard errors ( $n = 3$ ). ....  | 78 |
| Figure 25 Concentration-response curves for Ce and Er after ln-regression including 95% limit values regressions. ....   | 86 |
| Figure 26 Ce and Er cumulative mortality in <i>D. magna</i> along generations (F0, F1 and F2) normalized to negative controls. ....  | 89 |
| Figure 27 ROS production in <i>D. magna</i> exposed to Ce (panel A) and Er (panel B) along generations after normalization on negative controls. Results are presented as mean $\pm$ SD ( $n = 3$ ). Letters (a-e) indicate significant differences between treatments (exposure times: 3, 7, 14 and 21 days), while numbers (1-3) significant differences between generations (F0, F1 and F2); the level of significance was set at a $\leq 0.05$ (ANOVA). .... | 90 |
| Figure 28 Antioxidant enzyme activities after normalization on negative controls; error bars represent standard deviations. Letters (a-f) indicate significant differences between exposure times (3, 7, 14 and 21 days), while numbers (1-3) between generations (F0, F1 and F2); the level of significance was set at $\alpha = 0.05$ ; CAT, SOD and GST were expressed as U/ $\mu$ g protein; A, C and E are referred to Ce and B, D and F to Er. ....        | 92 |
| Figure 29 Real-time PCR analysis of the ATP-binding cassette (ABC) genes expression after treatment with Ce (A, B, C, and D) and Er (E, F, G and H) in <i>D. magna</i> F0, F1 and F2; gene expressions were evaluated with Student t-Test on control and treated daphnids; results are presented as mean $\pm$ standard  |    |

deviation (n =3) normalized to negative controls. Letters (a–e) indicate significant differences between contact times (3, 7, 14 and 21 days), while numbers (1–3) significant differences between generations (F0, F1 and F2); the level of significance was set at  $\alpha=0.05$ . ..... 95

Figure 30 Ce and Er uptake ( $\mu\text{g/g}$ ) including negative controls considering F0, F1 and F2 exposure scenarios. .... 98

Figure 31 Concentration-response curves for La ( $Y = 68.72 * X + 37.09$ ,  $R^2 = 0.9555$  std.err. = 6.976) and Ce ( $Y = 75.34 * X + 35.38$   $R^2 = 0.9563$ ; std.err. = 8.350) normalized to negative controls after semi-log regression, including 95% limit values (n = 4). ..... 104

Figure 32 La (0.4 mg/L) and Ce (0.5 mg/L) cumulative growth inhibition of *R. subcapitata* after 3, 7, 14, 21, and 28 days of exposure normalized to negative controls ( $\pm$ std.err.; n = 4); La:  $Y = 0.4991 * X + 11.15$ ,  $R^2 = 0.7890$ , std.err. = 2.307; Ce:  $Y = 1.108 * X + 6.446$ ,  $R^2 = 0.7714$ , std.err. = 5.773 ..... 105

Figure 33 ROS production in *R. subcapitata* exposed to La and Ce lasting 28 days after normalization on protein content. Results are presented as mean  $\pm$  std.err. (n = 4) in U/mg protein. Letters (a-f) indicate significant differences between exposure times (7, 14, 21, and 28) within treatments (La and Ce), while numbers (1–3) highlighted significant differences within exposure times (7, 14, 21, and 28) between treatments (La and Ce) ( $p < 0.05$ , Tukey's test). ..... 106

Figure 34 Antioxidant enzyme activities after normalization on protein content; CAT (A) and SOD (B) were expressed as U/mg protein. Results are presented as mean  $\pm$  std.err. (n = 4). Letters (a–d) indicate significant differences between exposure times (7, 14, 21, and 28) within treatments (La and Ce), while numbers (1–3) highlighted significant differences within exposure times (7, 14, 21, and 28) between treatments (La and Ce) ( $p < 0.05$ , Tukey's test). ..... 107

Figure 35 La and Ce uptake ( $\mu\text{g/g}$ ) in algal biomass at day 7, 14, 21, and 28 after normalization on negative controls; data are in  $\mu\text{g/g}$  ( $\pm$ std.err.; n = 3). ..... 109

Figure 36 Concentration-response relationship of Ce, Dy, Eu, La and Nd exposed to *A. fischeri*; concentrations in the x-axis are expressed as mg/L..... 115

Figure 37 Concentration-response relationship of Ce, Dy, Eu, La and Nd exposed to *P. tricornutum*; concentrations in the x-axis are expressed as mg/L. .... 119

## List of Tables

|  |    |
|--|----|
| Table 1 Abundance of REEs in the Earth's Crust (Adapted from Wedepohl, 1995 [37]) .....  | 19 |
| Table 2 Lanthanum-based and Cerium-based catalysts employed in heterogeneous Fenton-like oxidation.....  | 22 |
| Table 3 REE abundances in environment.....   | 24 |
| Table 4 Selected REE-related literature: adverse effects.....  | 26 |
| Table 4 (continued) Selected REE-related literature: adverse effects .....   | 27 |
| Table 5 Selected REE-related literature: hormetic effects in growth endpo.....   | 29 |
| Table 6 Data from ICP-MS analysis of elements (as mg/kg) occurring in the Taranto soil samples listed in their REE and HM concentrations. Other analyzed elements (As, B, Sb, and Ti) displayed concentrations < 1 mg/kg.....                                      | 39 |
| Table 7 Data from ICP-MS analysis of elements (as mg/kg) occurring in the Taranto soil samples listed in their REE and HM concentration.....   | 44 |
| Table 8 Data from ICP-MS analysis of elements (as mg/kg) occurring in the Augusta- Priolo soil samples listed in their REE and HM concentrations. ...  | 48 |
| Table 9 Analyzed metal levels in BoP sediment samples. Data of elements with levels < 1 mg/kg (Se, Cd and Sb) are not reported.....  | 58 |
| Table 10 Analyzed REE levels in BoP sediment samples . Data of elements are expressed as mg/kg and data of elements with levels < 1 mg/kg are not reported. Concentration sums are both expressed with and without Sc and Y. ....                                  | 60 |
| Table 11 Analyzed PAH levels in BoP sediment samples. Data levels are reported as µg/kg.....   | 61 |
| Table 12 Nominal and real concentrations (A) of testing solutions of Ce, Gd, La, and Nd at pH 4 and 6 at standard errors (B); N = nominal concentration, R = real concentration; concentrations are in mg/L.....   | 71 |
| Table 13 EC5, EC10, and EC50 values for Ce, Gd, La and Nd at pH =4 and 6; values are in mg/L; n.a. = not available; REEs= rare earth elements; EC = effective concentration; average EC values are provided ±95% confidence limit values in brackets (n = 3). .... | 73 |

|   |     |
|---|-----|
| Table 14 Primer sequences of the genes used for real time protein chain reaction (RT-PCR).....  | 84  |
| Table 15 Ce and Er concentrations ( $\mu\text{g/L}$ ) during the exposure period corrected for background concentrations of Ce and Er in the control water.....   | 86  |
| Table 16 Chronic toxicity effects on growth rate, day of first brood, and offspring produced for parental animal for both Ce and Er .....   | 88  |
| Table 17 Nominal and measured (ICP-MS) La and Ce concentrations (mg/L) and the relative std.err. (n = 3).....   | 104 |
| Table 18 Nominal and measured (ICP-MS) Ce, Dy, Eu, La and Nd concentrations (mg/L).....   | 114 |
| Table 19 EC5, EC10, and EC50 values for Ce, Dy, Eu; La and Nd on <i>A. fischeri</i> ; values are in mg/L; n.a. = not available; REEs = rare earth elements; EC = effective concentration; average EC values are provided $\pm 95\%$ confidence limit values in brackets (n = 3). .....    | 116 |
| Table 20 EC5, EC10, and EC50 values for Ce, Dy, Eu; La and Nd on <i>P. tricornutum</i> ; values are in mg/L; n.a. = not available; REEs = rare earth elements; EC = effective concentration; average EC values are provided $\pm 95\%$ confidence limit values in brackets (n = 3). ..... | 120 |

## Publications

The thesis is based on the following co-authored papers.

| Paper   | Impact factor | Citations |
|---|---------------|-----------|
| <b>Siciliano A.</b> , Libralato G., Comparative toxicity of rare earth elements in <i>Phaeodactylum tricornutum</i> and <i>Aliivibrio fischeri</i> . <i>Under Preparation</i>   | /             | /         |
| <b>Siciliano A.</b> , Libralato G. Catalytic activity of Rare Earth Elements in heterogeneous Fenton-like oxidation of wastewater contaminants: a review. <i>Under Preparation</i>  | /             | /         |
| Tommasi F., Thomas P.J., Lyons D.M., Pagano G., Oral R., <b>Siciliano A.</b> , Toscanesi M., Guida M., Trifuoggi M. Evaluation of rare earth element-associated hormetic effects in candidate fertilizers and livestock feed additives. <i>Submitted</i>  | /             | /         |
| Tommasi F., Pagano G., Oral R., Thomas P.J., Ecclese K.M., Tezc S., Toscanesi M., Lombardo F., <b>Siciliano A.</b> , Dipierro N., Gjataa I., Guida M., Libralato G., Lyons D.P., Buričh P., Kovačičh I., Trifuoggi M.(2021) Topsoil multi-endpoint pollution and toxicity in the petrochemical area at Augusta-Priolo (eastern Sicily, Italy). <i>Submitted</i>   | /             | /         |
| <b>Siciliano A.</b> , Guida M., Serafini S., Micillo M., Galdiero E., Carfagna S., Salbitani G., Tommasi F., Lofrano G., Padilla Suarez E.G., Gjata I., Brouziotis A.A., Trifuoggi M., Liguori R., Race M., Fabbricino M., Libralato G. (2021) Long-term multi-endpoint exposure of the microalga <i>Raphidocelis subcapitata</i> to lanthanum and cerium. <i>Science of the Total Environment</i> , 790, art. no. 148229, . DOI: 10.1016/j.scitotenv.2021.148229 | 7.963 (Q1)    | 1         |
| <b>Siciliano A.</b> , Guida M., Pagano G., Trifuoggi M., Tommasi F., Lofrano G., Padilla Suarez E.G., Gjata I., Brouziotis A.A., Liguori R., Libralato G. (2021) Cerium, gadolinium, lanthanum, and neodymium effects in simplified acid mine discharges to <i>Raphidocelis subcapitata</i> , <i>Lepidium sativum</i> , and <i>Vicia faba</i> . <i>Science of the Total Environment</i> , 787, art. no. 147527, . DOI: 10.1016/j.scitotenv.2021.147527            | 7.963 (Q1)    | 1         |

| Paper   | Impact factor | Citations |
|---|---------------|-----------|
| Oral R., Pagano G., Ferrara L., Toscanesi M., Mozzillo M., Gravina M., Natalc G.D., Thomas P.J., Tezc S., <b>Siciliano A.</b> , Guida M., Trifuoggi M.(2020) Sediment pollution and toxicity in a formerly industrialized bay in central mediterranean (POZZUOLI, Italy). Fresenius Environmental Bulletin, 29 (10), pp. 9498-9510.   | 0.489 (Q3)    | 0         |
| Galdiero E., Carotenuto R., <b>Siciliano A.</b> , Libralato G., Race M., Lofrano G., Fabbricino M., Guida M. (2019) Cerium and erbium effects on <i>Daphnia magna</i> generations: A multiple endpoints approach. Environmental Pollution, 254, art. no. 112985, . DOI: 10.1016/j.envpol.2019.112985  | 8.071 (Q1)    | 7         |
| Oral R., Pagano G., <b>Siciliano A.</b> , Toscanesi M., Gravina M., Di Nunzio A., Palumbo A., Thomas P.J., Tommasi F., Burić P., Lyons D.M., Guida M., Trifuoggi M. (2019) Soil pollution and toxicity in an area affected by emissions from a bauxite processing plant and a power plant in Gardanne (southern France). Ecotoxicology and Environmental Safety, 170, pp. 55-61. DOI: 10.1016/j.ecoenv.2018.11.122        | 6.291 (Q1)    | 9         |
| Trifuoggi M., Pagano G., Oral R., Gravina M., Toscanesi M., Mozzillo M., <b>Siciliano A.</b> , Burić P., Lyons D.M., Palumbo A., Thomas P.J., D'Ambra L., Crisci A., Guida M., Tommasi F. (2018) Topsoil and urban dust pollution and toxicity in Taranto (southern Italy) industrial area and in a residential district. Environmental Monitoring and Assessment, 191 (1), art. no. 43, . DOI: 10.1007/s10661-018-7164-7 | 2.513 (Q2)    | 8         |



# INTRODUCTION

---

Rare Earth Elements (REEs) as identified by the International Union of Pure and Applied Chemistry (IUPAC) include a group of 17 metals characterized by similar physicochemical characteristics. Of these elements, 15 belong to the lanthanide or lanthanoid series with atomic numbers between  $Z= 57$  and  $Z = 71$ , as follows: lanthanum (La), cerium (Ce), praseodymium (Pr), neodymium (Nd), promethium (Pm), samarium (Sm), europium (Eu), gadolinium (Gd), terbium (Tb), dysprosium (Dy), holmium (Ho), erbium (Er), thulium (Tm), ytterbium (Yb), and lutetium (Lu). Two more elements become a member of them: scandium (Sc,  $Z = 21$ ) and yttrium (Y,  $Z = 39$ )[1].

The REEs are commonly divided into two distinct subgroups: light (LREEs) and heavy (HREEs). The LREEs are La, Ce, Pr, Nd, Pm, and Sm, while the HREEs include Eu, Gd, Tb, Dy, Ho, Er, Tm, Yb, Lu, and Y [2]. The LREEs are characterized by smaller atomic masses, higher solubility and alkalinity. The HREEs present higher atomic masses, smaller solubility and alkalinity [3].

First discovered in 1878 in Sweden, they were believed to be some of the most uncommon elements [4]. REEs have been found to be relatively abundant in the Earth's crust, and they are referred to as 'rare' because they do not exist as individual native metals such as gold, copper and silver and are rarely concentrated into mine ores [5].

REEs represent key-roles in present-day life, as related to their indispensable involvement of many relevant technologies, as reviewed by Gwenzi et al. (2018) [6].

The use of REEs, especially of lanthanides, in technological devices altered their biogeochemical cycles and their presence in the e-waste made them a new category of potential emerging contaminants (EC) [7, 8]. Apart from industrial applications, REEs have found an extensive use in Chinese agriculture as fertilizers to increase crop yield, and in zootechny as feed additives aimed at increasing animal growth and egg laying, with likely prospects of their utilization outside China[9].

So, in the last decades, an extensive and growing body of literature on REE-associated effects in a number of biota and of test models has raised environmental concern about REE exposures [10-13]. These studies demonstrated that REEs exhibit beneficial effects as well as a moderate to high toxicity towards aquatic biota, including bacteria, microalgae, plants, vertebrates, and invertebrates [5, 14-19]. Their mechanisms of action and behaviour in biological systems are far from being completely understood, but it seems dependent on their concentration and physico-chemical conditions of the exposure media. Similarities in their mode of action were evidenced, but not univocally [20], in relation to their ionic radii and coordination numbers with some essential elements, i.e., Ca, Mn, Mg, Fe, and Zn [21]. As for human REE exposures in mining areas and REE extraction and manufacturing, a body of evidence points to REE bioaccumulation and excretion, while research gateways may prompt efforts to evaluate potential health risks in REE-exposed workers [8, 22-24]. Altogether, persuasive evidence points to recognized or potential health risks associated with REE exposures in environmental and human health.

Unfortunately, as is the case for many other environmental pollutants, it was stated that most literature reported on few REEs, and gaps into the knowledge persist on the health and environmental effects of other REEs [24]. In these cases, the ecological relevance was often insufficiently considered in terms of concentrations, model organisms and, most importantly, chemical mixtures.

Often during biological effect assessments, chemical isolation, purification, concentrations and dose-response relationships less can provide relevant information about effective concentration but these procedures fail to model interactive agonistic, antagonistic and synergistic effects of each chemical constituent in the chemical mixture detected in the sample. As such, the importance of working with whole field samples (for example, soil, sediment, etc.) and with concentrations environmentally relevant becomes important.

Considering the differences between field and laboratory tests, as well as the lack of data on the effects of the REEs that can be identified across their supply chain and in natural scenarios, this thesis conducted a set of tests under laboratory and field conditions to assess the effects of the REEs applied alone and REEs present in

mixture on soils/sediments, in order to provide information about the effects on artificial and natural environment, under different conditions and using different test species. This work is not a life-cycle assessment, however, it does to identify environmental compartments (i.e., aquatic environment and terrestrial environment) that may be at risk, when that information is available in the literature or an association can be made with experimental data.

**Chapter 1** is devoted to a brief introduction to discovery and occurrence of REEs. It is, also, quickly summarized physicochemical characteristics, biological effects and present uses of REEs.

The experimental data included eight case studies and was divided in two parts.

The first part of the thesis deals with the study of field effects and/or measured whole sediment/soil toxicity to understand the behaviour of REE multi-toxicant. Mixtures of toxicants or other stressors can result in either additive, synergistic or antagonist toxicity.

**Chapter 2** assessed REEs composition in a set of surface soil samples collected in the industrial areas of Taranto (Italy), Gardanne (France) and Augusta Priolo (Italy) evaluating the toxicity towards bioassay model (nematodes).

In **Chapter 3**, the study was extended evaluating sediment pollution and toxicity in the Bay of Pozzuoli (Italy), characterized by high anthropic pressure and by previous industrial facilities. Analyses were carried out to evaluate the content of REEs and the toxicity as whole sediment suspensions to sea urchins, or as elutriate in diatoms in sediment samples collected along five transects from the coast.

The second part of the thesis, presented the study of laboratory effects of REEs as single-toxicant and single-species or multi-species toxicity tests that underpin most of the information used to derive toxicant water quality. This study included controllable test conditions (e.g., solution chemistry, temperature) to match environmental site-specific conditions or standard test water composition. Therefore single-toxicant toxicity tests were the cornerstone for generating data for toxicant guideline values.

**Chapter 4** aimed at evaluating the adverse effects of four REEs (Ce, La, Gd and Nd) on green microalgae and macrophyte, considering a background multi-endpoint approach (i.e., growth inhibition, germination index, and genotoxicity) to

check the effect of spiked simplified acid mine drainage (AMD), a viable source of REEs, and to investigate the role of two pH values (4 and 6) in potential toxicity modification.

In the **Chapter 5**, the long-term chronic exposure to two REEs (Ce and Er) on crustaceans at environmentally relevant concentrations of freshwater scenario was investigated. Static renewal toxicity tests were carried out on a multi-endpoint and multi-generational basis. Effects included the following endpoints: organisms' size, parental reproduction, organisms' survival, determination of reactive oxygen species (ROS), enzymatic activity, gene expression of ABC transporter, and uptake. In **Chapter 6**, the same approach as in **Chapter 5** was employed, to explore the effects of long-term exposure to two other REEs (Ce and La) on microalgae. Environmentally relevant concentrations looked at potential generational adaptations in microalgae supporting bioconcentration and hence their possible transfer up to the food web. The multi-endpoint approach included the assessment of algal growth rate, determination of ROS, enzymatic activity, and uptake from exposure media.

The **Chapter 7** was to complete comparative toxicity data on REEs across taxonomically distant species characterized by different habitats and by different sensitivities to xenobiotics. This Chapter was aimed to evaluate the effects of five REEs on bioluminescent bacteria and for the first time on diatoms using similar experimental protocols under the same conditions. Moreover, the results in terms of toxicity are compared with those reported in literature, to rank the susceptibility of the different species to REE-induced harm.

The **general conclusions** of this project suggest that the responses to REEs may be controlled in different species and in different environmental scenarios depending on their capability to manage stress induced by these emerging contaminants

# CHAPTER 1

---

In this chapter, part of the results was presented based on original contribution submitted to international journal Environmental Monitoring and Assessment (EMAS) on December 14, 2021 and on contribution under preparation:

1. **Siciliano A.**, Libralato G. Catalytic activity of Rare Earth Elements in heterogeneous Fenton-like oxidation of wastewater contaminants: a review. Under Preparation
2. Tommasi F., Thomas P.J., Lyons D.M., Pagano G., Oral R., **Siciliano A.**, Toscanesi M., Guida M., Trifuoggi M. Evaluation of rare earth element-associated hormetic effects in candidate fertilizers and livestock feed additives. Submitted

## 1.1 DISCOVERY AND OCCURRENCE OF REES

The history of the discovery of REEs is a complex subject full of controversy. In one of the versions, which started in 1787, Carl Axel Arrhenius, a lieutenant in the Swedish army, found an interesting and dense black mineral in a trip near the village of Ytterby (Sweden). In 1794, Johan Gadolin, a chemist and mineralogist, examined a sample of this mineral and found that the black mineral contained 38% of a new “earth”, naming it Ytterby. Three years later, the Swedish chemist Anders Gustav Ekeberg renamed this earth as yttrium [3, 25, 26]. In another version, the first registration occurred in 1751, when a mineralogist and chemist Axel Frederik Cronstedt described an unusually heavy reddish mineral (later called cerite), in the Bastnas mine (Sweden). Later in 1803, a chemist Wilhelm Hisinger isolated an earth that named cerium [25]. As time passed and the development of new technologies, it was discovered that these two earths (yttrium and cerium) were a complex mixture of other elements. Currently, the rare earth family consists of 17 transition metals located in group 3 of the periodic table (Figure 1).

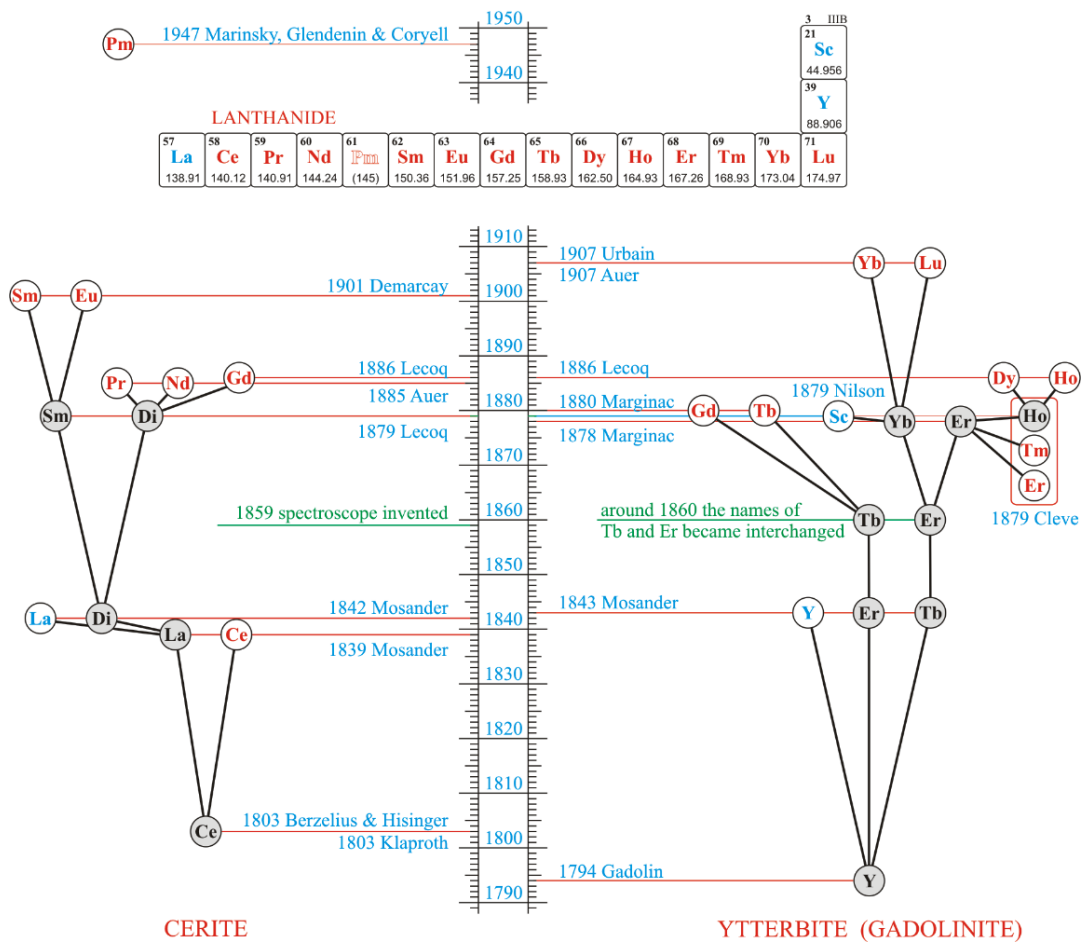


Figure 1 REE history The complex compositions of the two starting minerals cerite and gadolinite (ytterbite) are revealed in the flow chart of discoveries of the elements.

REEs are relatively abundant in the Earth’s crust and widely distributed in the world, but the discovered minable concentrations are less common than for most other ores [27, 28]. These elements are present in more than 270 minerals in a wide range of concentrations [29, 30] but almost entirely concentrated in only three minerals: bastnasite, monazite, and xenotime [31]. REEs are indeed not rare compared to some well-known precious metals such as Au and Pt and the range in crustal abundance vary from Ce, the 25th most abundant element of the 78 common elements in the Earth's crust at 60 parts per million, to thulium and lutetium, the least abundant rare-earth elements at about 0.5 part per million (Table 1) [3, 32, 33]. Pm is the only synthetic element that do not occur naturally in earth’s crust [34]. Known reserves of REEs (approximately 120 million tons) are extensively distributed worldwide. They mainly occur in China, Russia, United States,

Australia, Brazil, India, Malaysia, Thailand, Vietnam, Canada and South Africa [35]. China has the largest reserves (approximately 44 million tons) and appears as the world's largest REE producer (about 58% of the total production). Brazil is the second country in REE reserves (approximately 21 million tons), followed by Russia, with approximately 12 million tons [35, 36].

| Elements                          | Crustal Abundance<br>(parts per million) |
|-----------------------------------|--|
| Cerium ( $_{58}\text{Ce}$ )       | 60.0                                     |
| Lanthanum ( $_{57}\text{La}$ )    | 30.0                                     |
| Neodymium ( $_{60}\text{Nd}$ )    | 27.0                                     |
| Yttrium ( $_{39}\text{Y}$ )       | 24.0                                     |
| Scandium ( $_{21}\text{Sc}$ )     | 16.0                                     |
| Praseodymium ( $_{59}\text{Pr}$ ) | 6.7                                      |
| Samarium ( $_{62}\text{Sm}$ )     | 5.3                                      |
| Gadolinium ( $_{64}\text{Gd}$ )   | 4.0                                      |
| Dysprosium ( $_{66}\text{Dy}$ )   | 3.8                                      |
| Erbium ( $_{68}\text{Er}$ )       | 2.1                                      |
| Ytterbium ( $_{70}\text{Yb}$ )    | 2.0                                      |
| Europium ( $_{63}\text{Eu}$ )     | 1.3                                      |
| Holmium ( $_{67}\text{Ho}$ )      | 0.8                                      |
| Terbium ( $_{65}\text{Tb}$ )      | 0.7                                      |
| Lutetium ( $_{71}\text{Lu}$ )     | 0.4                                      |
| Thulium ( $_{69}\text{Tm}$ )      | 0.3                                      |
| Promethium ( $_{61}\text{Pm}$ )   | $10^{-18}$                               |

*Table 1 Abundance of REEs in the Earth's Crust (Adapted from Wedepohl, 1995 [37])*

## 1.2 PROPERTIES AND USES OF REES

The REEs have very similar chemical and physical properties, and this uniformity may be explained by the electronic configuration of the atoms with valence located in the inner 4f subshell orbital, shielded by 5s<sup>2</sup> and 5p<sup>6</sup> outer closed (full) subshells. Atomic nucleus is not shielded from increasing atomic number which causes the 4f orbitals surround closer the nucleus and the atomic radius of the atom to decrease (lanthanide contraction) [38-40]. Generally they are electropositive and reach an

oxidation state +3, particularly stable, only the elements Ce and Eu can also be present with valence +4 and +2, respectively [38].

The REEs are malleable, soft, ductile, and great conductors of heat and electricity [41] which allow their applications [3, 6]. These elements are used extensively for a variety of high technology applications and traditional industries such as agriculture, automotive, metallurgy, nuclear, petroleum, and textiles, at an unprecedented rate and consequently humans are daily exposed to these elements [3, 8, 24, 35, 42]. Since they are extremely important ingredients, these elements are called "The Vitamins of Modern Industry"[14, 43, 44]. Figure 2 presents a summary of the uses of REEs in high technology and other industrial applications. REEs are mainly used in permanent catalysis (24%), magnets (23%), polishing (18%), metallurgy (8%), and batteries (8%) [45].

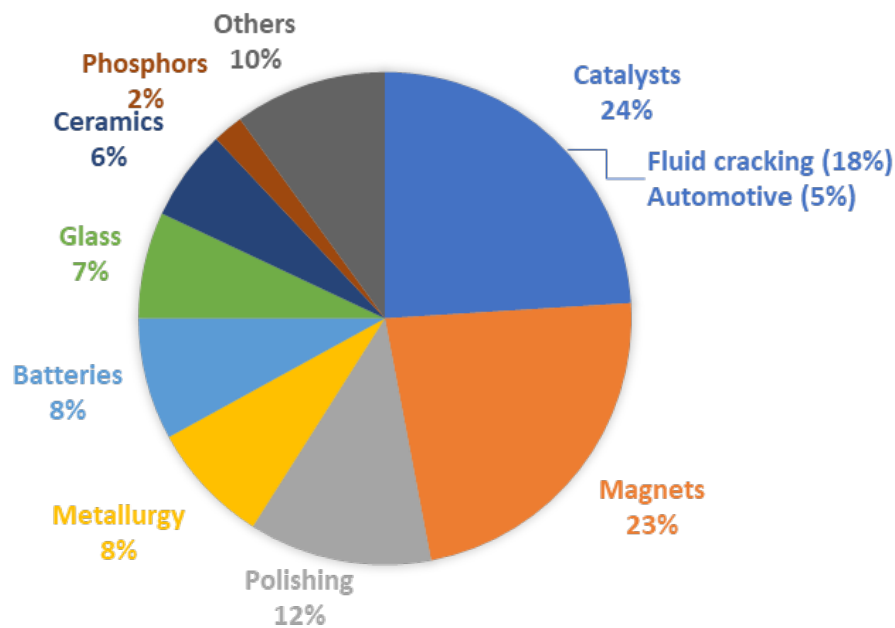


Figure 2 REEs (%) consumption in various application. Adapted from Roskill (2015) [45].

Catalyst applications (largely Ce and La) are for both industrial and auto catalysts including solid oxide fuel cells[46], the purification of vehicle exhaust gases [47], catalytic cracking [48], hydrogenation, dehydrogenation, hydration, dehydration, steam, carbon dioxide, and oxidative conversion of methane [49], due to the high mobility of oxygen and the stabilization of unusual oxidation states in their structure [50, 51]. Recently, the application of REEs in adsorption [52], photocatalysis [53]

and Fenton-like reaction [54, 55] has been reported gaining an outstanding role in pollution abatement also. A list of studies employing La and Ce in Fenton-like reaction is presented in Table 2.

Phosphors (particularly on Eu and Tb) are important for visual display in screens and low energy lighting [32]. Another area for expansion will be rare earth magnets (Nd, Pr, Sm and Dy) particularly for alternative energies as wind turbines, electric and hybrid cars and missile guidance systems. Glasses containing Er are important for fibre optical amplifiers required in high speed optical communication networks [32, 68]. REEs have also found an extensive use in medicine; for example, Gd in magnetic resonance imaging contrast agents or Y in the development of drugs for cancer treatment [69-72]. REEs are also used in agriculture as fertilizers to increase crop yield, and in zootechny as feed additives to promote animal growth [3, 9].

| Catalyst   |            | Oxidant   |              | Temperature (°C) | pH  | Reaction time (minute) | Target compound       | Degradation (%) | Mineralization (%) | References |
|--|------------|---|--------------|------------------|-----|------------------------|-----------------------|-----------------|--------------------|------------|
| Composition  | Dose (g/L) | Composition   | Dose (mM/L)  |                  |     |                        |                       |                 |                    |            |
| LaFeO <sub>3</sub> /lignin-biochar   | 0.25       | H <sub>2</sub> O <sub>2</sub>   | 4.4          | 21               | -   | 75                     | Ofloxacin             | 95.6            | -                  | [56]       |
| La <sub>0.7</sub> Sr <sub>0.3</sub> Mn <sub>0.85</sub> Fe <sub>0.15</sub> O <sub>3</sub> | 0.10       | H <sub>2</sub> O <sub>2</sub> ,<br>H <sub>2</sub> C <sub>2</sub> O <sub>4</sub> | 12.0,<br>1.0 | 21               | 4.0 | 120                    | Methyl orange         | 94.0            | 82.0               | [57]       |
| Ti – LaFeO <sub>3</sub>  | 0.70       | H <sub>2</sub> O <sub>2</sub>   | 14.0         | 40               | 8.0 | 180                    | Carbofuran            | 90.6            | -                  | [58]       |
| LaFeO <sub>3</sub>   | 0.30       | H <sub>2</sub> O <sub>2</sub>   | 20.0         | 21               | 5.5 | 300                    | Carbamazepine         | 92.0            | -                  | [59]       |
| LaFeO <sub>3</sub>   | 1.40       | H <sub>2</sub> O <sub>2</sub>   | 23.0         | 20               | 5.5 | 120                    | Sulfamethoxazole      | 98.0            | -                  | [60]       |
| CeO <sub>2</sub> -LaCuO <sub>3</sub>   | 0.4        | H <sub>2</sub> O <sub>2</sub>   | 12.5         | 25               | 7.0 | 350                    | Bisphenol             | <b>99.8</b>     | 72.44              | [61]       |
| Ce-Cu composite  | 1.0        | H <sub>2</sub> O <sub>2</sub>   | -            | 50               | 4.0 | 120                    | 2,4-Dichlorophenol    | 99.5            | 82                 | [62]       |
| Fe <sub>3</sub> O <sub>4</sub> /CeO <sub>2</sub>   | 2.0        | H <sub>2</sub> O <sub>2</sub>   | 30           | 30               | 2.0 | 180                    | 2,4,6-trichlorophenol | 99.0            | 65                 | [63]       |
| CeO <sub>2</sub>   | 0.5        | H <sub>2</sub> O <sub>2</sub>   | 10           | 25               | -   | 480                    | Acid orange7          | 98.0            | -                  | [56]       |
| Ce-Cu composite  | 1.0        | H <sub>2</sub> O <sub>2</sub>   | -            | 50               | 4.0 | 120                    | 4- Chlorophenol       | 95.0            | 88                 | [62]       |
| Ce <sub>x</sub> CuO <sub>y</sub>   | 0.1        | H <sub>2</sub> O <sub>2</sub>   | 50           | 25               | 5.0 | 60                     | Fluconazole           | 94.0            | -                  | [64]       |
| CeO <sub>2</sub>   | 1.0        | H <sub>2</sub> O <sub>2</sub>   | 18           | 25               | -   | 300                    | Acid orange7          | 90.0            | -                  | [65]       |
| Fe <sup>0</sup> /CeO <sub>2</sub>  | 0.1        | H <sub>2</sub> O <sub>2</sub>   | 100          | 26               | 5.8 | 60                     | tetracycline          | 90.0            | -                  | [66]       |
| FeCeO <sub>x</sub>   | 1.5        | H <sub>2</sub> O <sub>2</sub>   | 80           | 35               | 5.0 | 150                    | Rhodamine B           | 90.0            | -                  | [67]       |
| CeO <sub>2</sub>   | 1.5        | H <sub>2</sub> O <sub>2</sub>   | 60           | 22               | 3.0 | 120                    | Orange II             | 85.0            | -                  | [61]       |
| Fe <sub>2</sub> O <sub>3</sub> -CeO <sub>2</sub>   | 0.5        | H <sub>2</sub> O <sub>2</sub>   | 8            | 45               | 3.0 | 120                    | Sulfamerazine         | 70.0            | -                  | [65]       |
| CeO <sub>2</sub>   | 1.5        | H <sub>2</sub> O <sub>2</sub>   | 116          | 22               | 3.0 | 120                    | Acid Green            | <b>60.0</b>     | -                  | [66]       |

Table 2 Lanthanum-based and Cerium-based catalysts employed in heterogeneous Fenton-like oxidation

### **1.3 ANTHROPOGENIC SOURCES AND ENVIRONMENTAL OCCURRENCE**

Because of the emerging technologies in a big way, the REE application boom would continue in near future also [5]. They are strategic resources but they are not renewable and are considered to be close to “peaking” [5, 73]. In fact, the rare earth supply chain is still linear and recycling barely reaches 1% of world production [73]. In this way, REEs enter the environment at various stages of their life-cycle particularly during disposal of consumer and industrial products (e.g. landfills), discharges from mining and mineral processing, and effluents/wastewaters from industrial processes that use REEs [5, 6, 38]. Anthropogenic REEs contamination can be of great concern in hot spots (e.g., ore mine tailings and abandoned mines)[24], but the alteration of their biogeochemical cycles suggests their potential role as widespread emerging contaminants [5-8, 24, 74-76] (Table 3). REEs have been detected in atmospheric particulates such as dust [77-79], marine systems [80-82], aquatic systems including drinking tap water[83-87], terrestrial and aquatic biota [88], and human foods [69, 89-91]. Soils in areas impacted by mining activities, not only related to REE extraction, and industry have been shown to contain REEs with concentrations up to 100 times higher than normal background levels [6]. About the aquatic environment, their main sources include waste and wastewaters from medical institutions, fertilizers, mining processing, high technology industries, petroleum refineries, and recycling plants (i.e., e-waste management) [6, 24, 75, 92]. According to Migaszewski review paper [38], REEs ranged between 1.1 and 161.0 µg/L in wastewater. In river water, lanthanides concentrations were lower than in wastewater and ranged between 7.9 and 212.0 ng/L [38], but on a local basis they can be up to 80–200 µg/L [93].

| REE    | mg/kg (ppm)           |                          |                              |                                | µg/L (ppb)                   |                                 | ng/L (ppt)                |                                |                     |                        | pM                                 |
|--------|-----------------------|--------------------------|------------------------------|--------------------------------|------------------------------|---------------------------------|---------------------------|--------------------------------|---------------------|------------------------|------------------------------------|
|        | Top soils Europe [94] | Soils (South China) [95] | Peat bog soils (Sweden) [96] | Stream sediments (Europe) [94] | Ore mine effluent (USA) [97] | Coal mine effluent (China) [98] | River water (Amazon) [97] | River water (Mississippi) [99] | Seawater (UK) [100] | Seawater (Japan) [101] | Seawater (Western Philippine) [99] |
| La     | 25.9                  | 57.0                     | 1.4                          | 41                             | 80.4                         | 7.77                            | 74                        | 19.7                           | 137.8               | 166                    | 77.0                               |
| Ce     | 52.2                  | 122                      | 2.1                          | 83                             | 161                          | 19.4                            | 212                       | 9.67                           | 18.6                | 276                    | 32.0                               |
| Pr     | 6.02                  | 12.2                     | 0.44                         | 9.22                           | 21.2                         | 2.78                            | n.d.                      | n.d.                           | 10.1                | 7.2                    | 12.0                               |
| Nd     | 22.4                  | 40.6                     | 0.99                         | 36.6                           | 92.3                         | 13                              | 127                       | 19.9                           | 10.2                | 31                     | 47.0                               |
| Sm     | 4.28                  | 7.76                     | 0.2                          | 6.91                           | 20.3                         | 2.98                            | 34.5                      | 4.5                            | 7.0                 | 7.5                    | 9.0                                |
| Eu     | 0.851                 | 2.36                     | 0.032                        | 1.15                           | 5.95                         | 0.87                            | 7.9                       | 1.11                           | 6.9                 | 2.1                    | 1.8                                |
| Gd     | 4.2                   | 7.14                     | 0.16                         | 6.32                           | 23.8                         | 3.78                            | n.d.                      | n.d.                           | 8.8                 | 10.1                   | 8.5                                |
| Tb     | 0.638                 | 1.15                     | 0.044                        | 0.958                          | 3.65                         | 0.7                             | n.d.                      | n.d.                           | 7.3                 | 1.7                    | 1.5                                |
| Dy     | 3.58                  | 6.29                     | 0.14                         | 5.4                            | 22                           | 4.06                            | 31.4                      | 7.56                           | 8.2                 | 10.8                   | 10.0                               |
| Ho     | 0.716                 | 1.16                     | 0.033                        | 1.09                           | 4.43                         | 0.87                            | n.d.                      | n.d.                           | 7.5                 | 2.6                    | 2.4                                |
| Er     | 2.1                   | 3.11                     | 0.05                         | 3.18                           | 11.9                         | 2.43                            | 16.6                      | 6.53                           | 8.2                 | 8.2                    | 8.0                                |
| Tm     | 0.312                 | 0.42                     | 0.014                        | 0.47                           | 1.48                         | 0.34                            | n.d.                      | n.d.                           | 7.6                 | 1.1                    | 1.1                                |
| Yb     | 2.09                  | 2.66                     | 0.072                        | 3.09                           | 8.2                          | 1.99                            | 15.3                      | 6.06                           | 8.4                 | 8                      | 7.6                                |
| Lu     | 0.307                 | 0.42                     | 0.014                        | 0.477                          | 1.12                         | 0.31                            | n.d.                      | n.d.                           | 7.9                 | 1.2                    | 1.2                                |
| ∑ REEs | 125.59                | 260.77                   | 5.689                        | 198.865                        | 457.73                       | 61.28                           | 518.7                     | 75.03                          | 254.5               | 533.5                  | 219.1                              |

Table 3 REE abundances in environment

REEs are mobilized and transported in various environmental compartments through multiple ways entering into the hydrosphere, lithosphere and atmosphere. Apart from also entering through natural ways as wind-driven (e.g., dust) and hydrological processes such as runoff, infiltration, recharge, and erosion, the anthropogenic activity is a big cause of these contaminants entering the ecosystem [102-104]. Besides transport processes, movement of REEs depends on the nature and speciation and geochemical conditions. Apart from these, there are other factors which influence the environmental behaviour of REEs such as salinity, pH, redox potential, dissolved organic matter, mineral phases, and type and concentration of chelating agents [38, 105-108].

#### **1.4 REES-ASSOCIATED ADVERSE EFFECTS**

After the pioneering studies in 1941 by Drobkov [109] on the effects of REEs on the development of peas, and between 1994 and 1995 by Jha and Singh [110, 111] assessing the induction of cytogenetic damage by two REEs (Pr and Nd) in mice and in broad bean (*Vicia faba*), a thriving literature over recent decades has provided established evidence for a number of REE-associated adverse effects in a number of test models, as summarized in Table 4. Studies of REE toxicity in plant models were carried out on several crop and native species, showing decreased seed germination, root elongation and mitotic activity for REE levels 5.0 mg/L [10-13, 20, 112, 113].

More extensive studies of REE-associated toxicity were conducted in several animal models including mammals (mice and rats), fish (*Danio rerio*), and sea urchins, providing evidence for several of adverse effects, including oxidative damage, lung and kidney toxicity, developmental and cytogenetic damage [114-116]. Altogether, the available body of literature on the adverse effects of REE exposures raises environmental health concerns.

| Test models              | Test REEs  | Endpoints  | Observed effects  | References |
|--------------------------|--|--|---|------------|
| <b>PLANTS</b>            |  |  |   |            |
| Triticum aestivum        | La and Ce [0.5 - 25 mg/L]  | Root elongation; dry weight of roots and shoots; content of mineral elements   | Decreased parameters  | [112]      |
| Brassica juncea          | La(III) [0.05 - 5.0 mg/L]  | Root elongation; Fe, Mn and Zn accumulation  | La [ $\geq 1.0$ mg/L] inhibited root elongation and metal accumulation          | [113]      |
| 5 Native and crop plants | La, Ce and Y [20 -2000 mg/kg]  | Germination and harvest  | Decreased germination   | [10]       |
| 6 Native and crop plants | Pr, Nd, Sa, Tb, Dy, Er [100 - 700 mg/kg]                             | Seed germination; speed of germination   | Decreased germination   | [13]       |
| Allium cepa              | La and Ce [0 - 200 mg/L]   | Root growth; mitotic index and frequency of aberrant cells   | Decreased growth; mitotic index and increased aberrant cells                    | [12]       |
| <b>ANIMALS</b>           |  |  |   |            |
| Mice (adult and fetal)   | CeCl <sub>3</sub> (gavage) [200 or 500mg/kg BW]                      | Pulmonary haemorrhage (adults) pulmonary and hepatic vascular congestion (neonatal)  | Increased pulmonary damage  | [117]      |
| Wistar rats              | LaCl <sub>3</sub> (gavage) [0.1 - 40 mg/kg]                          | Behavioural performance; [Ca <sup>2+</sup> ] <sub>i</sub> level; Ca <sup>2+</sup> -ATPase in hippocampal cells; oxidative stress | Increased Ca <sup>2+</sup> -ATPase; decreased activities of antioxidant enzymes | [118]      |
| Rats                     | CeO <sub>2</sub> (nanoparticles) [175 - 250 mg/kg]                   | Oxidative stress endpoints   | Increased oxidative stress in cortex, hippocampus, and cerebellum               | [119]      |
| Mice                     | La, Ce, and Nd (III) (by gavage); [10, 20, or 40 mg/kg BW/day] 6 wks | Accumulation in hepatocyte, nuclei and mitochondria  | Oxidative damage in hepatic nuclei  | [120]      |
| Sprague-Dawley rats      | CeO <sub>2</sub> nanoparticles                                       | Liver ceria levels; serum alanine  | Decreased liver weight; hydropic  | [121]      |

Table 4 Selected REE-related literature: adverse effects.

| Test models                              | Test REEs   | Endpoints   | Observed effects   | References |
|--|---|---|--|------------|
| <b>ANIMALS</b>                           |   |   |  |            |
| ICR Mice                                 | LaCl <sub>3</sub> , CeCl <sub>3</sub> , and NdCl <sub>3</sub> [20 mg/kg BW, i.p.] | Brain injury; oxidative stress  | Increased brain injury and   | [122]      |
| ICR Mice                                 | CeCl <sub>3</sub> (gavage) [2 - 20 mg/kg BW]                                      | hepatocyte ultrastructure; oxidative stress; kidney structure                         | increased ROS formation; inhibited   | [123]      |
| CD1 Mice                                 | CeO <sub>2</sub> nanoparticles [2 mg/m <sup>3</sup> ]                             | Pro-inflammatory cytokines; oxidative stress markers                                  | Increased pro-inflammatory condition   | [124]      |
| Mice                                     | CeCl <sub>3</sub> [2 mg/kg] via gavage  | Liver injury and gene-expressed profiles  | Decreased counts of white blood cells; lymphocytes; platelets; reticulocyte count; neutrophilic granulocyte percentages; A/G ratio | [125]      |
| Mice                                     | CeCl <sub>3</sub> (nasally instilled)   | Pro-inflammatory lung parameters; serum triglyceride levels                           | Oxidative stress and inflammatory cytokine expression; sinusoidal dilatation   | [126]      |
| <i>Caenorhabditis elegans</i>            | La <sup>3+</sup> [10 mM]  | Growth and reproduction   | Significant adverse effects  | [115]      |
| Zebrafish embryos                        | La <sup>3+</sup> or Yb <sup>3+</sup> [0.01 to 1 mM]                               | Developmental defects and mortality   | Increased damage   | [116]      |
| 3 Sea urchin species (embryos and sperm) | 7 REE chlorides [10 <sup>-6</sup> – 10 <sup>-4</sup> M]                           | Developmental defects; fertilization success; offspring anomalies; cytogenetic damage | Increased developmental defects; decreased fertilization; increased cytogenetic anomalies  | [114, 127] |

Table 5 (continued) Selected REE-related literature: adverse effects

## 1.5 REES-ASSOCIATED HORMETIC TRENDS

REE dose-response trends have been associated with hormesis, a phenomenon characterized by stimulation (Greek: hormào) of biological activities at lower concentrations compared to inhibition and toxicity at higher exposure concentrations [128]. As shown in Table 5, evidence for hormetic trends were reported in a set of studies conducted in several biota including plants, fungi, microbiota and animals. In particular, plant models including rice, bean, cabbage and orange were exposed to varying levels of La, Ce and Sc by testing some key endpoints including growth, germination, chlorophyll content and oxidative stress parameters. The results reported on concentration-related hormetic trends in the REEs exposed plants [129-132].

Low La concentrations enhanced the photosynthetic rate and total chlorophyll content and led to a higher incidence of binucleate cells, with a slight increase in root and shoot biomass in soybean [133], while ROS levels declined in rice [134]. Extending this work to bacteria, microbial communities increased growth kinetics when exposed to low REE concentrations [135, 136]. Several studies of REE-associated hormetic effects were conducted in animal models (Table 5)[137-139]. In view of likely developments in the production and use of REE-based fertilizers and feed additives, and in view of open questions persisting on the efficacy of using REE mixtures and their concentration related trends, ad hoc investigations are required aimed at verifying the single vs. combined use of REEs in these production and use scenarios.

| Test models                                 | Test REEs  | Endpoints  | Observed effects   | References |
|---|--|--|--|------------|
| <b>PLANTS</b>                               |  |  |  |            |
| Rice<br>( <i>Oryza sativa</i> )             | La(NO <sub>3</sub> ) <sub>3</sub><br>[20 – 1500 µg/mL]                 | Germination of rice seeds; chlorophyll contents; root growth             | Increased parameters   | [129]      |
| Broad bean<br><i>Vicia faba</i>             | LaCl <sub>3</sub><br>[108-195 µg/g]                                    | Superoxide dismutase; catalase; ascorbate peroxidase; HSP 70             | Hormetic effects   | [130]      |
| Chinese cabbage<br>( <i>Brassica rapa</i> ) | LaCl <sub>3</sub> and CeCl <sub>4</sub>                                | Soluble sugar, titratable acid, nitrate and vitamin C                    | La more effective than Ce; different data for autumn vs. spring plantation   | [131]      |
| Soybean ( <i>Glycine max</i> )              | La(III)<br>[5 – 150 µM]  | Growth; mitotic index; chlorophyll content high concentrations decreased | Low La concentrations stimulated, the photosynthetic rate                    | [133]      |
| Rice ( <i>Oryza sativa</i> )                | La(III)<br>[0.05 – 1.5 mM]   | Redox endpoints  | Increased catalase and peroxidase  | [134]      |
| <i>Capsicum annuum</i>                      | LaCl <sub>3</sub> [10 µM]  | Seedling height; shoot diameter  | Increased growth   | [140]      |
| Rice<br>( <i>Oryza sativa</i> )             | Sc(III)<br>[25 and 50 µM]  | Germination; oxidative stress parameters                                 | Improved germination; decreased oxidative stress                             | [141]      |
| <i>Phaseolus vulgaris</i>                   | Ce(NO <sub>3</sub> ) <sub>3</sub> 6H <sub>2</sub> O<br>[0.1 - 72.9 mM] | Survival rate and growth vs. water stress                                | Increased photosynthesis rate, chlorophyll content, and water use efficiency | [132]      |
| Orange<br>( <i>Poncirus trifoliata</i> )    | Ce(NO <sub>3</sub> ) <sub>3</sub> 6H <sub>2</sub> O<br>[0.25 – 4 mM]   | Growth kinetics; chlorophyll content                                     | Different hormetic effects   | [142]      |

Table 6 Selected REE-related literature: hormetic effects in growth endpoint.

| Test models   | Test REEs                                    | Endpoints   | Observed effects   | References |
|---|--|---|--|------------|
| <b>FUNGI AND MICROBES</b>                             |  |   |  |            |
| <i>Trichoderma atroviride</i> and <i>T. harzianum</i> | La and REE mix [0.003 to 900 mM]             | Accumulation of REEs in fungal biomass                        | Increased growth   | [143]      |
| <i>Escherichia coli</i>                               | 16 REEs                                      | Growth kinetics   | Different hormetic effects   | [136]      |
| Microbial communities                                 | Y(III) [ $\leq 20$ mg/L]                     | Ammonia-oxidizing bacteria                                    | Increased specific-oxygen-uptake-rate at $\leq 20$ mg/L; or decreased $>20$ mg/L | [135]      |
| <b>ANIMALS AND ANIMAL CELLS</b>                       |  |   |  |            |
| Human dermal fibroblasts                              | 14 REE [1–100 $\mu$ M]                       | Pro-fibrotic responses in tissue injury                       | Increased proliferation by low REE levels  | [137]      |
| Murine preosteoblast cell line MC3T3-E1               | LaCl <sub>3</sub> [ $10^{-9}$ – $10^{-3}$ M] | Proliferation; osteogenic differentiation, and mineralization | Upregulated below $10^{-6}$ M, downregulated at $10^{-3}$ M                      | [138]      |
| Mice  | CeO <sub>2</sub> nanoparticles               | ROS production  | Decreased ROS  | [139]      |
| Sprague-Dawley rats                                   | Y <sub>2</sub> O <sub>3</sub> [20-320 ppm]   | Body weight; spatial learning and memory; anogenital distance | Increased at 20 ppm; decreased at 320 ppm  | [66]       |

Table 5 Selected REE-related literature: hormetic effects in growth endpoint

## CHAPTER 2

---

In this chapter, part of results based on original contributions published in [144, 145] and submitted in Environmental Research (Tommasi F., Pagano G., Oral R., Thomas P.J., Ecclese K.M., Tezc S., Toscanesi M., Lombardo F., Siciliano A., Dipierro N., Gjataa I., Guida M., Libralato G., Lyons D.P., Buričh P., Kovačičh I., Trifuoggi M.(2021) Topsoil multi-endpoint pollution and toxicity in the petrochemical area at Augusta-Priolo (eastern Sicily, Italy)) is presented.

### **2.1 TOPSOIL POLLUTION AND TOXICITY IN INDUSTRIAL AREAS OF TARANTO, AUGUSTA, PRIOLO (SOUTHERN ITALY) AND GARDANNE (SOUTHERN FRANCE)**

The knowledge of natural contents of a contaminant in the soil is crucial for environmental and human health risk assessments. Regarding REEs, this issue deserves the attention and the support of scientific community, because our understanding on the biological role of these ECs is still in its early stages [146] and little is known about their effects in environment, when natural concentrations are altered in areas affected by anthropogenic activities. In these areas, many data are available on the quality of water and air [147, 148], while few studies concern the chemical composition and effects of dust and surface layers of soil on which numerous substances from air, water and industrial emissions accumulate. Even more scarce are the data relating to the presence of EC, such as REEs, despite the accumulation in the environment in relation to anthropic activity i.e. steel industry, has been reported in various parts of the world [149].

These studies was aimed at geospatially identifying pollutants, including REEs, present, and determining their concentrations and toxicity as complex mixtures, in topsoil samples close to industrial areas of Taranto Augusta and Priolo in southern Italy and Gardanne in southern France. Elemental analysis of soil was conducted by ICP-MS for 23 metals and a set of 16 REEs. Organic analyses focused on polycyclic aromatic hydrocarbons (PAHs) (16 parent homologs) and total aliphatic hydrocarbons (C10 - C40). Topsoil samples were tested for toxicity in bioassay

model: mortality in nematode *Caenorhabditis elegans*. The data obtained in the bioassay can allow exploration of geospatial patterns of effect in biota as a function of contaminant level providing key information that could inform future investigations, mitigation, and remedial measures.

### 2.1.1 Taranto case study

The industrial area neighbouring the city of Taranto (southern Italy, 40° 28' 34" N, 17° 13' 47" E) has been subject to environmental concerns for several years. A number of studies focused on health effects in local residents [150-152], or on the pollution status of the nearby enclosed inner bay, termed Mar Piccolo (Small Sea) [153-157]. Air pollution from the steel foundry, as solid and gaseous atmospheric emissions of PAHs, was well studied in 2005 [158]. As demonstrated in Figure 3, the Taranto industrial area hosts a steel foundry, an oil refinery, a power plant, and has hosted a set of dockyards that altogether imply the occurrence of multiple pollutants present as complex mixtures. It was recognized that dust deposition [158], released from the main industrial sources in Taranto (steel foundry, power plant, and oil refinery) and well known to residents as red wind impacted soil giving rise to inorganic and organic complex mixtures, both including metals and persistent organic pollutants [159-161]. Thus, wind-driven dust from polluted soils was expected to affect human health through breathable particulate matter [151].

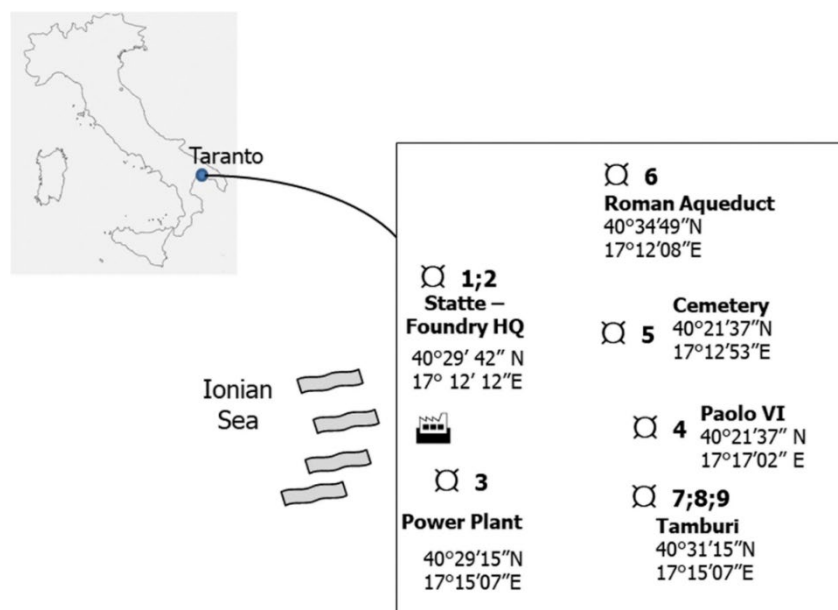


Figure 3 Outline of the Taranto industrial area and location of sampling sites.

## 2.1.2 Gardanne case study

Bauxite manufacturing by the Bayer process in alumina production is associated with a by-product, bauxite residue (BR), traditionally termed “red mud” [162, 163]. In turn, BR has raised environmental concern in areas affected by plant effluents as related to its recognized toxicity since early studies [164-168]. BR was considered as a complex mixture, whose main elemental components was aluminium and iron [169]. Recent reports have focused on the impacts of BR disposal areas, providing evidence for persistent alterations of soil and freshwaters composition near bauxite processing plants (BPPs) [161, 170, 171]. Management steps to suppress dusting from BR-polluted areas using phyto-stabilization has gained much interest [171] but the possibility of fugitive dusting from operational or legacy sites remains. As shown in Figure 4, the Gardanne (southern France, 43°45'25.98" N, 5°47'17.36" E) industrial area investigated herein includes a BPP and nearby PP, which are located close to the residential neighbourhoods of the town.

Furthermore, the recent literature has pointed to fly ash release from PPs, both including inorganics [172, 173] and several organic classes, such as PAHs [174, 175], combustion-derived nanoparticles (CDNP), and de novo formation of polychlorinated dibenzo-p-dioxins and dibenzofurans (PCDDs and PCDFs) [176, 177].

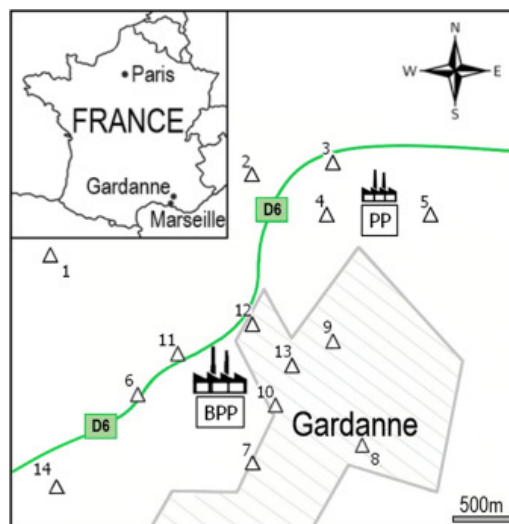


Figure 4 Map of Gardanne and of soil sampling points. Abbreviations: BPP – Bauxite Processing Plant; PP – Power Plant.

### 2.1.3 Augusta- Priolo case study

The combined facilities of oil refineries and related petrochemical industries in Augusta (southern Italy, 37°13'49"N 15°13'10"E) and Priolo (southern Italy, 37°10'N 15°11'E) represent the largest industrial footprint in this sector in the whole of Europe. These areas include two main oil refineries and a series of subsidiary facilities and harbours, with the area hosting a population of approximately 50,000 inhabitants (Figure 5).

Residents near these chemical plants have been extensively studied for multiple health risks [148, 178], and are included in epidemiological surveillance programs in Italy such as in the programme of public health intervention [148]. In particular, concerns among the population are prevalent as occupational exposures in petrochemical facilities have been found to increase the risks of various types of neoplasm in men and women [179-181]. Apart from the human health considerations, numerous ecotoxicological studies of environmental samples [182] using various bioassays on soil and marine sediment samples [183-185] confirmed that the risks from these industries extend beyond mere occupational exposures of workers to the wider environment. Amongst various xenobiotic compounds linked to adverse effects near petrochemical facilities, metal pollution has been often studied, with a particular focus on some priority HM and PAHs [184, 186].

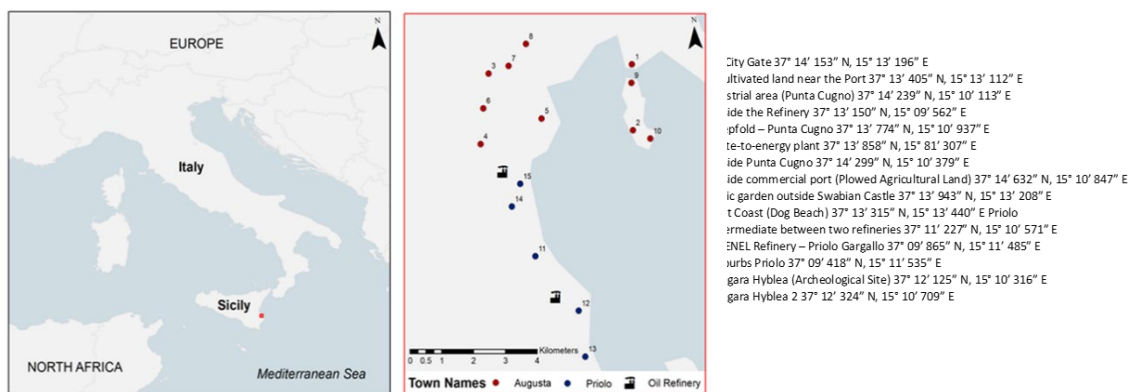


Figure 5 An overview map and localization of sampling sites in Augusta and Priolo.

## **2.2 METHODS**

### **2.2.1 Soil sample collection and processing**

Topsoil or dust samples were collected from the road, street edges or cultivated soil with a new and clean steel shovel. The top 20 cm was sampled after removal of stones and herbaceous debris. Lighter soil was collected with a small brush. Approximately 100 g of soil was collected at each location following protocols previously [187, 188]. Samples were carried to the laboratory in polystyrene 150-ml beakers. Samples were sieved in 2-mm mesh steel nets, ground in a ceramic pestle and eventually dried at 60 °C for 24 h, for subsequent analytical and bioassay evaluations.

### **2.2.2 Metal analysis**

Soil samples were analysed for a suite of trace elements, including 14 heavy metals (HM) and 10 REEs. For the determination of HM and REEs, soil samples were subjected to oxidative acid digestion using a mixture of acids at high temperature and pressure, assisted by microwave (Mars – CEM, Italy). Two different methods of digestion were used for HM and REE extraction. For the solubility of HM, the US EPA 3050B:1996 method was followed [189]. The acid digestion and subsequent extraction of REEs were made using an internal method that involved two steps. In the former step, nitric and hydrofluoric acid are used (0.25 g sample + 3.5 mL HNO<sub>3</sub> + 0.1 mL HF). The second step involved the addition of boric acid [6 mL H<sub>3</sub>BO<sub>3</sub> (4%)]. In both steps, the microwave operating parameters were set as follows: T = 180 °C; ramp (min:s) = 5:30; hold (min:s) = 9:30; pressure = 800 psi; power = 900–1050 W. The quantitative determination of trace elements was carried out using method UNI EN ISO 16171 [190] with ICP-MS analysis (inductively coupled plasma with mass spectrometry detection; Aurora M90 Bruker, USA). The detection limit (LOD) and limit of quantification (LOQ) were calculated using the method of blank variability for each investigated metal.

### 2.2.3 PAH and total organic analysis

Soil samples were analysed for total hydrocarbons (C10–C40) and PAHs contents. The dry soil samples were extracted with a mixture acetone/n-hexane 1:1 v/v and sonicated for 3 h by ultrasonic disruptor. A part of the extract was purified with anhydrous sodium sulphate (preheated at 550 °C for 2 h) and analysed by gas chromatography coupled with a mass spectrometer (Shimadzu 2010 Plus and MS-TQ8030-Shimadzu, Japan) for PAH analysis. Another part of the extract was purified on florisil column (2 g florisil with granulometry of 60–100 mesh and activated at 150 °C for 24 h) and analysed by gas chromatography with a flame ionization detector (FID) (Agilent 6890, USA) for the determination of total hydrocarbons (C10–C40). The detection limit (LOD) and limit of quantification (LOQ) were calculated and average values of LOD and LOQ were 0.03 and 0.1 µg/g for PAHs and 1.7 and 5.1 µg/g for total hydrocarbons, respectively. The precision, accuracy, and recovery were estimated with the certified matrix. The percentage of recovery was between 60%–120% for PAHs and 80%–110% for C10–C40.

### 2.2.4 *Caenorhabditis elegans* bioassays

The nematode *Caenorhabditis elegans* wild-type strain N2 variant Bristol is maintained on NGM (Nematode growth media) plates seeded with *Escherichia coli* (strain OP50-Uracil deficient) and stored at 20 °C was used ASTM E2172–01 [191]. The tests were performed using age-synchronous adult nematodes and achieved by lysis of the gravid nematodes with a bleaching mixture (10 g/l NaOH, 10.5 g/l NaOCl) followed by centrifuge washing with M9 (2.2 mM KH<sub>2</sub>PO<sub>4</sub>, 4.2 mM Na<sub>2</sub>HPO<sub>4</sub>, 85.6 mM NaCl, 1 mM MgSO<sub>4</sub>) and allowed to rest overnight in NGM agar plates. The nematode bioassay followed a slightly modified version of the ASTM Standard Method E2172–01 [191]. Topsoil or dust samples (2.33 g) were hydrated to 35–45% of their dry weight with K-medium in centrifuge tubes. Ten worms were transferred to each test tube and exposed to the samples for 24 h at 20 °C. All treatments were performed in four replicates, without feeding the

worms. Nematodes were extracted from the matrix by centrifugation with silica gel with a specific density of 1.13 g/ml (Ludox TM 50, Sigma-Aldrich, St. Louis, MO, USA). After centrifugation at 2000 rpm for 2 min, the supernatant of each sample was poured into 100-mm glass Petri dishes and washed with K-medium. The extracted individuals were then counted under a microscope ( $\times 40$  magnification). Control cultures were carried out by rearing nematodes unexposed to samples. Mortality was the measured endpoint and test acceptability was with 80% recovery and 90% control survival.

### **2.2.5 Statistical analysis**

Results of bioassays are given as mean  $\pm$  standard error. Differences between samples and control group were determined by two-tailed Student's t test. The significance of the difference among groups was evaluated by one-way analysis of variance (ANOVA) and further statistical *post hoc* comparisons with Tukey's multiple comparison test.

The trace element dataset was analysed through principal component analysis (PCA). The main goal of PCA is to reduce the dimensionality of a dataset consisting of many interrelated variables while retaining as much as possible of the variation present in the dataset. The same is accomplished by transforming the variables to a new set of variables, which are known as the principal components (PCs) and are orthogonal, ordered such that the retention of variation present in the original variables decreases by moving down in the order. A PCA, based on Pearson's correlation matrix, was used to investigate the relationships between the independent variables (trace metal concentrations) in the nine topsoil or dust samples. These statistical analyses were performed using R-Package.

## 2.3 RESULTS AND DISCUSSIONS

### 2.3.1 Taranto area

Previous reports in the literature identified environmental health risks in the Taranto industrial area, and in the Tamburi residential district [150, 152, 181]. While these reports focused on seawater and air quality [154, 156-158], or even health conditions among residents [150, 151], none attempted to determine the toxicological contributions of contaminated soil in this industrial area. A report from the Regional Environmental Authority (ARPA Puglia) included extensive data on soil pollution in Puglia region. This report considered soil pollution data from industrial and other sources, but did not include soil toxicity measures [192]. To the best of our knowledge, this is the first report on the spatial distribution of contaminants in soil and resultant toxicity in the Taranto industrial area and in a nearby residential district.

As shown in Table 6, sites 5 and 6 (aqueduct and cemetery) showed the highest levels of iron and of total (excluding iron) metals. Sites 1, 3, 7, and 9 (Statte, power plant, and Tamburi 1 and 3) also showed high levels of chromium and/or zinc. The total REE levels were detected at an intermediate concentration among metals [ $Cr \approx REEs > Pb$ ]. The levels of individual metals (from Fe to Sn, including REEs) at different sampling sites were evaluated by PCA. Other metals found at lower levels (i.e.,  $< 1 \text{ mg/kg}$ ; As, B, Sb, Co, and Cd) were excluded from further data analysis. As shown in Figure 6, the first component (PC1, horizontal axis) is negatively correlated with Fe, Mn, Zn, Cu, Cr, Ni, and Sn, while the second component (PC2, vertical axis) is positively correlated with REEs, Cu, and negatively with Pb and V. By overlapping these graphs (Fig. 6a, b), we can determine that sites 5 and 6 are characterized by excess levels of Cu, Sn, Mn, Cr, Zn, Fe, and Ni. The sites 2, 8, and 4 were not correlated with any of the metal signatures showing relatively low pollution levels.

| REEs | Y    | La       | Ce     | Pr     | Nd     | Sm    | Eu    | Gd    | Tb    | Dy    | Σ REEs  |        |
|------|------|----------|--------|--------|--------|-------|-------|-------|-------|-------|---------|--------|
|      | TA 1 | 0.698    | 1.565  | 2.689  | 0.157  | 0.615 | 0.121 | 0.036 | 0.128 | 0.000 | 0.096   | 6.104  |
|      | TA 2 | 0.351    | 0.668  | 1.219  | 0.073  | 0.293 | 0.065 | 0.000 | 0.070 | 0.000 | 0.053   | 2.791  |
|      | TA 3 | 0.703    | 1.536  | 3.026  | 0.164  | 0.653 | 0.129 | 0.035 | 0.137 | 0.000 | 0.101   | 6.484  |
|      | TA 4 | 0.789    | 2.624  | 5.098  | 0.276  | 1.053 | 0.196 | 0.044 | 0.208 | 0.026 | 0.132   | 10.446 |
|      | TA 5 | 0.498    | 1.318  | 2.637  | 0.138  | 0.545 | 0.104 | 0.032 | 0.110 | 0.000 | 0.074   | 5.456  |
|      | TA 6 | 0.564    | 1.511  | 3.169  | 0.150  | 0.604 | 0.108 | 0.031 | 0.123 | 0.000 | 0.084   | 6.344  |
|      | TA 7 | 0.437    | 1.958  | 3.634  | 0.136  | 0.512 | 0.082 | 0.024 | 0.101 | 0.000 | 0.065   | 6.949  |
|      | TA 8 | 0.478    | 1.206  | 2.258  | 0.129  | 0.507 | 0.101 | 0.026 | 0.107 | 0.000 | 0.076   | 4.887  |
|      | TA 9 | 0.309    | 0.895  | 1.818  | 0.093  | 0.355 | 0.068 | 0.000 | 0.076 | 0.000 | 0.052   | 3.664  |
| HMs  | Fe   | Mn       | Zn     | Cu     | Cr     | Pb    | Ni    | V     | Sn    | Co    | Cd      |        |
|      | TA 1 | 1158.853 | 52.873 | 35.846 | 5.493  | 6.382 | 4.139 | 2.036 | 1.212 | 1.168 | 0.28614 | 0.055  |
|      | TA 2 | 1448.670 | 32.531 | 17.146 | 2.567  | 1.939 | 2.407 | 1.640 | 1.991 | 0.147 | 0.18527 | 0.000  |
|      | TA 3 | 1931.247 | 46.468 | 48.007 | 11.179 | 2.789 | 4.389 | 2.483 | 1.540 | 2.045 | 0.31319 | 0.113  |
|      | TA 4 | 750.219  | 27.796 | 6.475  | 5.973  | 1.491 | 2.778 | 1.247 | 1.680 | 0.275 | 0.29197 | 0.029  |
|      | TA 5 | 4595.418 | 66.512 | 83.958 | 8.383  | 7.347 | 4.570 | 3.469 | 2.069 | 2.372 | 0.37331 | 0.106  |
|      | TA 6 | 5836.967 | 54.169 | 49.715 | 10.039 | 4.931 | 4.501 | 2.102 | 2.438 | 1.886 | 0.26349 | 0.090  |
|      | TA 7 | 5034.150 | 59.127 | 27.234 | 7.965  | 4.163 | 4.092 | 2.324 | 1.842 | 0.946 | 0.23078 | 0.061  |
|      | TA 8 | 2403.992 | 30.151 | 13.678 | 3.316  | 1.909 | 7.756 | 2.618 | 2.042 | 0.276 | 0.24188 | 0.043  |
|      | TA 9 | 2178.250 | 56.643 | 25.912 | 8.853  | 1.547 | 5.105 | 1.623 | 1.288 | 0.756 | 0.2904  | 0.057  |

Table 7 Data from ICP-MS analysis of elements (as mg/kg) occurring in the Taranto soil samples listed in their REE and HM concentrations. Other analyzed elements (As, B, Sb, and Ti) displayed concentrations < 1 mg/kg.

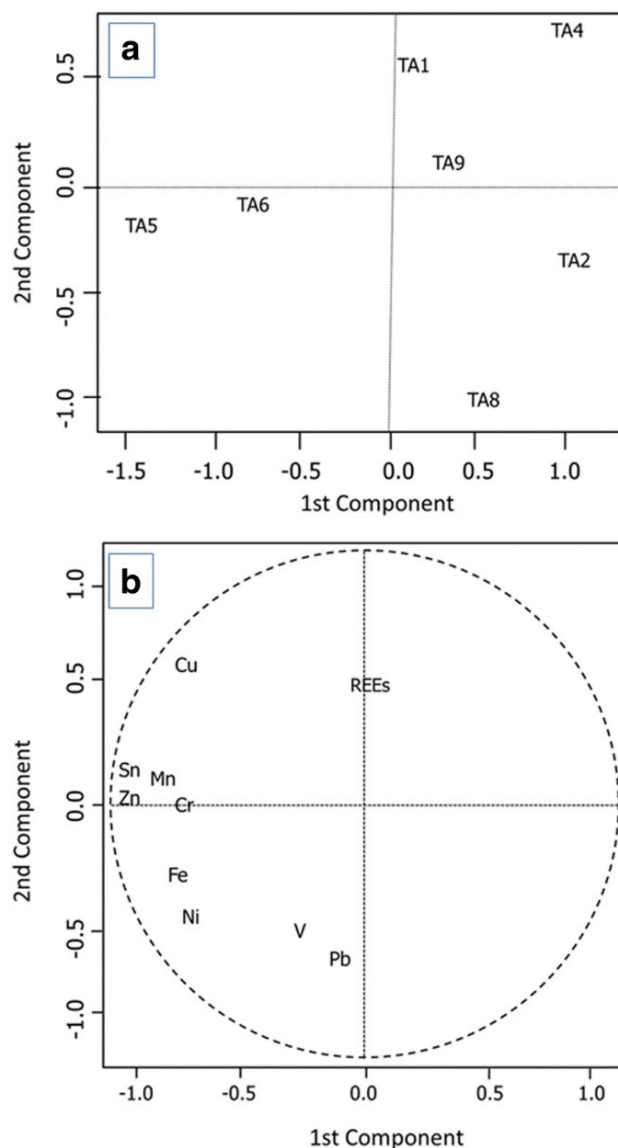


Figure 6 Principal component analysis (PCA) of metal levels identifying the most affected sites (5 and 6) (a), and the relative levels of individual metals (b).

The organic analysis was limited to determining total aliphatic hydrocarbons (C10–C40) and PAHs, although a range of other compound classes could be measured in future studies when searching for bioactive compounds in complex environmental mixtures.

Total hydrocarbons (C10–C40) showed the highest levels (2820 mg/kg dry weight, d.w.) at site 2 (Statte—Foundry Entrance), as shown in Figure 7, lower levels (1205 and 1019 mg/kg d.w.) at sites 3 and 6 (power plant and aqueduct) reaching almost background levels at the other sites (< 700 mg/kg). Unlike total hydrocarbons, PAH

levels showed the highest concentration (6.86 mg/kg) at site 4 (Paolo VI) and lower concentrations at sites 5 and 9 (cemetery and Tamburi 3) (5.44 and 6.31 mg/kg, respectively). Altogether, PAH levels were found to lie within an order of magnitude of each other ( $\leq 7$  mg/kg) and at these low levels (below national limits, Ministero dell'Ambiente 2006) would not be expected to generate significant adverse effects.

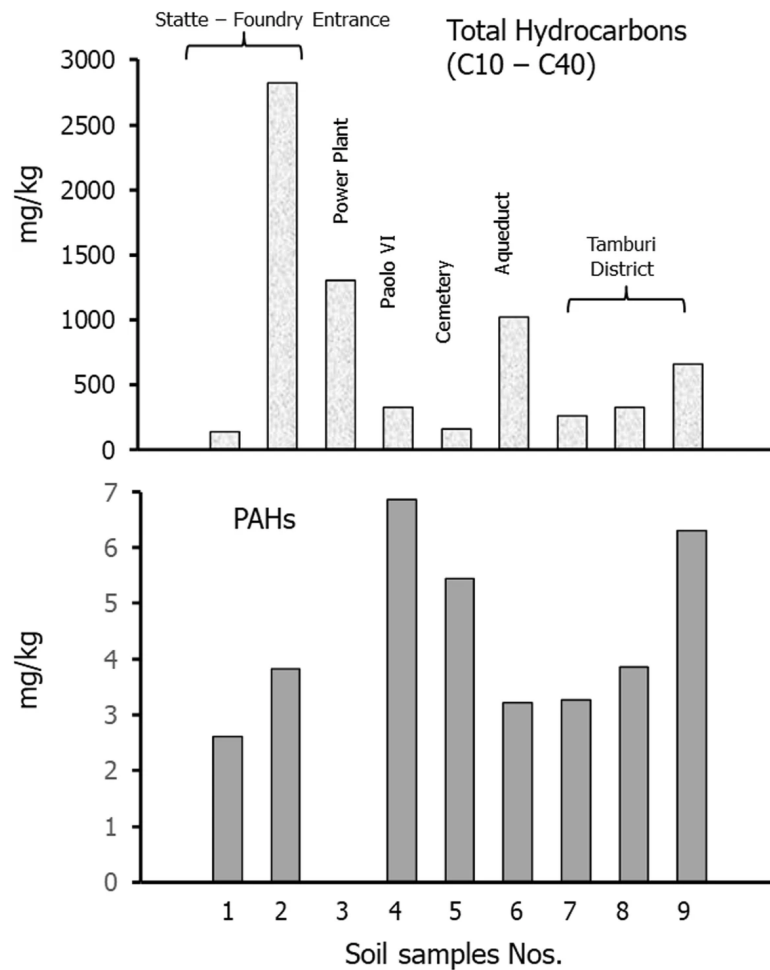


Figure 7 Measured levels of total hydrocarbons (C10-C40) and of PAHs in Taranto sampling sites

When nematodes were reared in hydrated soil samples (35–45% of dry wt.), mortality was evaluated after 24 h. All sites induced highly significant *C. elegans* mortality ( $p < 0.0001$ ), with sites 5 and 6 exerting the most severe toxicity. Mortality was observed, to a lesser extent, in soil samples from the other sites (Figure 8).

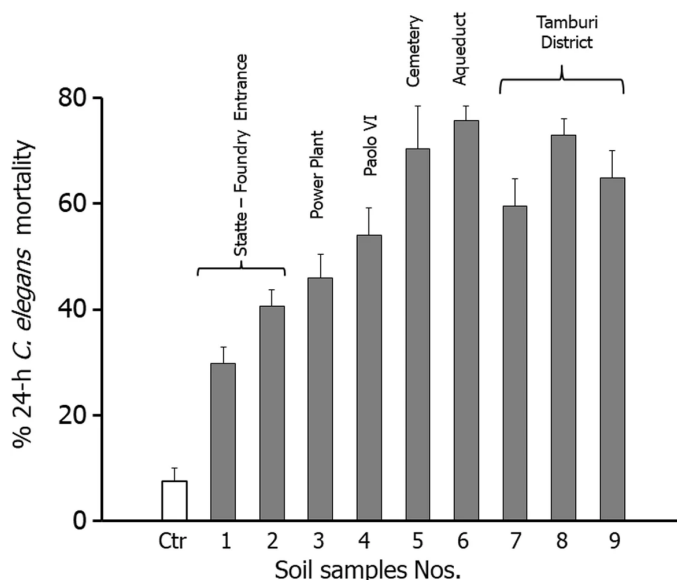


Figure 8 Twenty-four-hour mortality of *C. elegans* exposed to Taranto soil samples.

The overall results nematode bioassays concurred in identifying sites 5 and 6 (cemetery and aqueduct) as having the most toxic soil. Other sites such as the Tamburi neighbourhood and Paolo VI site were also toxic but to a lesser extent. Thus, one may recognize an unequivocal toxicity peak in soil samples from these sites. While sites 5 and 6 are in relatively isolated areas, of particular concern is the Tamburi neighbourhood with its approx. eighteen thousand inhabitants exposed to potentially toxic soil and street dust. Our findings add to existing reports on the importance of implementing mitigation measures in the Tamburi neighbourhood to limit human exposure to street dust and contaminated soils which could lead to impaired population health.

### 2.3.2 Gardanne area

Following acid oxidative digestion, metal concentrations were measured in soil samples. Iron and aluminium displayed the highest concentrations (> 1000 mg/kg) in samples from sites 1, 8, 9 and 13 (Table 7). Lower concentrations were found for Mn with a range of 18–34 mg/kg noted among the sites. The sum of REEs concentrations were found evenly distributed across sampling site and showed the fourth highest concentration at all the sites, with the highest concentrations of 20–

25 mg/kg noted at sites 1, 8 and 9 [REEs > Cr > Pb]. The other measured elements (Zn, Pb, V, Cr, Ni, Cu and B) showed far lower concentrations (1–6 mg/kg), except for Pb and Zn at site 5 (14 and 29 mg/kg). The lowest measured concentrations were found under limit of detection for Sn, As, and Sb (< 1 mg/kg).

As shown in Figure 9, the first component (PC1, horizontal axis) is positively correlated with REEs, Mn, Al, Fe, Cu and Cr while the second component (PC2, vertical axis) is negatively correlated with Ni and V. By overlapping these graphs (Fig. 9a, b), we can determine that sites 8 and 9 are characterized by excess levels of REEs, Mn and Fe. The site 3 was not correlated with any of the metal signatures showing relatively low pollution levels.

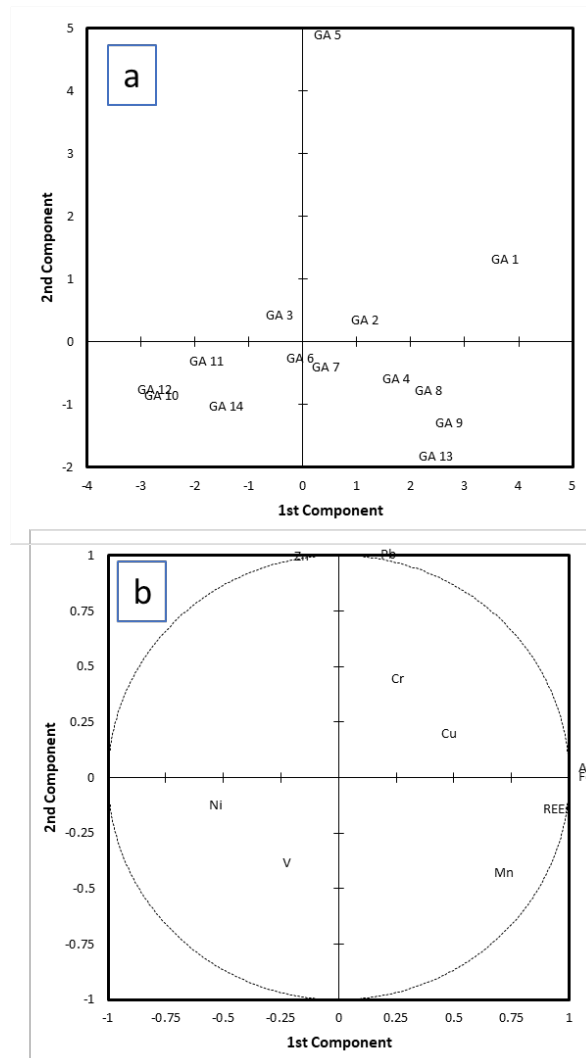


Figure 9 Principal component analysis (PCA) of metal levels identifying the most affected sites (8, 9 and 13) (a), and the relative levels of individual metals (b).

| REEs | Y     | La     | Ce   | Pr   | Nd  | Sm  | Eu   | Gd    | Tb  | Dy    | Σ REEs |       |
|------|-------|--------|------|------|-----|-----|------|-------|-----|-------|--------|-------|
|      | GA 1  | 1.1    | 5.4  | 9.6  | 0.6 | 2.1 | 0.4  | 0.1   | 0.4 | < 0.1 | 0.2    | 19.9  |
|      | GA 2  | 0.7    | 2.5  | 4.7  | 0.3 | 1.0 | 0.2  | < 0.1 | 0.2 | < 0.1 | 0.1    | 9.7   |
|      | GA 3  | 0.6    | 1.8  | 3.1  | 0.2 | 0.7 | 0.1  | < 0.1 | 0.2 | < 0.1 | 0.1    | 6.7   |
|      | GA 4  | 0.6    | 3.1  | 5.9  | 0.3 | 1.3 | 0.2  | < 0.1 | 0.2 | < 0.1 | 0.1    | 11.8  |
|      | GA 5  | 0.8    | 2.7  | 4.8  | 0.3 | 1.1 | 0.2  | < 0.1 | 0.2 | < 0.1 | 0.1    | 10.2  |
|      | GA 6  | 0.9    | 2.6  | 4.3  | 0.3 | 1.0 | 0.2  | < 0.1 | 0.2 | < 0.1 | 0.1    | 9.5   |
|      | GA 7  | 1.0    | 3.1  | 5.8  | 0.3 | 1.3 | 0.3  | 0.1   | 0.3 | < 0.1 | 0.2    | 12.3  |
|      | GA 8  | 1.0    | 5.2  | 9.6  | 0.6 | 2.2 | 0.4  | 0.1   | 0.4 | < 0.1 | 0.2    | 19.7  |
|      | GA 9  | 1.5    | 6.4  | 12.4 | 0.7 | 2.8 | 0.5  | 0.1   | 0.5 | < 0.1 | 0.3    | 25.3  |
|      | GA 10 | 0.7    | 2.1  | 4.1  | 0.2 | 0.9 | 0.2  | < 0.1 | 0.2 | < 0.1 | 0.1    | 8.5   |
|      | GA 11 | 0.3    | 1.0  | 1.9  | 0.1 | 0.4 | 0.1  | < 0.1 | 0.1 | < 0.1 | 0.1    | 4.1   |
|      | GA 12 | 0.2    | 1.3  | 2.5  | 0.1 | 0.4 | 0.1  | < 0.1 | 0.1 | < 0.1 | 0.0    | 4.7   |
|      | GA 13 | 1.0    | 3.8  | 7.6  | 0.4 | 1.5 | 0.3  | 0.1   | 0.3 | < 0.1 | 0.2    | 15.2  |
|      | GA 14 | 0.8    | 2.5  | 4.7  | 0.3 | 1.1 | 0.2  | 0.1   | 0.2 | < 0.1 | 0.1    | 10.0  |
| HMs  | Fe    | Mn     | Zn   | Cu   | Cr  | Pb  | Ni   | V     | Sn  | Al    | As     |       |
|      | GA 1  | 1154.4 | 25.5 | 6    | 3   | 5.8 | 5.8  | 2     | 3.7 | < 0.1 | 1209.6 | < 0.1 |
|      | GA 2  | 816.4  | 31.5 | 6.9  | 2   | 1.8 | 5.3  | 1.3   | 3.8 | < 0.1 | 821.5  | < 0.1 |
|      | GA 3  | 833.5  | 23.2 | 1    | 0.8 | 2.1 | 5.2  | 1     | 2.1 | < 0.1 | 859.4  | < 0.1 |
|      | GA 4  | 876.1  | 28.6 | 1.5  | 3.3 | 2.4 | 1.4  | 2.4   | 1.9 | < 0.1 | 916.1  | < 0.1 |
|      | GA 5  | 777.8  | 18.9 | 29   | 1.8 | 3.1 | 14.2 | 2.2   | 2.3 | < 0.1 | 835.4  | < 0.1 |
|      | GA 6  | 761.3  | 18.6 | 1    | 1   | 6.5 | 1    | 2.9   | 4.5 | < 0.1 | 811.1  | < 0.1 |
|      | GA 7  | 776.6  | 18.4 | 1.3  | 2.5 | 1   | 1    | 2.1   | 1.8 | < 0.1 | 776    | < 0.1 |
|      | GA 8  | 1008.8 | 28.4 | 1.3  | 1.5 | 1   | 4.6  | 2.4   | 2.7 | < 0.1 | 1019.9 | < 0.1 |
|      | GA 9  | 1040.9 | 25.7 | 0.5  | 0.7 | 1.2 | 1.1  | 2.6   | 0.9 | < 0.1 | 1130.7 | < 0.1 |
|      | GA 10 | 466.9  | 20   | 6.7  | 1.2 | 1.5 | 1    | 6     | 5.1 | < 0.1 | 468.6  | < 0.1 |
|      | GA 11 | 456    | 20.3 | 4.8  | 0.9 | 1.3 | 1.6  | 2.8   | 1.9 | < 0.1 | 594    | < 0.1 |
|      | GA 12 | 459.5  | 23.7 | 5.6  | 1.7 | 1.2 | 1    | 1.5   | 5.3 | < 0.1 | 506.4  | < 0.1 |
|      | GA 13 | 1038.9 | 34.4 | 1    | 1.5 | 1.9 | 1.3  | 2     | 6.3 | < 0.1 | 1085.9 | < 0.1 |
|      | GA 14 | 664.7  | 24.4 | 2.4  | 1.5 | 1.5 | 1.2  | 1.9   | 4.4 | < 0.1 | 667.4  | < 0.1 |

Table 8 Data from ICP-MS analysis of elements (as mg/kg) occurring in the Taranto soil samples listed in their REE and HM concentrations.

The sum of PAH concentrations showed highest values at sites 2 and 7 (10–15 mg/kg) (Figure 10a), without displaying excess PAH concentrations either close to the BPP or the PP. Unlike PAHs, total hydrocarbons (C10–C40) showed significantly excess concentrations in the area nearby the entrance of the BPP (sites 10 and 12), as shown in Figure 10b.

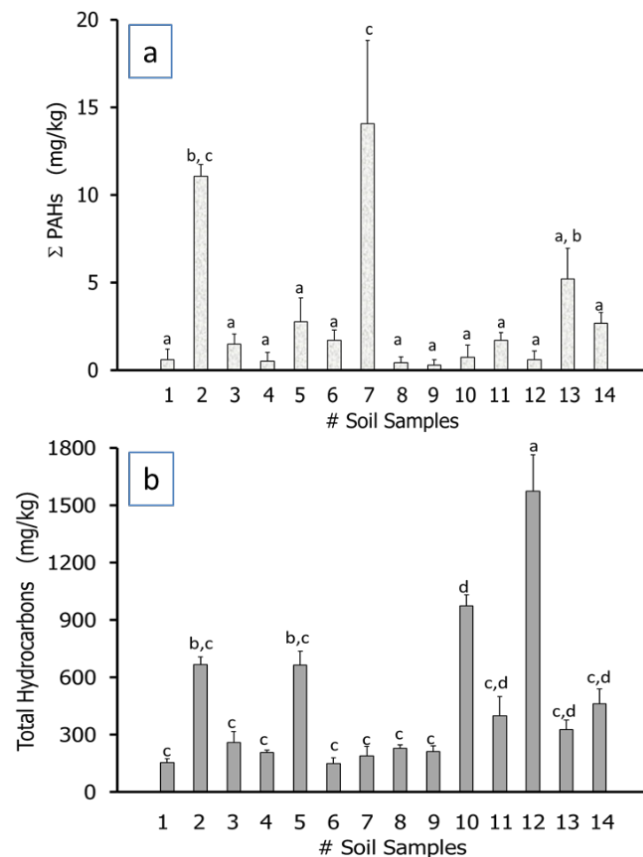


Figure 10 Concentrations of PAH sums in soil samples following organic extraction. Triplicate determinations; data ( $\mu\text{g/l}$ ) are expressed as means  $\pm$  SEM (a); concentrations of total hydrocarbons (C10–C40) in soil samples following organic extraction (b). LOD and LOQ were 1.7 and 5.1 mg/kg. Data with different letters (a–c) are significantly different ( $p < 0.05$ ).

The concentrations of a range of metals (Al, Fe, B, V, Zn and As) and analyses of total hydrocarbons (C10 to C40) indicated similar patterns in the Gardanne area close to the BPP (sites 9–12) and surrounding the PP sites 2–5. These findings were consistent with the literature where PP emissions are associated with multiple organic-based types of pollution [173-176], though the impact of the metal component in fly ash of waste-to-energy plants has also been investigated [172]. The established roles of polychlorinated biphenyls, polychlorinated dibenzo-p-

dioxins and polychlorinated dibenzofurans in PP-polluted soils [174] was not investigated in the present study although it may be speculated that the Gardanne PP emissions might also be a source of such pollutants thereby warranting ad hoc investigations. With respect to the finding of decreasing soil metal content with distance from point sources of pollutants, an exception was noted for site 1, which was located far from the BPP and PP, with high Al, Fe and B concentrations measured. This anomaly may be related to atmospheric deposition of BPP-derived dust based on prevailing weather patterns. Thus a further question arises on what the possible impacts of such deposition on surrounding agricultural land may be, taking into consideration the soils' natural composition. Another unexpected observation was found in the soil concentrations of total hydrocarbons that displayed two peaks, close to the PP (sites 2 and 5) and close to the BPP (sites 10 and 12). It should be noted that sites 10 and 12 are located near to the entrance to the BPP and are affected by intensive truck traffic involved in bauxite transportation, hence the likely source of high concentrations of aliphatic hydrocarbons, and as reported previously in heavy traffic areas [193].

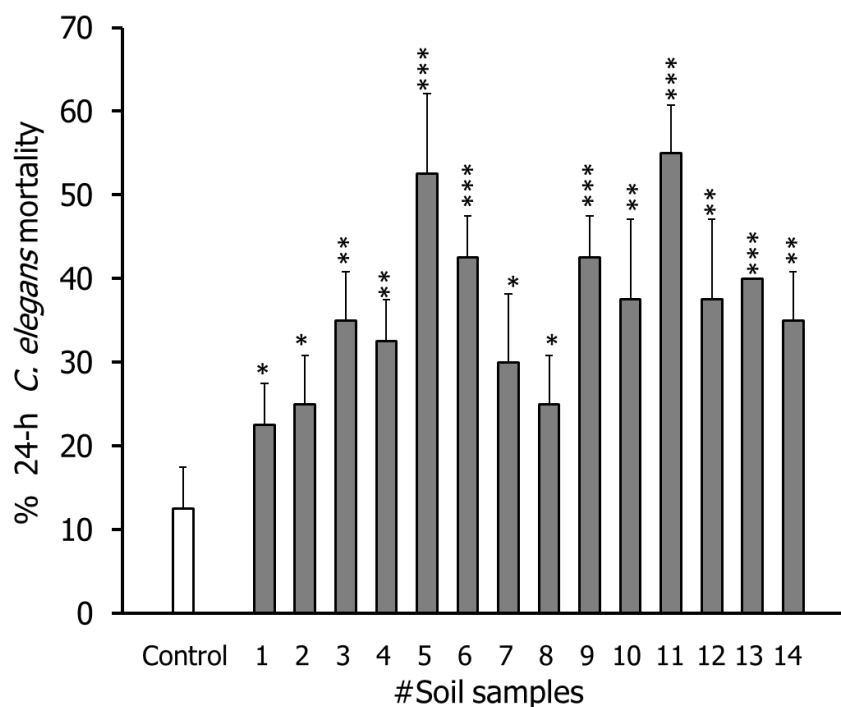


Figure 11 24-h % Mortality of *Caenorhabditis elegans* exposed to  $\cong 40\%$  (dry wt/ vol) of soil samples.

By exposing *C. elegans* to soil samples ( $\cong$  30% wt/vol), a significantly increased 24-h mortality was observed for all soil samples, though the highest mortality frequencies were detected following exposures to soil samples from sites 5 and 11 (Figure 11).

The already high concentrations of pollutants have generally led to significant soil toxicity in *C. elegans* ( $p < 0.05$ – $0.01$ ), with even greater significance for the 24-h mortality endpoint for sites 5 and 11 ( $p < 0.001$ ). Altogether, the nematode bioassay data corroborated the analytical evidence for increased pollution in two distinct areas, close to the BPP and to the PP.

### 2.3.3 Augusta-Priolo areas

Total metal concentrations failed to show any major differences among the soil sampling sites, except for lower concentrations found at sites 5 and 9 in Augusta (Table 8). Unlike total metal concentrations, REEs were found to show major differences in topographic distribution, with the highest concentrations found at sites 4, 7 and 8 in Augusta, and at sites 11, 14 and 15 in Priolo, where REE concentrations in the range of approximately 20-40 mg/kg were noted. These values were 2- to 5- fold higher than the highest REE levels found at industrial facilities in Gardanne and in Taranto [144, 145], where maximum REE levels were measured at 25 and 10 mg/kg, respectively. Lower, yet relevant REE levels were found at other Augusta sites (14 to 16 mg/kg; sites 3, 5, 6 and 10). The lowest REE levels were found at sites 1 and 9 in Augusta (an old city gate and a public garden), and at sites 12 and 13 in Priolo. The results of the PCA revealed that together, the first four components explain 67.3% of the variance. In Figure 12a, the contaminant groups (metals and REEs) cluster together. Most of the variance in this plot appears to be driven by a few sites, notable site 3, associated with HMs, and sites 6,8 and 13, associated with REEs.

| REEs | Y  | La     | Ce    | Pr     | Nd    | Sm    | Eu     | Gd     | Tb    | Dy     | Σ REEs |        |
|------|----|--------|-------|--------|-------|-------|--------|--------|-------|--------|--------|--------|
|      | 1  | 11.5   | 18.1  | 32.2   | 4.4   | 13.0  | 2.8    | 1.1    | 8.6   | 0.8    | 1.7    | 94.0   |
|      | 2  | 6.6    | 18.2  | 33.7   | 4.6   | 12.7  | 2.5    | 1.0    | 8.6   | 0.7    | 1.2    | 89.7   |
|      | 3  | 11.9   | 46.3  | 82.3   | 10.6  | 28.5  | 6.2    | 2.8    | 20.4  | 1.5    | 2.2    | 212.8  |
|      | 4  | 14.6   | 81.9  | 129.6  | 16.4  | 48.8  | 8.2    | 3.2    | 36.2  | 2.6    | 3.5    | 345.0  |
|      | 5  | 9.9    | 22.5  | 39.8   | 5.2   | 16.0  | 3.1    | 1.2    | 11.5  | 1.0    | 1.7    | 111.8  |
|      | 6  | 13.9   | 29.1  | 55.5   | 7.9   | 22.6  | 4.2    | 1.5    | 16.2  | 1.4    | 2.4    | 154.6  |
|      | 7  | 8.7    | 22.7  | 40.3   | 4.8   | 14.8  | 3.0    | 1.0    | 11.2  | 1.0    | 1.6    | 109.1  |
|      | 8  | 20.6   | 41.5  | 86.9   | 10.8  | 32.3  | 5.7    | 2.0    | 24.0  | 2.0    | 3.5    | 229.4  |
|      | 9  | 3.3    | 7.0   | 11.9   | 1.6   | 5.0   | 1.6    | 0.7    | 3.8   | 0.4    | 0.6    | 35.9   |
|      | 10 | 11.5   | 18.1  | 32.2   | 4.4   | 13.0  | 2.8    | 1.1    | 8.6   | 0.8    | 1.7    | 78.0   |
|      | 11 | 13.7   | 36.6  | 65.6   | 8.4   | 24.7  | 4.6    | 1.8    | 16.7  | 1.5    | 2.6    | 176.2  |
|      | 12 | 11.0   | 21.2  | 33.7   | 4.6   | 13.5  | 2.7    | 1.0    | 9.4   | 0.8    | 1.6    | 99.5   |
|      | 13 | 15.9   | 48.0  | 62.3   | 8.7   | 25.2  | 4.7    | 1.6    | 19.0  | 1.5    | 2.6    | 189.5  |
|      | 14 | 13.4   | 51.4  | 97.8   | 12.5  | 35.9  | 6.1    | 2.3    | 27.9  | 2.1    | 2.5    | 251.8  |
|      | 15 | 3.0    | 8.2   | 9.7    | 1.4   | 4.1   | 1.0    | 0.4    | 3.5   | 0.3    | 0.5    | 32.1   |
| HMs  | V  | Cr     | Mn    | Co     | Ni    | Cu    | Zn     | As     | Sr    | Cd     | Pb     |        |
|      | 1  | 86.11  | 38.29 | 248.50 | 4.92  | 22.72 | 40.39  | 126.32 | 23.18 | 551.39 | 0.52   | 26.43  |
|      | 2  | 100.48 | 27.96 | 252.29 | 5.67  | 18.46 | 49.73  | 178.13 | 16.55 | 235.95 | 0.63   | 40.24  |
|      | 3  | 119.31 | 45.67 | 249.35 | 7.22  | 32.58 | 73.20  | 195.43 | 8.71  | 194.20 | 0.68   | 82.15  |
|      | 4  | 169.21 | 84.29 | 702.37 | 31.41 | 97.31 | 123.21 | 558.98 | 10.99 | 759.75 | 1.34   | 47.33  |
|      | 5  | 90.86  | 20.56 | 303.64 | 5.64  | 17.21 | 32.88  | 108.84 | 13.40 | 164.94 | 0.35   | 11.24  |
|      | 6  | 128.47 | 42.12 | 365.38 | 9.94  | 35.63 | 30.67  | 77.94  | 27.10 | 242.03 | 0.48   | 15.49  |
|      | 7  | 103.88 | 27.36 | 333.89 | 7.59  | 30.14 | 51.05  | 146.19 | 18.77 | 323.68 | 0.67   | 326.34 |
|      | 8  | 131.37 | 40.79 | 510.78 | 12.07 | 24.40 | 38.03  | 66.46  | 23.20 | 273.73 | 0.42   | 18.86  |
|      | 9  | 68.77  | 9.73  | 69.54  | 1.75  | 10.29 | 65.49  | 183.57 | 4.92  | 96.92  | 0.30   | 12.36  |
|      | 10 | 82.17  | 11.07 | 249.29 | 4.24  | 19.53 | 15.60  | 43.59  | 21.67 | 521.26 | 0.31   | 32.75  |
|      | 11 | 137.14 | 69.89 | 642.11 | 18.86 | 70.63 | 47.68  | 114.41 | 15.47 | 192.77 | 1.03   | 26.88  |
|      | 12 | 98.23  | 23.20 | 263.59 | 7.70  | 32.55 | 39.45  | 247.45 | 16.47 | 229.84 | 1.09   | 90.83  |
|      | 13 | 120.31 | 37.51 | 540.58 | 11.16 | 42.55 | 46.06  | 259.46 | 17.29 | 189.27 | 0.74   | 60.27  |
|      | 14 | 140.39 | 51.34 | 572.12 | 16.07 | 72.36 | 39.47  | 83.06  | 16.74 | 667.91 | 0.83   | 70.01  |
|      | 15 | 92.08  | 16.92 | 133.27 | 3.13  | 23.90 | 206.11 | 263.51 | 7.89  | 145.14 | 0.64   | 20.74  |

Table 9 Data from ICP-MS analysis of elements (as mg/kg) occurring in the Augusta- Priolo soil samples listed in their REE and HM concentrations.

The higher levels found in this study compared to the other industrial facilities are consistent with their use both in oil refining (La) and in the preparation of catalytic additives (Ce) to diesel oil [194-196]. Whether such elevated levels of REEs should be a cause for concern is not yet clear, especially since REEs are finding increasing use in agriculture and animal feeds as growth stimulants [42]. Given the needed use of REEs in oil refining and in the production of diesel catalytic additives, further investigations may be warranted on occupational exposures to oil products and exhaust microparticulate matter in this region [8].

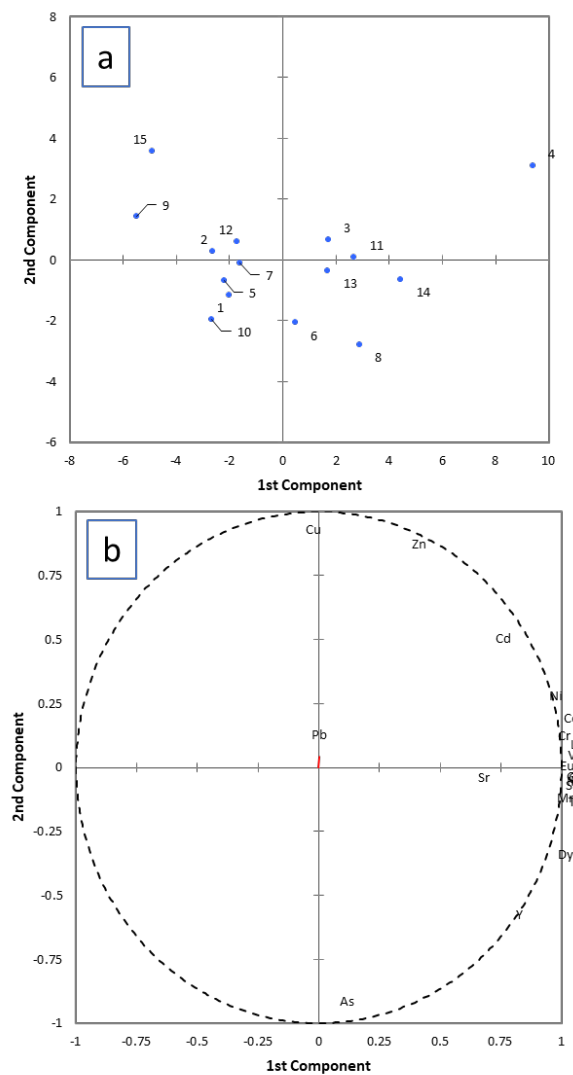


Figure 12 Principal component analysis (PCA) of metal levels identifying the most affected sites of Augusta-Priolo(a), and the relative levels of individual metals (b).

Total PAHs and C10-C40 hydrocarbons were found at different concentrations according to the sampling sites, as shown in Figure 13. PAHs displayed the highest concentrations at sites 8 and 12, while lesser though still significant concentrations were found at sites 1-2 and 4-6 at Augusta, and site 11-13 at Priolo. PAHs were not found to represent a significant environmental load at sites 14-15. Total C10-C40 hydrocarbons were present at the highest concentrations at sites 3 and 13, with lesser concentrations noted at the other sites.

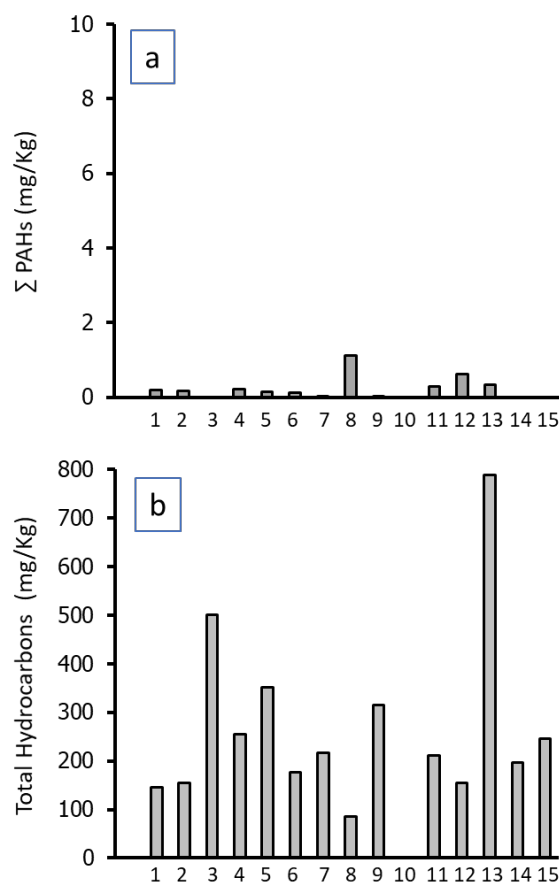


Figure 13 Concentrations of PAH sums in soil samples following organic extraction (a); concentrations of total hydrocarbons (C10–C40) in soil samples following organic extraction (b); data ( $\mu\text{g/Kg}$ ).

Topsoil-exposed *C. elegans* displayed different mortality rates. The only site displaying highly significant mortality was 8, while other sites displayed lesser, yet significant *C. elegans* mortality, namely 1,3,4, 6, 10 and 11. No significant effects were found for topsoil from the other six sites (2, 5, 7, 9, 12,13,14 and 15).

The site 8, one of the most polluted sites, displayed the highest adverse effects, unlike relatively unpolluted sites, such as 10-15, located in town suburbs or at an archaeological site. This relevant analytical finding of elevated hydrocarbon and metal concentrations is consistent with the elevated hydrocarbon and metal concentrations found and with the proximity of specific sites to oil processing facilities.

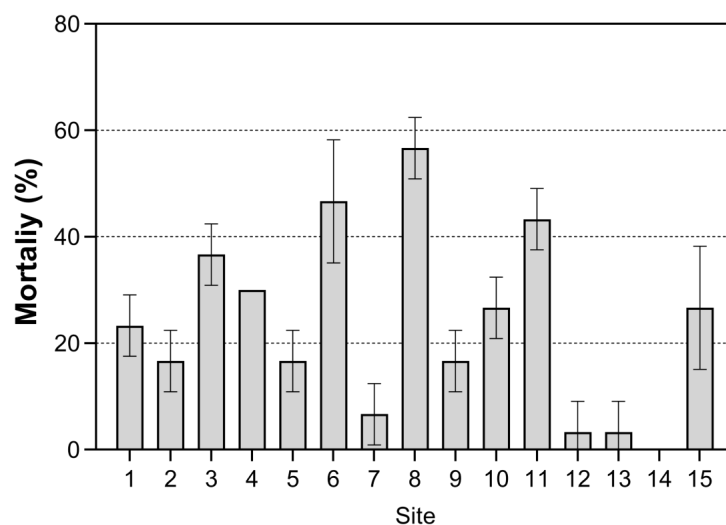


Figure 14 24-h % Mortality of *C. elegans* exposed to  $\cong 40\%$  (dry wt/vol) of Augusta- Priolo soil samples.

## 2.4 CONCLUSIONS

This study provided a multi-parameter map of topsoil pollution and toxicity close to the petrochemical industries located near Taranto (Italy), Gardanne (France) and Augusta and Priolo (Italy). It was demonstrated that some of the more prominent and heavily polluted sampling sites were identified with associated biological effects on *C. elegans*. In turn, this finding agrees with the occupational REE exposure in workers exposed to diesel exhaust microparticulate matter. Whether, and if so to what extent, the analytical and bioassay data may raise some concern in terms of environmental and human health, is a sensitive question warranting further investigations and remediation efforts.

# CHAPTER 3

---

In this chapter, the results based on original contributions published in [197].

## **3.1 SEDIMENT POLLUTION AND TOXICITY IN A FORMERLY INDUSTRIALIZED BAY IN CENTRAL MEDITERRANEAN (POZZUOLI, ITALY)**

Numerous investigations reported studies about the role of REEs as natural tracers of biogeochemical processes [198] and of water mass circulation in the marine environment [199-202]. Due to the coherent correlations between REE concentrations and contents of clay and metals (i.e. Fe, Mn, Al) are widely used as tracers of sources and processes controlling trace element distribution in marine sediments [107, 203]. The REE distribution in sediments is largely controlled by scavenging processes, in particular by Fe–Mn–oxides [204], by sedimentary provenance, by redox conditions of the overlying water column [205], and by potential anthropogenic inputs [206].

However, mechanisms for REE mobilization in different sediments and the potential risks of long-term exposure to REE-abundant environment are not adequately understood.

Integrating data on sediment chemical load with data on the adverse effects to benthic organisms may provide tools for a comprehensive assessment of sediment pollution and toxicity, and may allow us to identify the bioactive compound(s) in the environmental mixture that might be driving toxicological response [207].

This study was aimed at evaluating sediment pollution and toxicity in the Bay of Pozzuoli (BoP) (Tyrrhenian Sea, southern Italy), characterized by high anthropic pressure and by previous industrial facilities. Analyses were carried out to evaluate the content of REEs, HMs, C10 - C40 and PAHs in sediment samples collected along five transects from the coast. Sediment samples were tested for toxicity as whole sediment (WS) suspensions to sea urchins (*Arbacia lixula*), or as elutriate (EL) in diatoms (*Phaeodactylum tricornutum*).

### 3.1.1. Pozzuoli case study

The BoP (southern Italy, 40°49'23"N 14°07'20"E) has been subject to industrial processes and emissions for several decades, including a steel foundry, an asbestos/cement plant, a cable factory, and two harbours. Several studies were conducted focusing on the state of environmental pollution in the coastal zones facing the former industrial site of Bagnoli. High levels of HMs, PAHs, and polychlorinated biphenyls (PCBs) were previously reported [208-211]. Some studies [208, 212] reported that natural volcanic activity also contributed to increased environmental pollutants. A recent study reported on excess HMs and PAHs levels in sediments from the BoP [213, 214], which exceeded the Italian environmental guidelines used to assess the potential toxicity of sediments for aquatic ecosystems [215, 216]. Outstanding levels of individual PAHs were found throughout the BoP, with mean values (MV) exceeding the Italian environmental guidelines from 127-fold (naphthalene) (MV = 4.42 µg/g) to 446-fold [benzo(a)pyrene] (MV = 8.48 µg/g) [214]. The report by Trifuoggi et al. [213] also highlighted that sediment concentrations of As, Cd, Cr, Cu, Hg, Ni, Pb, and Zn significantly exceeded the Italian environmental guidelines. Two main sources could be identified in the BoP, both the Bagnoli industrial area to the east, and the industrial and harbour areas to the west. A new sediment sampling campaign was carried out in the BoP, along five transects with a total of 14 sampling sites, as shown in Figure 15.

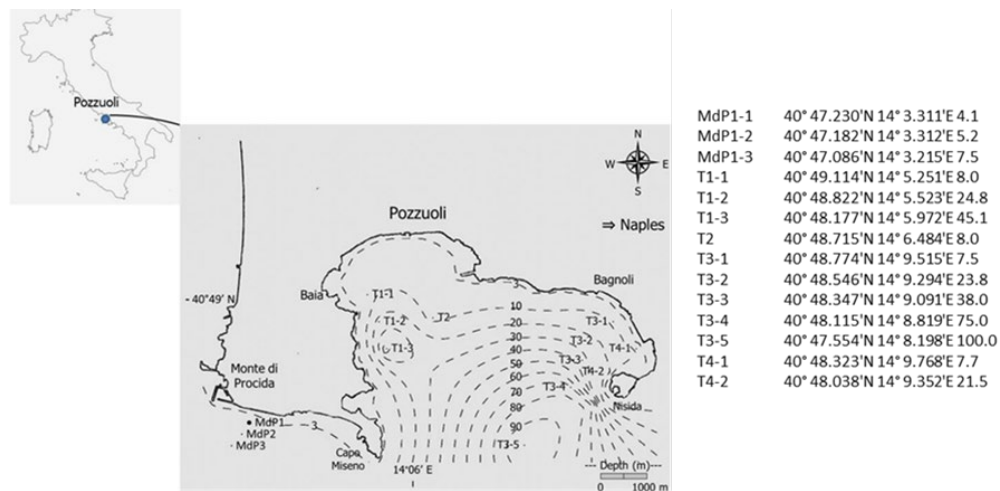


Figure 15 Sediment sampling sites along five transects in the present study: Monte di Procida (MdP) and four transects (T1-T4) in the Bay of Pozzuoli.

Sediment sampling was performed in 14 BoP sites, as shown in Figure 1, by a Van Veen grab along 5 transects, positioned on a coast-offshore alignment. Nine sampling sites (T1-1 to T1-3, T2, and T3-1 to T3-5) were selected in part due to their proximity to the locations studied by Trifuoggi et al. [213]. Further 6 sampling sites were chosen in the “hot area” facing the brownfield site of Bagnoli (T4-1 to T4-2), and outside of the BoP, nearby Monte di Procida (MdP1 to MdP3), expected to be relatively less polluted. Sea depth was measured by an echograph and varied between 4 and 20 m inshore and up to a 100-m depth offshore (Figure 15), and determined by DGPS (Differential Global Positioning System).

## **3.2 METHODS**

### **3.2.1 Sediment sampling and handling**

Sediment samples were collected in plastic bags (for heavy metal analyses) and aluminium foil (for PAH analyses), sent in an ice box to the laboratory, and then frozen at  $-20\text{ }^{\circ}\text{C}$  until bioassay evaluations. As for conducting chemical analyses, samples were stored at  $+4\text{ }^{\circ}\text{C}$  for 2d, thereafter dried at  $40\text{ }^{\circ}\text{C}$ , then ground and sieved (2 mm). Two days before running bioassays, frozen sediment samples were thawed by storing at  $+4\text{ }^{\circ}\text{C}$ . Dry weight was measured for each sample after drying 5-g sediment aliquots at  $60\text{ }^{\circ}\text{C}$  for 24 h. Dry weight content ranged from 57 to 84% (data not shown). Any bias from freezing-and-thawing material in bioassays was both justified by the need to reconcile the duration of sampling campaign with running bioassays, and by the homogeneous sample alterations due to freezing-and-thawing. The average heavy metal recovery was estimated 60 to 120%, 60 to 80% for PAHs, and 80 to 100% for total aliphatic hydrocarbons (C10-C40).

### **3.2.2 Metal analysis**

Sediment samples were sieved at a 2-mm mesh. All analyses were conducted on the sieved aliquots. Metal content was determined for 17 priority metals and 16 REEs. Sediment samples were subjected to the same procedure reported in section 2.2.2.

### 3.2.3 PAH and total hydrocarbon analysis

Sediment samples were analysed for their PAH content following the method reported in section 2.2.3, and the analysed homologs were: Acenaphthene; Acenaphthylene; Anthracene; Benzo(*a*)anthracene; Benzo(*b*)fluoranthene; Benzo(*k*)fluoranthene; Benzo(*g,h,i*)perylene; Benzo(*a*)pyrene; Chrysene; Dibenzo(*a,h*)anthracene; Fluorene; Fluoranthene; Indenopyrene; Naphthalene; Phenanthrene, and Pyrene. Total hydrocarbons (C10 – C40) in A/H extract, purified with florisil, were analysed by gas chromatography with Flame Ionization detector (FID) (Agilent 6890, USA).

### 3.2.4 Sea urchin bioassays

Sea urchins from the species *A. lixula* were collected from the Bay of Naples by the staff of the Stazione Zoologica Anton Dohrn (SZAD, Naples, Italy). Sea urchin embryo cultures were reared by exposure to WS [217]. Controls were conducted as untreated negative controls in natural filtered seawater (FSW) from SZAD Aquarium, 3.5% salinity, pH 8. This FSW source was obtained by aspiration of sea water by a collection system 1 km offshore, followed by settling and filtering. This procedure ensured homogeneity of the SW tanks collected for the assays, which was filtered again before sediment testing. No standard sediment was utilized as an additional control. In embryotoxicity tests, WS aliquots (0.1% dry wt eq/vol) were placed in culture plate wells [Falcon™ Tissue Culture Plates (6 wells, 10 ml/well, code # 353046)], and then suspended in 9 ml FSW. 1-ml zygote aliquots (10 min post-fertilization, p-f) were added to sediment suspensions and incubated at 18 °C in the dark for 72 h. Sperm bioassays were performed on *A. lixula* sperm suspensions: a 100-µl sperm pellet was suspended in 10 ml of stirred WS samples (0.5 % wt eq/vol) for 1 h. Triplicate 100-µl aliquots of sperm supernatant inseminated 6-replicate, 10-ml egg suspensions. Thus, the ensuing offspring embryos developed without contact with WS particulate matter. Sperm fertilization success (fertilization rate, FR = % fertilized eggs) was measured by scoring the percent of fertilized eggs in live cleaving embryos (1 to 3 h p-f). Thereafter, 72 h p-f, the offspring of exposed sperm were scored for developmental defects. Each

bioassay was run in six replicates. The observations of larvae were performed on the first 50 plutei scored in each of six replicate cultures 72 h pf, and immobilized by 10<sup>-4</sup> M chromium sulphate 5 min prior to observation. The following outcomes in embryogenesis abnormalities were scored as: i. pathologic (P1), malformed plutei, and ii. pathologic embryos (P2), arrested at blastula/gastrula stages and unable to differentiate up to the pluteus stage. The total percentages of P1 + P2 were scored blind by trained readers, each one evaluating a complete set of cultures.

### **3.2.5 Algal bioassays**

Sediment samples were subjected to elutriation, carried out by mixing sediment to sea water in a solid to liquid ratio of 1:4; shaking for 24 h, and filtering the EL in a 0.45 µm membrane filter. All samples were stored at 4 °C until use. An ISO protocol 10253 [218] was used to measure the algal growth inhibition with *P. tricornerutum*. The starting *P. tricornerutum* inoculum was obtained from MicroBioTests Inc. (Gent, Belgium) (PT190608) and subcultured in the laboratory. The cultures were carried out according to the ISO standard protocol (ISO 10253). Artificial seawater (ASW) of the algal test was used as control; ASW was prepared according to the ISO standard protocol (ISO 10253). For the control and for each sample, 3 replicates were inoculated with 10<sup>6</sup> algal cells l<sup>-1</sup> in well plates and incubated for 72 h at 23 ± 2 °C under continuous illumination. The specific growth rate (µ) of *P. tricornerutum* in each replicate was calculated from the logarithmic increase in cell density in the interval 0–72 h. Results were expressed as the mean (± SEM) of the percentage inhibition of cell growth vs. negative controls.

### **3.2.6 Statistical Analysis**

Results of bioassays are given as mean ± standard error. Statistical analyses were completed in SPSS Statistics 20. Levene's test was applied to check the homogeneity of variance. Differences between the samples and the control group were determined by two-tailed Student's t-test. A normality test was performed and the significance of the difference among the groups was evaluated by One-way of Analysis of Variance (ANOVA). Mean comparison of the samples with Tukey's difference post-hoc test was performed and shown in the figures. Chi-Square and

Mann-Whitney U Test was applied where ANOVA assumptions were not fulfilled. Correlations between the measured concentrations of total PAH, total heavy metals, Al(III) and Fe(III) of each station and the results of each biotest were analysed by Pearson Correlation Test. Differences were considered significant when  $p < 0.05$ .

### 3.3 RESULTS AND DISCUSSIONS

Table 9 reported the detected metal levels except for Al(III) and Fe(III) whose level showed first the highest levels, ranging from 7,000 to 35,000 mg/kg dry weight (Figure 16). The levels of the other metals showed consistent differences among sampling transects, which were observed by either considering all metals except for Al(III) and Fe(III), or for Al(III) alone, or for Fe(III) alone, as shown in Figure 16. A consistent finding was the excess metal levels in the intermediate T3 sampling sites (T3-3 and T3-4), and in the T4-2 sampling site.

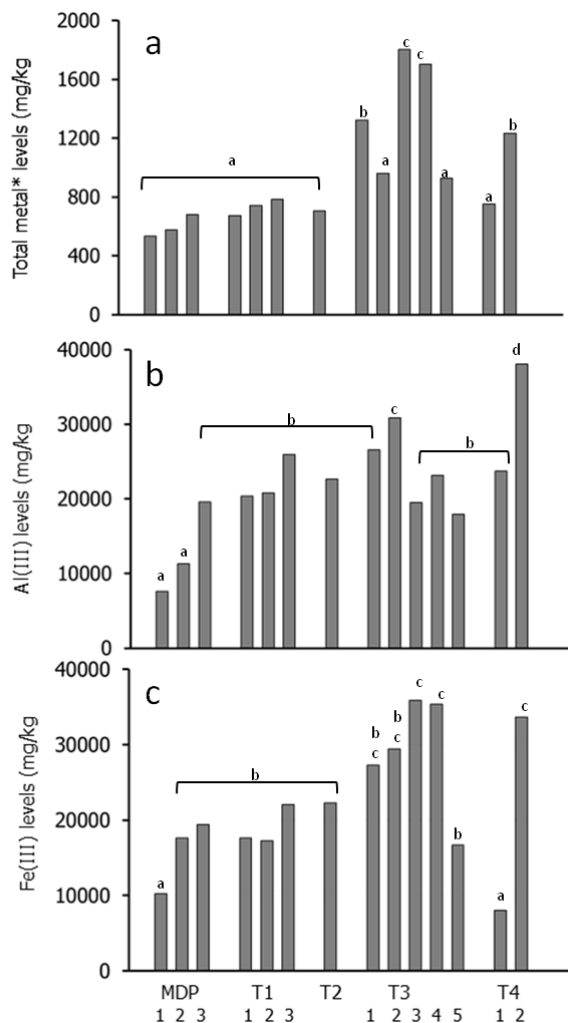


Figure 16 Metal levels in sediment samples showed highest levels in T3 and T4 as consistently observed in total metal levels (a) [excepted Al(III) and Fe(III)] and in Fe(III) (b) and Al(III) (c) levels. Data with different letters (a–n) are significantly different (Tukey's,  $p < 0.05$ ).

| Sample #    | Be  | B    | V    | Cr   | Mn    | Co  | Ni   | Cu   | Zn    | As   | Sn    | Ba    | Ti   | Pb    | ∑ HMs   |
|-------------|-----|------|------|------|-------|-----|------|------|-------|------|-------|-------|------|-------|---------|
| <b>MdP1</b> | 0.4 | 1.5  | 16.8 | 4.4  | 457.1 | 3.6 | 7.1  | 1.3  | 19.4  | 8.5  | 0.24  | 5.3   | 0.11 | 6.0   | 531.7   |
| <b>MdP2</b> | 0.4 | 1.5  | 33.8 | 4.5  | 461.1 | 4.2 | 5.0  | 0.9  | 28.9  | 9.5  | 0.76  | 17.5  | 0.20 | 9.5   | 577.8   |
| <b>MdP3</b> | 0.8 | 13.3 | 29.9 | 13.2 | 476.5 | 5.1 | 9.6  | 2.0  | 44.8  | 13.8 | 1.33  | 52.4  | 0.19 | 17.0  | 679.8   |
| <b>T1-3</b> | 1.4 | 19.5 | 27.4 | 18.3 | 266.6 | 2.8 | 11.1 | 21.9 | 124.7 | 16.9 | 6.30  | 63.1  | 0.40 | 93.4  | 673.8   |
| <b>T1-4</b> | 1.5 | 15.1 | 27.5 | 19.6 | 285.0 | 3.4 | 7.6  | 23.8 | 134.7 | 15.3 | 7.70  | 83.9  | 0.51 | 115.7 | 741.2   |
| <b>T1-5</b> | 1.9 | 18.0 | 32.0 | 21.8 | 331.8 | 4.4 | 7.2  | 18.6 | 136.2 | 13.4 | 6.07  | 87.6  | 0.43 | 103.7 | 783.1   |
| <b>T2-3</b> | 1.6 | 18.6 | 36.5 | 10.3 | 361.3 | 3.9 | 4.5  | 6.0  | 87.7  | 22.6 | 4.83  | 77.1  | 0.19 | 69.6  | 704.8   |
| <b>T3-1</b> | 1.9 | 12.2 | 37.3 | 8.6  | 842.6 | 2.2 | 2.6  | 6.0  | 181.4 | 45.5 | 8.86  | 66.8  | 0.76 | 106.5 | 1,323.1 |
| <b>T3-2</b> | 2.4 | 30.2 | 40.3 | 8.3  | 479.2 | 2.8 | 2.7  | 5.3  | 179.7 | 47.5 | 7.76  | 57.0  | 0.41 | 97.5  | 961.1   |
| <b>T3-3</b> | 2.1 | 20.7 | 44.0 | 27.7 | 756.1 | 3.7 | 10.1 | 33.9 | 471.0 | 22.8 | 19.44 | 88.8  | 0.53 | 302.2 | 1,803.0 |
| <b>T3-4</b> | 1.7 | 21.3 | 40.4 | 29.9 | 535.8 | 4.4 | 9.9  | 45.4 | 523.4 | 22.0 | 16.37 | 102.4 | 0.52 | 349.2 | 1,702.9 |
| <b>T3-5</b> | 2.0 | 6.6  | 23.6 | 21.8 | 322.9 | 4.1 | 5.8  | 25.7 | 272.5 | 19.6 | 3.16  | 53.0  | 0.36 | 165.9 | 926.9   |
| <b>T4-1</b> | 0.7 | 10.4 | 20.9 | 2.0  | 541.3 | 1.9 | 1.8  | 3.1  | 44.4  | 14.1 | 2.22  | 85.4  | 0.19 | 22.7  | 751.2   |
| <b>T4-2</b> | 2.2 | 16.7 | 48.8 | 8.5  | 635.4 | 3.2 | 1.8  | 7.9  | 237.7 | 52.6 | 5.79  | 92.4  | 0.38 | 119.7 | 1,233.0 |

Table 10 Analyzed metal levels in BoP sediment samples. Data of elements with levels < 1 mg/kg (Se, Cd and Sb) are not reported.

Among the outcomes of REE analysis (Table 10), Sc levels were found highest and evenly distributed among sampling sites, approximately ranging from 40 to 130 mg/kg dry wt, and suggesting a geological, non-anthropogenic occurrence of Sc in the BoP.

Among the lanthanoids, La displayed highest levels in the MDP and T1 transects, and at sites T3- 2 and T3-4. Highest Ce levels were found at sites MDP-2, T1-3, T2, T3-3, T3-4 and T3-5. By summing lanthanoid levels, and the elements with levels < 1 mg/kg (heavy REEs), highest levels of light REE sum were observed at sites MDP-2, T1-3 and T2, while lower levels of REE sum were found in transects T3 and T4.

The occurrence of relevant REE levels in the BoP was suggested by the known REE release in fly ash [219], and by the previous activity of a coal-operating steel foundry in the Bagnoli area [220].

A relevant finding pointed to highest scandium levels throughout the sampling sites that might be of natural origin. Apart from Sc, the sum of light REE content failed to show any consistent distribution with metal levels in sampling sites (Tables 8 and 9), since highest REE levels were found in the presumed “clean” Mdp transect and not in the most polluted – and toxic – T3 and T4 transects.

It should be recalled, however, that the BoP is also characterized by its well-established volcanic activity, which has contributed to sediment pollution and toxicity [208].

The sediment samples showed dramatic differences in PAH levels among the sampling transect, by two orders of magnitude, from the Mdp transect (chosen as a relatively unpolluted site, out of BoP) to T3 transect, displaying PAH levels in the order of thousands up to hundred thousands g/kg dry weight, respectively, as shown in Table 11.

| #Sample | Sc   | Y     | La   | Ce   | Pr   | Nd   | Sm   | Gd   | Σ REEs | Σ REEs<br>(- Sc and Y) |
|---------|------|-------|------|------|------|------|------|------|--------|------------------------|
| MdP_1   | 73.9 | 7.16  | 12.8 | 42.4 | 3.79 | 15.0 | 2.98 | 2.93 | 161.0  | 79.9                   |
| MdP_2   | 92.8 | 6.15  | 26.2 | 76.3 | 6.31 | 29.5 | 5.17 | 4.79 | 247.2  | 148.2                  |
| MdP_3   | 102  | 3.65  | 15.5 | 48.4 | 3.41 | 14.2 | 2.45 | 2.53 | 192    | 86.4                   |
| T1-1    | 96.7 | 1.73  | 10.2 | 26.0 | 1.93 | 11.4 | 1.46 | 1.39 | 150.8  | 52.4                   |
| T1-2    | 103  | 3.91  | 13.7 | 32.9 | 2.39 | 15.5 | 1.99 | 1.84 | 175    | 68.3                   |
| T1-3    | 126  | 10.50 | 24.8 | 60.8 | 3.20 | 27.8 | 2.77 | 2.55 | 258    | 122.0                  |
| T2      | 75.5 | 4.23  | 21.7 | 58.9 | 3.45 | 19.0 | 2.39 | 2.42 | 187.6  | 107.9                  |
| T3-1    | 84.8 | 1.38  | 2.65 | 12.4 | 0.81 | 3.3  | 0.74 | 0.70 | 106.7  | 20.56                  |
| T3-2    | 64.9 | 1.78  | 4.48 | 18.3 | 1.18 | 4.5  | 0.92 | 0.85 | 96.8   | 30.17                  |
| T3-3    | 67.2 | 3.04  | 0.69 | 39.9 | 1.64 | 19.1 | 1.37 | 1.27 | 134.3  | 64.01                  |
| T3-4    | 64.7 | 2.70  | 5.35 | 39.3 | 1.59 | 17.7 | 1.36 | 1.25 | 133.9  | 66.54                  |
| T3-5    | 56.6 | 4.87  | 0.63 | 38.3 | 2.46 | 18.3 | 2.26 | 1.97 | 125.5  | 63.96                  |
| T4-1    | 38.0 | 1.74  | 0.34 | 20.0 | 1.45 | 5.3  | 0.87 | 0.91 | 68.5   | 28.81                  |
| T4-2    | 96.0 | 1.18  | 2.28 | 12.7 | 0.70 | 2.8  | 0.64 | 0.57 | 116.9  | 19.76                  |

*Table 11 Analyzed REE levels in BoP sediment samples . Data of elements are expressed as mg/kg and data of elements with levels < 1 mg/kg are not reported. Concentration sums are both expressed with and without Sc and Y.*

|                        | MdP<br>1       | MdP<br>2    | MdP<br>3    | T1_1         | T1-2         | T1_3         | T2          | T3-1          | T3-2          | T3_3          | T3_4          | T3-5          | T4-1         | T4-2          |
|------------------------|----------------|-------------|-------------|--------------|--------------|--------------|-------------|---------------|---------------|---------------|---------------|---------------|--------------|---------------|
| Naphthalene            | < 10           | 61          | 103         | 345          | 241          | 69           | 123         | 6742          | 1159          | 8832          | 5431          | 3306          | 1414         | 5236          |
| Acenaphthylene         | < 10           | 74          | 106         | 455          | 359          | 305          | 96          | 8564          | 3215          | 9309          | 5466          | 3638          | 1220         | 5911          |
| Acenaphthene           | < 10           | 50          | 63          | 82           | 89           | 89           | 56          | 5188          | 684           | 2319          | 957           | 2021          | 528          | 2933          |
| Fluorene               | < 10           | 40          | 55          | 87           | 141          | 79           | 74          | 4670          | 1332          | 1944          | 70            | 1713          | 513          | 2855          |
| Phenanthrene           | < 10           | 102         | 178         | 1289         | 968          | 1155         | 371         | 33370         | 5622          | 27076         | 8999          | 7271          | 3282         | 17923         |
| Anthracene             | < 10           | 90          | 148         | 499          | 461          | 379          | 167         | 20474         | 3739          | 10776         | 5170          | 3980          | 1459         | 17457         |
| Fluoranthene           | < 10           | 344         | 840         | 6238         | 4186         | 5997         | 689         | 104456        | 19835         | 117153        | 52776         | 23739         | 11404        | 58808         |
| Pyrene                 | < 10           | 284         | 681         | 4576         | 3234         | 4471         | 522         | 83420         | 13910         | 82916         | 36919         | 18773         | 9536         | 51575         |
| Benzo[a]anthracene     | < 10           | 158         | 320         | 2389         | 2344         | 2199         | 259         | 39614         | 9155          | 33947         | 17528         | 10837         | 4875         | 31385         |
| Chrysene               | < 10           | 150         | 322         | 2657         | 2156         | 2476         | 261         | 40565         | 8705          | 38448         | 19826         | 11526         | 4916         | 31769         |
| Benzo[b]fluoranthene   | < 10           | 198         | 406         | 3429         | 2978         | 3121         | 335         | 37692         | 7781          | 46905         | 27189         | 11169         | 6057         | 36148         |
| Benzo[k]fluoranthene   | < 10           | 167         | 316         | 2679         | 1945         | 2393         | 253         | 26703         | 6757          | 31799         | 17372         | 8888          | 4522         | 26205         |
| Benzo[a]pyrene         | < 10           | 220         | 428         | 3498         | 2815         | 3141         | 333         | 13389         | 4515          | 45610         | 26301         | 5491          | 1970         | 13305         |
| Indeno[1,2,3-cd]pyrene | < 10           | 215         | 381         | 2944         | 2743         | 2420         | 322         | 19911         | 5439          | 38363         | 20627         | 6790          | 3951         | 31046         |
| Dibenz[a,h]anthracene  | < 10           | 133         | 167         | 511          | 657          | 449          | 154         | 6244          | 3698          | 8832          | 7015          | 2368          | 920          | 5712          |
| Benzo[ghi]perylene     | < 10           | 187         | 348         | 2759         | 2032         | 2259         | 305         | 17586         | 4855          | 33436         | 19965         | 6280          | 3443         | 24527         |
| <b>∑ PAHs</b>          | <b>&lt; 10</b> | <b>2474</b> | <b>4861</b> | <b>34438</b> | <b>27349</b> | <b>31004</b> | <b>4319</b> | <b>468587</b> | <b>100401</b> | <b>537664</b> | <b>271611</b> | <b>127792</b> | <b>60010</b> | <b>362796</b> |

Table 12 Analyzed PAH levels in BoP sediment samples. Data levels are reported as µg/kg

Thus, Figure 17 represented log transformation of total PAH levels, where T3 displays highest PAH levels, in particular in samples T3-1, T3-3, as well as sample T4-2, with PAH levels ranging from  $\approx 300,000$  to  $500,000$  g/kg. On the other hand, the Mdp and T2 transects showed lowest PAH levels, in the order of  $\approx 4,000$  to  $5,000$  g/kg, and the T1 transect displayed intermediate levels, close to  $35,000$  g/kg. The levels of total hydrocarbons (C10 – C40) were found parallel to PAH levels across the transect and sampling sites (Figure 18), with highest values at sites T3-3 and T3-4, whereas lower levels of total hydrocarbons were detected at sites T1-1, T1-3, T3- 1, T3-2, and T4-1; the three MDP sites showed minimal levels of total hydrocarbons ( $<10$  mg/kg).

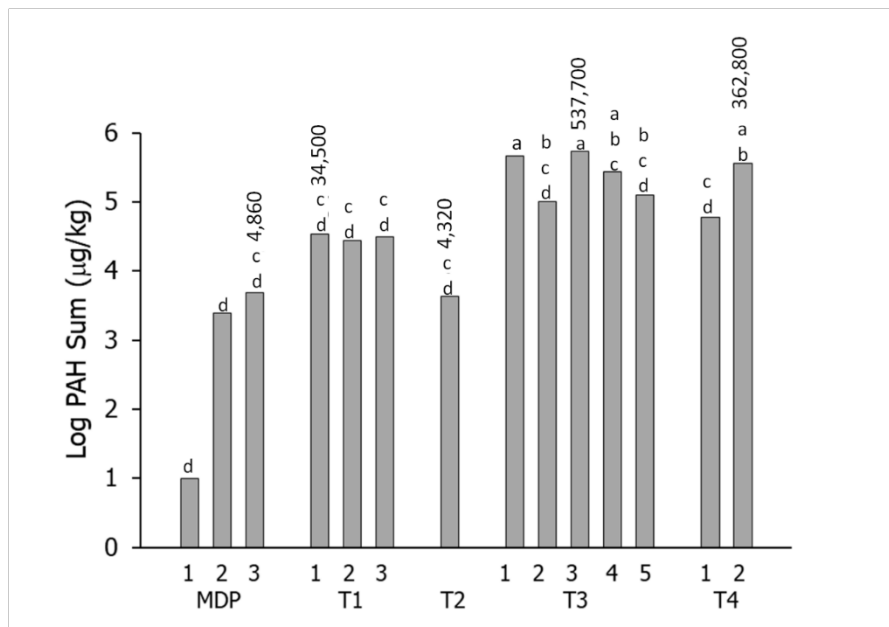


Figure 17 Logarithmic expression of total PAH levels showed dramatic differences between two sites (Mdp and T2) showing PAH levels in the order of  $4,000$  mg/kg and sites T3 and T4 displaying PAH levels in the order of 2- to  $500,000$  mg/kg. Data with different letters (a–d) are significantly different (Tukey's,  $p < 0.05$ ).

The results provided consistent evidence for excess sediment pollution at intermediate distances from coast to offshore, in terms of PAH, total hydrocarbons (C10 – C40), and of metal content, paralleling the toxicity test findings.

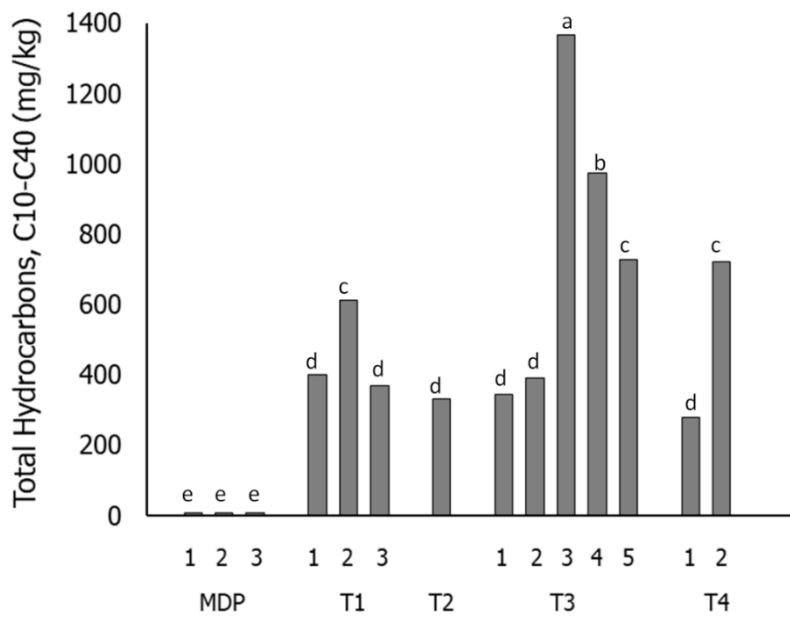


Figure 18 Levels of total hydrocarbons (C10 – C40) showing highest levels at sites T3-3 T3-4 and T4-3. Data with different letters (a–d) are significantly different (Tukey's,  $p < 0.05$ ).

By exposing *A. lixula* embryos to 0.1% WS samples, impaired larval development and increased developmental defects (DD) were observed for samples from most of WS sampling sites. As shown in Figure 19, a noteworthy bell-shaped trend was detected for WS samples from transect 3 (T3), facing the Bagnoli brownfield, where samples T3-3 and T3-4 displayed the highest DD rate (>50%) compared to T3-1 and T3-2 (closer to the coast) and to T3-5 (offshore). By exposing embryos to 0.5% WS, the observation of larvae was biased by excess sediment in culture wells, interfering with larval counts (data not shown).

When *A. lixula* sperm were suspended in 0.5% WS for 1 h, fertilization was unaffected by most of WS samples, except for two sites, MDP1-2 and T3- 4, which showed a significantly decreased fertilization rate (FR =  $53.67 \pm 16.68$  and  $39.83 \pm 4.59$  respectively, vs. control FR =  $95.39 \pm 1.56$ ). On the other hand, the offspring of WS-exposed sperm underwent a significant DD increase (Figure 20). Again, the transect T3 facing the Bagnoli brownfield exerted the most severe effects.

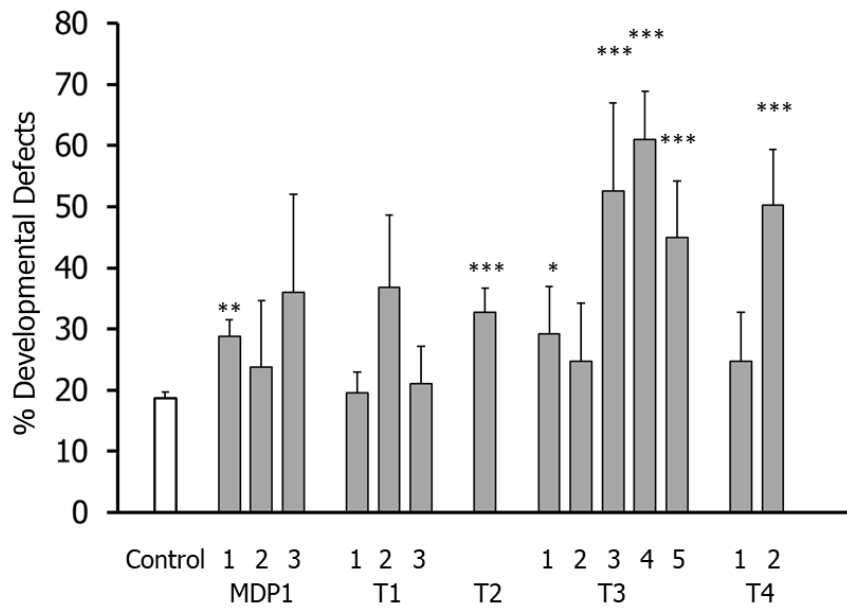


Figure 19 Percent developmental defects in sediment (WS)-exposed sea urchin (s-u) larvae showing bell-shaped rates in the five sites of the T3 transect and highest rates at sites T4-2 and T4-3. Asterisks indicate the results of two-tailed Student t-tests:  $p < 0.05$ ;  $**p < 0.01$ ;  $***p < 0.001$ .

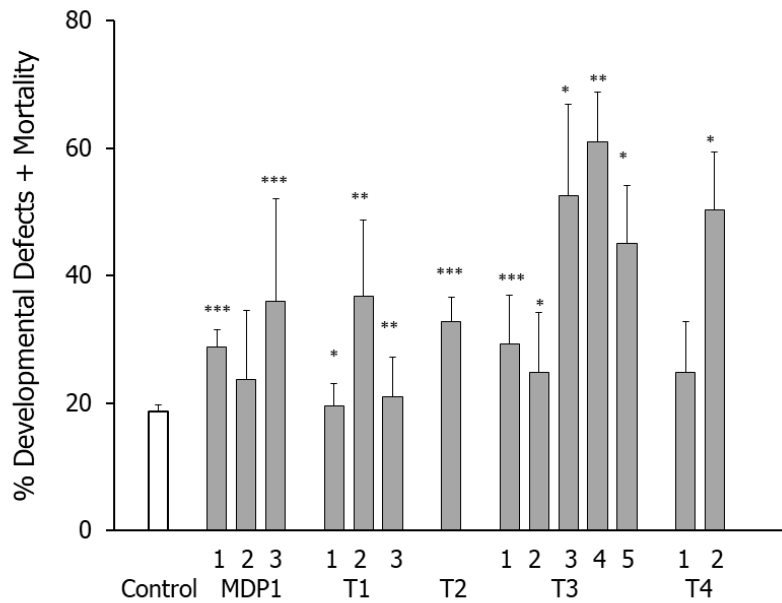


Figure 20 The offspring of sediment-exposed sperm displayed significant damage in terms of developmental defects and mortality at several sites across all transects. Asterisks indicate the results of two-tailed Student t-tests:  $*p < 0.05$ ;  $**p < 0.01$ ;  $***p < 0.001$ .

By exposing *P. tricornutum* diatoms to sediment EL, an overall growth inhibition was observed compared to control growth rate ( $\mu = 1.9$ ), with most significant data for sites MDP1-1, T2, T3-3 and T3-4 (Figure 21). Interestingly, this bell-shaped trend for T3 transect in diatom growth inhibition overlapped with the analogous observation for T3 sites in sea urchin embryotoxicity assay and for the analytical data.

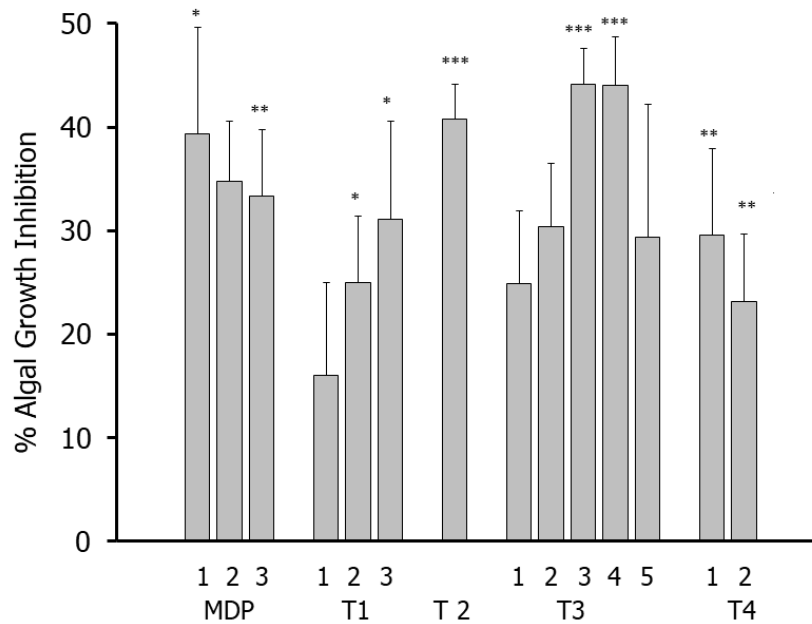


Figure 21 Exposure of *P. tricornutum* to sediment EL resulted in significant growth rate inhibition vs. controls (growth rate  $\mu = 1.9$ ). The data are normalized with control. Again sites from transect 3 displayed a bell-shaped trend with T3-3 and T3-4 resulting in highest growth rate inhibition. Asterisks indicate the results of two-tailed Student t-tests: \* $p < 0.05$ ; \*\* $p < 0.01$ ; \*\*\* $p < 0.001$ .

In order to compare the contaminant distributions and the responses, Pearson Correlation Test was carried out in order to verify the correlation between  $\Sigma$ PAH,  $\Sigma$ HeavyMetals,  $\Sigma$ Al(III) and  $\Sigma$ Fe(III) values vs. sea urchin embryotoxicity data (P1+P2) and *P. tricornutum* percent inhibition values. Raw data were used instead of log-transformed data. SPSS v20 used for the statistical analysis. The correlation between: The correlation between:

- $\Sigma$ PAHs and embryotoxicity was slightly positive and significant, with  $p < 0.05$ ;  $r = 0.28$ ;
- $\Sigma$ HMs and embryotoxicity was  $p < 0.05$ ;  $r = 0.27$ ;
- $\Sigma$ Al(III) and embryotoxicity was not significant ( $p < 0.063$ );

d)  $\Sigma\text{Fe(III)}$  and embryotoxicity was  $p < 0.05$ ;  $r = 0.30$ .

Correlation between algal percent inhibition and analytical data failed to show any significant data, except for  $\Sigma\text{Fe(III)}$  ( $p < 0.05$ ;  $r = 0.33$ ).

A noteworthy finding was both observed in embryotoxicity bioassay (WS in sea urchins) and as growth inhibition in algal growth bioassay (EL in diatoms), displaying nonmonotonic toxicity trends within transects, which were more completely expressed by transect 3 along five sampling points. Namely, an increase in sediment toxicity was observed at intermediate distances between coastline and offshore (T3-3 and T3-4), in agreement with analogous findings in pollutant concentration. It may be recalled that this topographic distribution of sediment pollution toxicity is not new, as similar nonmonotonic trends in sediment pollution and toxicity were reported in previous studies of Toulon Bay, Naples Bay and Izmir Bay [221, 222]. In particular, the report by Romaña et al. [221] found a nonmonotonic trend in sediment toxicity which was consistent with the preferential deposit area of the suspended matter originating from the point discharge of wastewater effluent in Toulon Bay, at an intermediate distance from coast to offshore. Sea urchin sperm bioassays failed to display spermiotoxicity for most of samples, while inducing severe offspring damage and mortality following sperm exposure to T3-3, T3-4 and T4-2 (Figure 20). It should be noted that the embryos/larvae generated by exposed sperm are not in contact with sediment, but may only be affected by a transmissible damage from sperm pronuclei to zygotes, thus resulting in developmental damage and embryonic/larval defects and mortality. As well-established events in several organisms, dominant lethal mutations have been associated to male exposures resulting in offspring damage in a long line of studies since the 1930s' (reviewed by [217]). In sea urchins, sperm exposures to a number of physical and chemical agents have been associated to cytogenetic and/or developmental damage and/or mortality (reviewed by [217]). Altogether, one may assume that the findings of sperm exposure to WS suspensions vs. offspring damage rely on distinct toxicity mechanisms compared to prolonged exposures of embryos/larvae.

### **3.4 CONCLUSIONS**

Unconfined to the present results, this study should warrant further investigations on sediment toxicity in the BoP and in other impacted marine areas using a combination of chemical characterization methods and bioassay-guided evaluations. Sediment from the Bay of Pozzuoli displayed PAH, hydrocarbon and metal pollution, along with significant toxicity to sea urchin early life stages and to algal growth. The highest levels of PAHs, total hydrocarbons and metals were found along the two transects, T3 and T4, closest to the Bagnoli brownfield. Consistent with those analytical findings, the effects found in two toxicity bioassays followed nonmonotonic trends along transects from coastline to offshore, prompting further investigations at the community level.

# CHAPTER 4

---

In this chapter, the results based on original contributions published in [20].

## **4.1 THE EFFECTS OF CERIUM, GADOLINIUM, LANTHANUM, AND NEODYMIUM IN SIMPLIFIED ACID MINE DISCHARGES**

The acid mine drainage (AMD) is an acid leachate characterized by low pH (i.e., approximately  $\text{pH} < 5$ , but it depends on a site-by-site basis) and an important concentration of sulphates and dissolved metal(loid)s [223]. It is derived from the sulphide oxidative dissolution promoted by mining activity and it constitutes one of the main pollution process of natural watercourses [224]. This acidic sulphate water is geochemically characterized by high mobilization REEs. AMD has recently raised a great deal of attention as a potential significant source of REEs directly able to affect environmental and human health, if not adequately collected and treated. REE contents reported in AMD [225-228] and from consistently showed several orders of magnitude above the medians of natural waters. The median concentration of REEs in European Union stream sediment was 198.9 mg/kg [94], reaching 457.7  $\mu\text{g/L}$  in USA ore mine effluent and 61.3  $\mu\text{g/L}$  in China coal mine effluent, while in surface water their concentration ranged from 75.03  $\mu\text{g/L}$  up to 518.7  $\mu\text{g/L}$  [38]. Zhao et al. [98] indicated that the REE-sulphate complexes are the main form of dissolved REEs concentration in acid mine wastewater representing more than 60% of the total amount, followed by free metal species form. The presence of REEs in AMD and its acidic pH can increase their mobility and bioavailability in the various environmental compartments with potential negative effects on a one health approach, especially in mining areas (i.e., both active or abandoned sites) [225, 229-231]. When the intensity of acidity reaches a baseline ecotoxicity threshold, it can affect organisms through direct acute damage and indirect acidified soil and water [232-234]. Thus, the combined REEs pollution and acid conditions from AMD could adversely affect the structure and function of aquatic ecosystem changing the productivity and the abundance in biomass or even could lead to the elimination of aquatic species [235, 236].

Relatively scarce information is available to date about the REEs toxicity at low pH levels in addition to scarce information on REEs-associated biological effects, including bioassays on model organisms, and human health effects [7, 24, 74, 76]. Only few papers evidenced that low pHs (i.e., mine wastewater) can modify their biological activity increasing aquatic toxicity [237, 238], where a relevant role is also played by organic and inorganic ligands [10]. Primary producers can be highly sensitive indicators of toxic effects due to the aquatic exposure to REEs dissolved in AMD. As a parallelism, we must remember that the notorious Itai-Itai disease was caused by the consumption of rice contaminated by cadmium from cultures irrigated with AMD [239]. d'Aquino L et al. [143] stated that few data about REEs effects on macrophytes were available from the scientific literature and, to the best of our knowledge, such scarcity persist today. The need to investigate photosynthetic organisms in relation to AMD contamination (i.e., surface water polluted by uncontrolled and untreated AMD, and direct irrigation with contaminated AMD) pushes ahead the present research topic. This study evaluated the adverse effects of four rare elements (Ce, La, Gd and Nd) on *Raphidocelis subcapitata* (green microalgae), and *Lepidium sativum* (macrophyte), and *Vicia faba* (macrophyte) considering a background multi-endpoint approach (i.e., growth inhibition, germination index, and genotoxicity) to check the effect of spiked simplified AMD investigating the role of two pH values (4 and 6) in potential toxicity modification.

## **4.2 MATERIALS AND METHODS**

### **4.2.1 Analytical methods**

Trichloride anhydrous salts of Ce (III), La(III), Gd(III), and Nd(III) were purchased from Sigma-Aldrich (Italy). All chemicals were of analytical grade. Testing solutions were prepared from 1 M stock solutions per element in ultra-pure distilled water stored at 4 °C. Stock solutions were diluted to the final test concentrations using freshwater medium (ISO, 2012a) buffered at pH values 4 and 6. The pH was measured with a pH-meter (Mettler Toledo Five Easy, Milan, Italy). The experimental design included 4 exposure concentrations (i.e., 0.01, 0.1, 1, and 10

mg/L – nominal concentrations). Real concentrations were determined by Inductively Coupled plasma mass spectrometry (ICP-MS, Aurora Bruker M90, Bremen, Germany) following previously established protocols and quality assurance and quality control laboratory procedures according to [240]. The limits of detection (LOD) and quantification (LOQ) were as follows for Ce, Gd, La, and Nd: 0.0010, 0.0018, 0.0006, and 0.0011 µg/L as LOD; and 0.0035, 0.0058, 0.0021, and 0.0037 µg/L as LOQ. Analyses were carried out in triplicate.

#### **4.2.2 Algal growth inhibition test**

The algal growth inhibition test (72 h) with *R. subcapitata*, formerly known as *Selenastrum capricornutum* and *Pseudokirchneriella subcapitata*, was carried out based on ISO 8692 [241]. The algal density was determined by spectrophotometric analysis (DR5000, Hach Lange GmbH, Weinheim, Germany). The percentage inhibition of the cell growth (IG, %) was calculated as the difference between the growth rate of the control and of the sample and expressed as the mean ( $\pm$  standard deviation). Toxicity tests were carried out in triplicate.

#### **4.2.3 Phytotoxicity test**

The *L. sativum* germination and root elongation toxicity tests were performed according to ISO 11269 [242]. Macrophyte seeds (n = 10) were exposed on filter paper Whatman n. 1 imbibed with 3 mL of testing solution in triplicate in Petri dishes. Samples were incubated at  $25 \pm 1$  °C in darkness and the number of seeds germinated and the length of the developing roots were measured after 3 days. Controls were carried out in distilled water. Germination (%), and root elongation inhibition were combined to calculate the germination index (GI, %) [243].

#### **4.2.4 Micronucleus test**

*V. faba* was investigated for genotoxicity according to ISO 29200 [244]. Macrophyte seeds (n = 5) were exposed on filter paper Whatman n. 1 imbibed with 6 mL of testing solution in triplicate in Petri dishes. After incubating in the dark at

22 ± 2 °C for 96 h, the root tips of germinated seeds were fixed for 24 h in 1:3 acetic acid: ethanol solutions, then were cut, stained in Schiff's Reagent using Feulgens method, and squashed on microscope slides [244]. The micronucleus frequency MCN (%) was evaluated in 10<sup>3</sup> cells from *V. faba* seeds using ImageJ [245].

## 2.5. Data analyses

Median effect concentrations (EC50), EC5 and EC10 were calculated as mean values and relative 95% confidence limit values [74], for *R. subcapitata* and *L. sativum*. Differences between treatments were assessed via one-way analysis of variance (ANOVA) after the verification of normality (Shapiro-Wilk's test) and homoscedasticity (Levene's test). The *post-hoc* Tukey's test accounted for differences within groups setting the statistical significance at p < 0.05. Statistical analysis was carried out via SigmaPlot (Systat Software, San Jose, CA).

## 4.3 RESULTS AND DISCUSSION

All endpoints were calculated on real concentrations summarized in Table 12.

| A  |   | pH 4  |      |      |       | pH 6  |      |      |       |
|----|---|-------|------|------|-------|-------|------|------|-------|
| Ce | N | 14.02 | 1.40 | 0.14 | 0.01  | 14.01 | 1.40 | 0.14 | 0.014 |
|    | R | 10.22 | 1.43 | 0.13 | 0.01  | 10.22 | 1.43 | 0.13 | 0.010 |
| Gd | N | 15.72 | 1.57 | 0.15 | 0.01  | 15.72 | 1.57 | 0.15 | 0.015 |
|    | R | 5.72  | 1.64 | 0.16 | 0.01  | 5.72  | 1.66 | 0.15 | 0.012 |
| La | N | 13.89 | 1.38 | 0.13 | 0.01  | 13.89 | 1.38 | 0.13 | 0.013 |
|    | R | 5.32  | 1.20 | 0.12 | 0.01  | 5.42  | 1.21 | 0.12 | 0.012 |
| Nd | N | 14.42 | 1.44 | 0.14 | 0.01  | 14.42 | 1.44 | 0.14 | 0.014 |
|    | R | 6.51  | 0.71 | 0.07 | 0.005 | 6.51  | 0.71 | 0.07 | 0.005 |
| B  |   | pH 4  |      |      |       | pH 6  |      |      |       |
| Ce | R | 2.39  | 0.33 | 0.03 | 0.002 | 2.39  | 0.33 | 0.03 | 0.002 |
| Gd | R | 1.34  | 0.38 | 0.03 | 0.003 | 1.34  | 0.38 | 0.03 | 0.002 |
| La | R | 1.24  | 0.28 | 0.02 | 0.002 | 1.27  | 0.28 | 0.02 | 0.002 |
| Nd | R | 1.52  | 0.16 | 0.01 | 0.001 | 1.52  | 0.16 | 0.01 | 0.001 |

Table 13 Nominal and real concentrations (A) of testing solutions of Ce, Gd, La, and Nd at pH 4 and 6 at standard errors (B); N = nominal concentration, R = real concentration; concentrations are in mg/L.

In Figure 22, the results of the IG (%) of *R. subcapitata* were reported at pH 4 and 6, respectively, for Ce (Fig. 22 A and B), Gd (Fig. 22 C and D), La (Fig. 22 E and F), and Nd (Fig. 22 G and H). A linear regression model was considered to fit data concentration-response relationships. All equations and the relative standard errors were included in Fig. 22 (A–H).

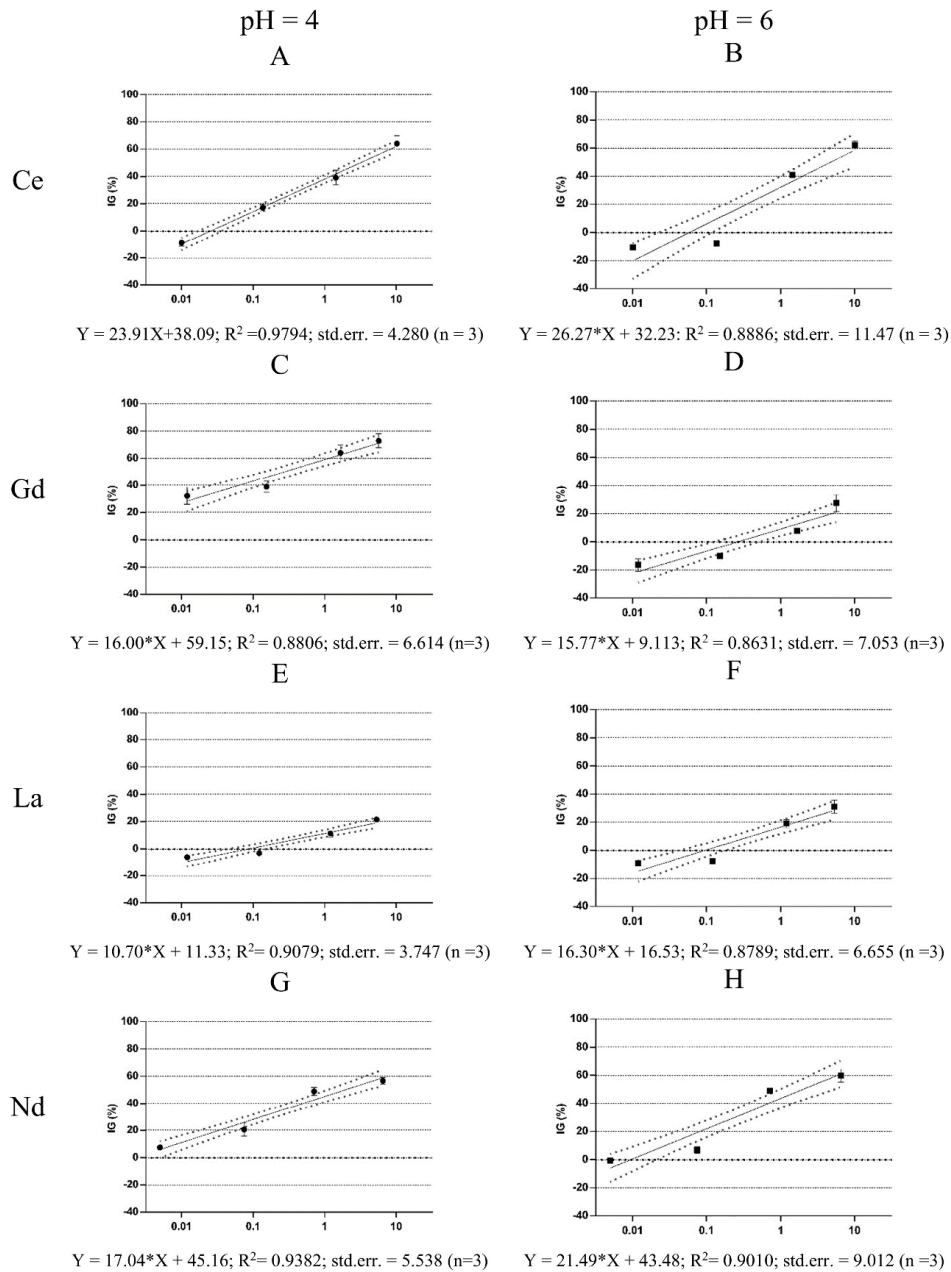


Figure 22 Concentration-response relationship at pH 4 and 6 of Ce (A and B), Gd (C and D), La (E and F), and Nd (G and H) exposed to *R. subcapitata*; concentrations in the x-axis are expressed as mg/L; IG = inhibition of growth.

These equations allowed the determination of EC50, EC10, and EC5 that were summarized for both pH values in Table 13.

|               |           | EC5                         | EC10                      | EC50                      |
|---------------|-----------|-----------------------------|---------------------------|---------------------------|
| <b>pH = 4</b> | <b>Ce</b> | 0.04<br>(0.02-0.10)         | 0.07<br>(0.03-0.16)       | 3.15<br>(1.36-7.19)       |
|               | <b>Gd</b> | 0.0004<br>(0.000009- 0.012) | 0.0008<br>(0.00002- 0.02) | 0.267<br>(0.009-5.3)      |
|               | <b>La</b> | 0.256<br>(0.007-1.15)       | 0.751<br>(0.02-3.21)      | n.a.                      |
|               | <b>Nd</b> | 0.004<br>(0.0001-0.096)     | 0.008<br>(0.0003-0.187)   | 1.860<br>(1.036 to 3.341) |
| <b>pH = 6</b> | <b>Ce</b> | 0.09<br>(0.00- 0.25)        | 0.014<br>(0.00- 0.38)     | 4.75<br>(0.04- 10.99)     |
|               | <b>Gd</b> | 0.553<br>(0.012-0.096)      | 1.136<br>(0.023- 0.211)   | n.a.                      |
|               | <b>La</b> | 0.196<br>(0.002-0.366)      | 0.398<br>(0.005-0.714)    | n.a.                      |
|               | <b>Nd</b> | 0.01<br>(0.001-2.16)        | 0.0276<br>(0.002-3.64)    | 1.856<br>(0.973 – 3.540)  |

*Table 14 EC5, EC10, and EC50 values for Ce, Gd, La and Nd at pH =4 and 6; values are in mg/L; n.a. = not available; REEs= rare earth elements; EC = effective concentration; average EC values are provided  $\pm$ 95% confidence limit values in brackets (n = 3).*

For Ce, La and Nd, biostimulation effects were detected at the first two lowest exposure concentrations for both pH 4 and 6, and also for Gd at pH 6. Microalgae growth impairment occurred for Ce, La, and Nd at 1 and 10 mg/L (nominal concentrations) at pH 4 and 6, and for Gd at pH 6. For microalgae exposed to Gd at pH 4, all exposure concentrations evidenced a concentration-response significant toxic effect up to 73% at 5.72 mg/L. REEs biostimulation effects in unicellular green algae were already reported for nano-CeO<sub>2</sub> considering photosynthesis inhibition and ROS formation as endpoints [246] and Ce(NO<sub>3</sub>)<sub>3</sub> for growth inhibition [247]. The exposure to Ce at pH 4 showed effects not significantly different from the exposure at pH 6 with a correlation coefficient of  $R^2 = 0.93$  (Fig. 21 A and B). Only, at 0.137 mg/L the effect of pH 6 exposure was still biostimulation and significantly different ( $p < 0.001$ ) from the same concentration at pH 4 treatments being about 25% lower. Ce effects ranged between -10% (0.01 mg/L) and 64% (10.225 mg/L). Indeed, the EC50 of Ce at pH 4 was 3.15 (1.36–7.19) mg/L and Ce EC50 at pH 6 was 4.75 (0.04–10.99) mg/L (Table 13). These

EC50 values are not significantly different ( $p > 0.05$ ). For Gd, a significant difference in the concentration-response curves can be observed in Fig. 21 (C and D), at pH 6 the EC50 value in the investigated concentration range cannot be detected and only EC5 and EC10 values were calculated (i.e., maximum effect of 23% at 5.72 mg/L). At pH 4 (Fig. 21 C), significant differences ( $p < 0.001$ ) between treatments were highlighted. The maximum detected effect was 73% at 5.72 mg/L. Gd EC50 at pH 4 was 0.267 (0.01–5.30 mg/L). For Gd exposure at pH 6, only EC5 and EC10 values were calculated (Table 13). For La, effects ranged between –6% (0.01 mg/L) and 21% (5.32 mg/L) (Fig. 21 E and F). At 0.01 mg/L and 0.12 mg/L of La no significant differences ( $p > 0.05$ ) were observed between treatments at pH 4 and pH 6. At 1.207 mg/L, the inhibitory effect of pH 6 exposure was significantly different ( $p < 0.01$ ) from the corresponding concentration at pH 4 treatments being about 8% greater. On the contrary, at 5.321 mg/L, the inhibitory effect of pH 6 exposure was significantly different ( $p < 0.001$ ) from the 5.321 mg/L at pH 4 being about 10% lower. The EC50 after 72 h of exposure was not determined in both pH exposure scenarios, while EC5 and EC10 values were summarized in Table 13. About *R. subcapitata* exposure to Nd, the effects varied between 7.4% and 56.7% for pH 4, and –0.9% and 59.7% for pH 6 (Fig. 21 G and H). Significant differences ( $p < 0.05$ ) were evidenced amongst treatments at the first two lowest exposure concentrations, while no significant differences ( $p > 0.05$ ) were observed within treatments at the remaining concentrations. At 0.005 mg/L, the inhibitory effect of pH 6 exposure was significantly different ( $p < 0.01$ ) from the same concentration at pH 4 treatments being about 8% lower. At 0.075 mg/L, the inhibitory effect of pH 6 exposure was significantly different ( $p < 0.001$ ) from the 0.075 mg/L at pH 4 being about 14% lower. The EC50 values of Nd at pH 4 and 6 were not significantly different ( $p < 0.01$ ) being 1.860 mg/L and 1.856 mg/L, respectively (Table 13). These data were partly in agreement with previous studies [10, 248, 249]. The comparison of the growth inhibition effects at pH 4 and 6 evidenced only limited differences between the two exposure scenarios, except for Gd where low pH values can increase the effect on the targeted species. REEs were ranked in increasing order of toxicity at pH 4 according to the estimates obtained. For EC50: La < Ce < Gd < Nd; EC10: La < Ce < Nd < Gd and EC5: La < Ce < Nd < Gd. The toxicity

trend evidenced that the most toxic elements at pH 4 were Nd and Gd, while La was the less toxic. At pH 6, the general toxicity decreased and kept similar values compared to pH 4. At both pH, Gd and La EC50 values could not be obtained. REEs were ranked in increasing order of toxicity at pH 6, EC50: La  $\approx$  Gd < Ce < Nd; EC10: Gd < La < Nd < Ce and EC5: Gd < La < Ce < Nd. In general, the ecotoxicity did not always increase with the increase in the atomic number of the investigated REEs with *R. subcapitata* as reported in previous studies [76, 250, 251], and the general scarcity of experimental data can make it difficult to fully discuss. For example, EC50 value of Ce (4.4 mg/L) according to [250] was very similar to both EC50s at pH 4 and 6, but the pH of testing solutions was not displayed, while the Gd EC50s were significantly different compared to [250] (1.257 mg/L).

Several authors [247, 252, 253] highlighted that the formation of insoluble REEs species in exposure media or of precipitates in the presence of free ion concentration due to the changes in pH levels might be responsible of the differential responses.

In Figure 23, the results about the GI (%) of *L. sativum* were reported at pH 4 and 6, respectively, for Ce (Fig. 23 A and B), Gd (Fig. 23 C and D), La (Fig. 23 E and F), and Nd (Fig. 23 G and H). GI values between 80% and 120% are considered as acceptable, while, if 120% inhibition or biostimulation effects are identified [243]. As a general overview of the obtained results, the GI always evidenced inhibitory effects at the two highest tested concentrations for all the investigated REEs at both pHs. Similarly, all GI values were always >80% and < 120%, so any biostimulation effect was displayed as well.

Considering the exposure of *L. sativum* to Ce, the number of *L. sativum* germinated seeds was 100% in the control test, but when Ce solutions at 0.137 mg/L, 1.431 mg/L and 10.225 were used the number of seeds was reduced of about 80% both at pH 4 and 6 (data not shown). At 0.01 mg/L, the number of germinated seeds was not significantly different from the negative control (< 10% effect). No significant differences ( $p > 0.05$ ) were observed at 0.137 mg/L and 10.225 mg/L of Ce for both pH values, while at 0.01 mg/L and 1.431 mg/L statistical differences in the effects were evidenced ( $p < 0.05$ ) within pH 4 and pH 6 treatments (Fig. 23 A and B). Ce germination index ranged between 81% (0.010 mg/L) and 54% (10.225 mg/L) at pH 4, and between 90% (0.010 mg/L) and 64% (10.225 mg/L) at pH 6. The number of *L. sativum* germinated seeds after Gd exposure significantly ( $p < 0.05$ ) decreased

from 0.154 mg/L, up to 5.721 mg/L. Effects of Gd at pH 4 were not significantly different from those at pH 6 with a correlation coefficient of  $R^2 = 0.98$  (Fig. 23 C and D). The Gd GI ranged between 83% (0.012 mg/L) and 50% (5.721 mg/L) at pH 4, and between 86% (0.012 mg/L) and 60% (5.721 mg/L) at pH 6.

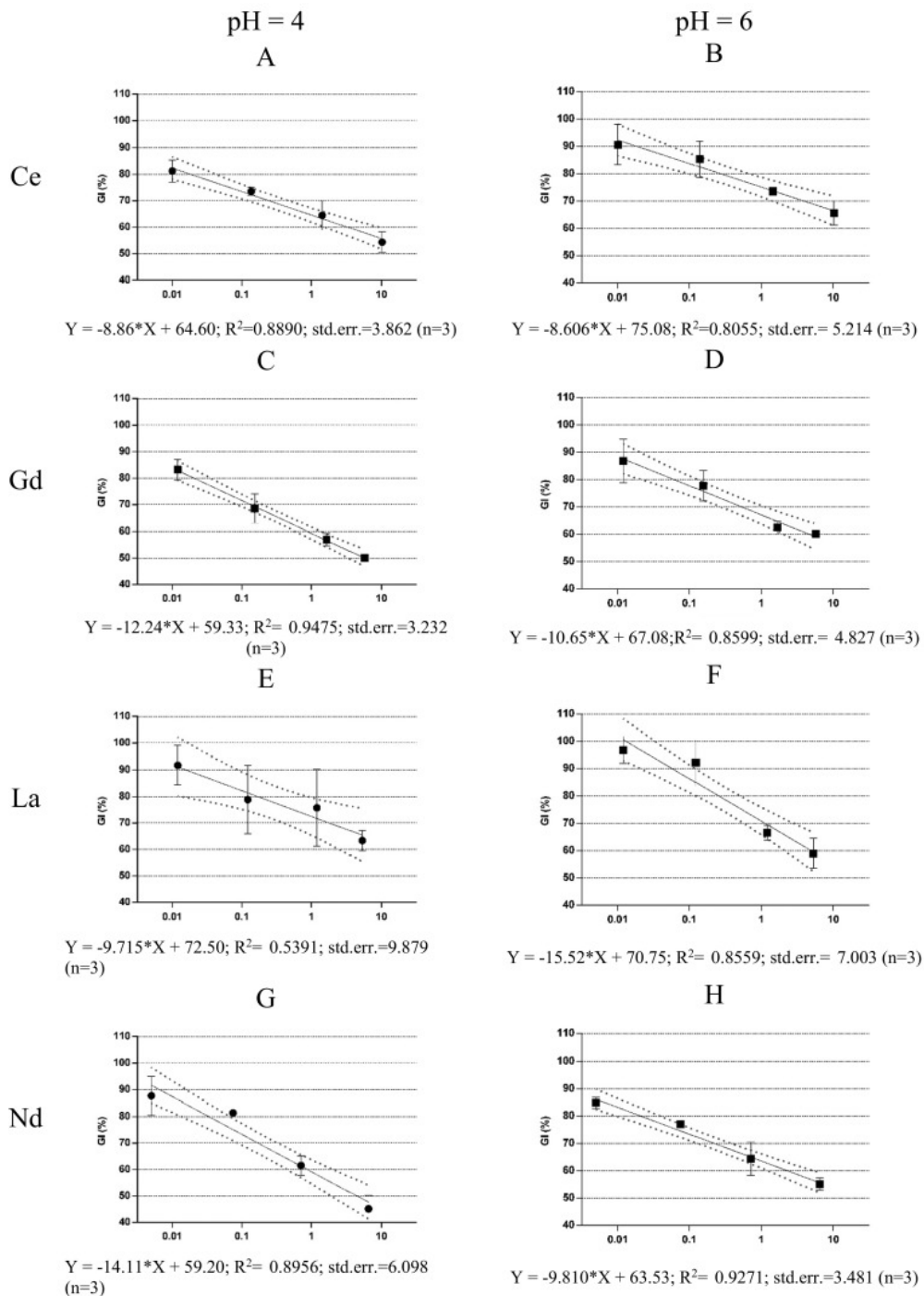


Figure 23 Concentration-response relationship at pH 4 and 6 of Ce (A and B), Gd (C and D), La (E and F), and Nd (G and H) exposed to *L. sativum*; concentrations in the x-axis are expressed as mg/L; GI = germination index.

About the exposure to La, the number of germinated seeds was reduced up to 90% at pH 4 and 80% at pH 6. No significant differences ( $p > 0.05$ ) were evidenced between treatments at the different pHs in the considered concentration range (Fig. 23 E and F). At pH 4, only the lowest exposure concentration (0.012 mg/L) showed a GI significantly different (90%) than all other treatments (63%–78%) being the only one presenting no effect. At pH 6, the highest concentrations (5.321 mg/L and 1.207 mg/L) showed slight adverse effects ranging between 59% and 66%, while the two lowest treatment presented no effect. In Nd exposure, the number of *L. sativum* germinated seeds was reduced up to 80% at 0.710 and 6.510 mg Nd/L for both pH 4 and 6 (data not shown). Significant differences ( $p < 0.05$ ) were observed only at 6.510 mg/L for both pH values, while at 0.005 mg/L, 0.075 mg/L and 0.710 mg/L no significant difference between treatments was detected ( $p > 0.05$ ). The germination index showed a similar toxicity trend to the previous REEs exposure, but with higher toxicity level (45%) at 6.510 mg/L (pH 4). Indeed, the GI values ranged between 45% and 87% for pH 4, while between 55% and 84% for pH 6 (Fig. 23 G and H).

Currently, few data are available about *L. sativum* exposure to REEs including all endpoints. Wang et al. [254] reported that  $Ce^{3+}$  (14 mg/L),  $La^{3+}$  (13.8 mg/L), and  $Nd^{3+}$  (14 mg/L) in *Lepidium meyenii* enhanced hyperhydricity and the activities of antioxidative enzymes in adventitious shoots like peroxidase (POD), catalase (CAT), ascorbate peroxidase (APX), superoxide dismutase (SOD), monodehydroascorbate reductase (MDHAR) and glutathione reductase (GR), but most adventitious shoots grew normally. Thomas et al. [10] highlighted that La and Ce at “high pH” ( $5.95 \pm 0.02$  and  $6.74 \pm 0.03$ , in that order) had no impact on seed germination in the tested species at any concentration, whereas Ce supplied at “low pH” ( $4.08 \pm 0.02$ ) induced negative effects (i.e., inhibition concentration on 10% exposed population, IC10, mg/kg dry soil (d.s.)) on seed germination in *Asclepias syriaca* (54.6 mg/kg d.s.), *Desmodium canadense* (165.9 mg/kg d.s.), *Panicum virgatum* (166.8 mg/kg d.s.), *Raphanus sativus* (150.4 mg/kg d.s.), and *Solanum lycopersicum* (195.34 mg/kg d.s.).

The frequency distribution of micronuclei in *V. faba* exposed to Ce (0.010 mg/L), Gd (0.012 mg/L), La (0.012 mg/L), and Nd (0.005 mg/L) was reported in Figure 24

for both pH 4 and 6. No significant differences ( $p < 0.05$ ) were evidenced between the negative controls and the treatments at pH 6. At pH 4, effects were significantly different ( $p < 0.05$ ) from negative controls for La, Nd, and Gd being approximately from three- to four-fold compared to negative controls. The MNF confirmed that Gd at pH 4 is significantly toxic like for *R. subcapitata* and *L. sativum*.

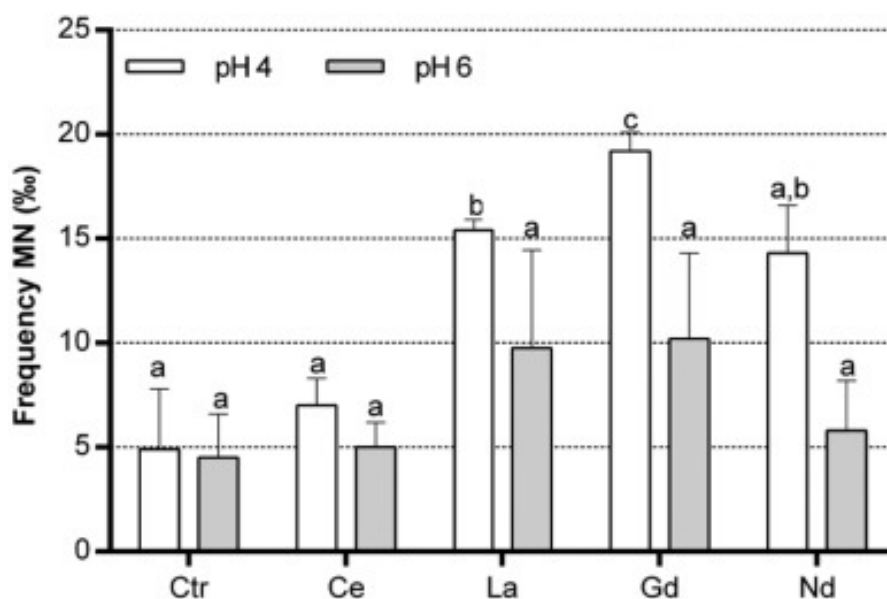


Figure 24 Frequency of micronuclei (MC) in *V. faba* root exposed to Ce (0.010 mg/L), Gd (0.012 mg/L), La (0.012 mg/L), and Nd (0.005 mg/L) at pH = 4 and 6; letters (a-c) correspond to significantly different data (Tukey's test,  $p < 0.05$ ); ctr = negative control; error bars indicate standard errors ( $n = 3$ ).

For Nd, an increased MNF mitotic and chromosomal aberrations in *V. faba* were also evidenced by Jha and Singh [110], similarly to our findings. For La, Wang et al. [130] highlighted some hormetic effects in *V. faba*, but the MNF was not investigated. Only Ce presented no mutagenicity effects either at pH 4 or 6. The pH has a significant role in changing the effects of Gd, La, and Nd to *V. faba* inducing mutagenicity at low values (pH 4).

#### 4.4 CONCLUSIONS

The effects of Ce, Gd, La, and Nd were assessed in a simplified acid mine discharge investigating the role of pH 4 and 6 in changing the toxicity profiles of three photosynthetic organisms. A multiple-endpoint approach (i.e., growth inhibition, germination index, and mutagenicity) was used to investigate real exposure scenarios. Results evidenced that pH 4 can increase the toxicity of the selected REEs increasing the amount of free trivalent ions compared to pH 6. In summary, the toxicity trends were as follows: i) for microalgae (i.e., considering the EC50 values): 1) La < Ce < Nd < Gd at pH 4; 2) Nd < Ce < Gd  $\approx$  La at pH 6; ii) for *L. sativum* (i.e., considering the GI(%) at the highest exposure concentration): 1) La < Ce < Gd < Nd at pH 4; 2) Ce < Gd  $\approx$  La  $\approx$  Nd at pH 6; iii) for *V. faba* (i.e., MNF): 1) Ce < La  $\approx$  Nd < Gd at pH 4; 2) Ce  $\approx$  La  $\approx$  Nd  $\approx$  Gd at pH 6. The sensitivity of the considered biological models was *R. subcapitata* > *V. faba* > *L. sativum*, suggesting that microalgae can have an important role as well as *V. faba* in the risk assessment of REEs. Gd was the most toxic element at pH 4, followed by La and Nd, and Ce. At pH 6, their effects significantly decreased, and Nd evidenced the highest toxicity. Gd, La and Nd evidenced at pH 4 their potential mutagenicity, that was not present at pH 6. According to the considered exposure scenarios, potential significant negative effects could be exerted especially by Gd, La, and Nd in acidic aquatic environments to microalgae and macrophytes, but they can be reduced by controlling the pH. Several gaps into the knowledge still remain about REEs toxicity effects and their potential uptake by aquatic species including the transfer through the food web and potential mechanism of adaptation and detoxification.

# CHAPTER 5

---

In this chapter, the results based on original contributions published in [74].

## 5.1 CERIUM AND ERBIUM EFFECTS ON *DAPHNIA MAGNA* GENERATIONS

The goal of ecotoxicity testing is to develop data that can ensure appropriate protection of public health from the adverse effects of exposures to contaminant. Current approaches to REE toxicity testing rely primarily on observing adverse biological effects in homogeneous groups of organisms exposed to high doses of the element. However, the relevance of biological studies for the assessment of environmental risks at much lower concentrations is becoming object of interest. Apart from the high costs of the studies and time-consuming, adequate coverage of different life stages, of endpoints of public concern, such as developmental toxicity is a continuing concern.

As mentioned in the previous sections, most literature on REE ecotoxicity reported on few REEs, namely Ce and La, and only few publications report ecotoxicity for different REEs performed under identical experimental conditions [250].

Gaps into the knowledge persist on the health and environmental effects of other REEs [76]. Furthermore, most information about acute toxicity of REEs referred to concentrations not relevant under an environmental viewpoint and only few studies investigated the potential effects of REEs on a long-term basis in freshwater [15, 255].

A study investigated the potential hazard of Ce, La, Gd, Nd) and Pr to freshwater microcrustaceans considering both acute (*Thamnocephalus platyurus* - 24 h, *Daphnia magna* - 48 h, and *Heterocypris incongruens* - 6 days) and chronic (21 days with *D. magna*) assays [15]. Acute toxicity as median lethal concentration (LC50) of Ce (as Ce(NO<sub>3</sub>)<sub>3</sub>) was  $33.0 \pm 1.2$  mg/L and  $26.3 \pm 3.5$  mg/L for *T. platyurus* and *D. magna* in artificial freshwater (AFW), respectively, while it was >50 mg/L for both Ce and Er in natural lake waters (from two different lakes as nominal concentrations).

The 21 days chronic test with *D. magna* evidenced for Ce (as Ce(NO<sub>3</sub>)<sub>3</sub>) a LC50 in lake water of 0.30 (0.23e0.36) mg/L. Another study assessed the effects of 11 REEs on *Hydra attenuata* showing a LC50 value of 0.33 (0.24e0.45) mg/L for Ce (CeCl<sub>3</sub> 5H<sub>2</sub>O) and 0.40 (0.32 e 0.57) mg/L for Er (ErCl<sub>3</sub> 6H<sub>2</sub>O) [255]. The sensitivity of *H. attenuata* for Ce is very similar to *D. magna* chronic test [15].

According to Sneller et al. [256], the derived maximum permissible concentration (MPC) for Ce is 22.1 mg/L for fresh surface water. No MPC is currently available for Er. The present research aimed at investigating the long-term chronic exposure of *D. magna* to Ce and Er at environmentally relevant concentrations. Static renewal toxicity tests were carried out on a multi-endpoint and multi-generational basis.

Effects included the following endpoints: organisms size, parental reproduction, organisms survival, determination of reactive oxygen species (ROS), enzymatic activity, gene expression of ABC transporter, and uptake.

## **5.2 MATERIAL AND METHODS**

### **5.2.1 Chemicals, testing solutions, and analytical characterization**

Chemicals were purchased from Sigma Aldrich (Saint Louis, USA) as cerium chloride (CeCl<sub>3</sub> 7H<sub>2</sub>O) (purity > 99.99%) and erbium chloride (ErCl<sub>3</sub> 6H<sub>2</sub>O) salts. Stock solutions were prepared in deionized water (1 g/L; total organic substance < 1 mg/L).

Treatment solutions were prepared in artificial freshwater ISO 6341 [257] at least 24 h before the organisms exposure. The analytical determination of Ce and Er in treatment solutions was carried out via inductively coupled plasma mass spectrometry (ICP-MS NexION 350X, PerkinElmer, Inc., MA, USA). Analyses were carried out on samples collected after day 3, 7, 14, 21, 24, 28, 35, 42, 45, 49, 56, and 63.

### **5.2.2 A multi-endpoint experimental approach with *D. magna* (organisms' size, parental reproduction, organisms' survival)**

Daphnids populations were cultured for several generations at Hygiene Laboratory of the Department of Biology of the University of Naples Federico II in ISO medium [257] and daily fed (i.e. 5 days a week) with microalgae *R. subcapitata*. Acute toxicity test with *D. magna* were carried out according to [257].

Neonates (< 24 h old) were isolated for testing and used for multigenerational chronic semi-static toxicity tests according to OECD 211 guidelines [258] modified considering: i) 30 daphnids in six replicates in 1 L beakers with medium renewed twice a week [259]; 2) the first brood instead of the third one due to delayed reproduction of organisms (according to screening tests – data not presented here) and subsequent extent of the test duration.

Three subsequent generations (F0 (parental), and F1 and F2 (filial) of *D. magna* were exposed to treatments and negative controls for at least 21 days per each generation. Averagely during the whole exposure period, freshwater parameters were as follows: T = 20 ± 2 °C; pH = 7.8 ± 0.2; hardness = 160 ± 16 mg/L; ionic strength = 0.0165 mol/L; dissolved oxygen = 6.5 ± 0.5 mg/L.

The end of the whole multigenerational test was delayed up to 72 days waiting for the appearance of the new generations [260]. The F0 first brood neonates constituted the F1 generation; the F1 first brood neonates constituted the F2 generation. All generations were exposed in the same way. Briefly, daphnids were used as parental generation (F0) and exposed to sub-lethal environmentally relevant concentrations of Ce and Er (1 µg/L, nominal concentration) as reported in the Introduction.

Class A glass beakers were used as test containers after acid washing (10% HCl in deionised water overnight), deionised water rising and oven sterilisation (120 °C overnight).

After 3, 7, 14, and 21 days (similarly to [260]) from F0, F1 and F2 exposures, organisms were assessed for the variation of adults' size (< 24 h old), average number of offspring produced per survived organism, survival (i.e. survivors at the end of each generational exposure compared to the exposed organisms), and growth

as the variation of length per unit time (mm/day). The same daphnids collected after 3, 7, 14, and 21 days of exposure of F0, F1 and F2 were further investigated for gene expression, determination of ROS, enzymatic activity, and uptake.

The growth as length variation per unit time (mm/day) was determined according to [260] by measuring the length of daphnids from the top of the head to the base of the apical spine. After 3, 7, 14, and 21 days, organisms were transferred from their beaker into a Petri dish and observed by carefully removing excess water until no movement of the organisms was observed. Organisms' pictures were taken by a stereo-microscope camera (Leica EZ4 HD) and processed with ImageJ2 [261]. Daphnids' growth rates ( $g_r$ ) were calculated from individual dry masses ( $L_1$  and  $L_2$ ) at successive times ( $t_1$  and  $t_2$ ) according to [262]:  $g = (\ln(L_2) - \ln(L_1)) / (t_2 - t_1)$ .

### **5.2.3 Reactive oxygen species and enzymatic activity**

After 3, 7, 14, and 21 days of exposure of F0, F1 and F2, samples (10 organisms from three of the six replicates containing each 30 daphnids) were randomly collected to analyse ROS production and the activation of antioxidant defence including superoxide dismutase (SOD), catalase (CAT), and glutathione S-transferase (GST). Each sample was homogenized with 0.1 mL of 50 mM potassium phosphate buffer solution (PBS) (pH 7.4) with 0.5 mM EDTA using a sterile pestle. Homogenates were centrifuged for 20 min at 15000g (4 °C). The protein concentration of each sample was measured in three replicates using a spectrophotometer (Hach-Lange DR 5000) according to [263] method. ROS content and activity of SOD, CAT and GST were measured using Sigma-Aldrich kits according to manufacturer's similarly to [264].

### **5.2.4 Gene expression**

After 3, 7, 14, and 21 days of exposure of F0, F1 and F2, samples (10 organisms from three of the six replicates containing each 30 daphnids) were randomly collected to analyse the expression of *abcb1* (ATP binding cassette subfamily B

member 1) and *abcc1/3*, *Abcc4* and *Abcc5* (ATP binding cassette subfamily C) genes according to [265].

Target genes' mRNA was quantified with quantitative real-time polymerase chain reaction (Real-Time qPCR) (Power SYBR Green Master Mix kits, Life Technologies, Thermo Fisher Scientific, Waltham, MA, USA). Total RNA was extracted from *D. magna* at day 3, 7, 14 and 21 for F0, F1 and F2. Samples were treated using Tri-Reagent (Sigma, St. Louis, MO, USA) according to the manufacturer's recommendations. From an amount of 1 µg of total RNA, cDNAs were synthesized using the Super Script VILO cDNA synthesis kit (Life Technologies, Thermo Fisher Scientific, Waltham, MA, USA) following the manufacturer's instructions.

Real-time qPCR was carried out in 96-well optical reaction plate in a 20 µL total reaction volume. The reaction solution and amplification reactions were in accordance to [266] and [267], respectively. A melting curve analysis of PCR products was performed from 60 °C to 95 °C in order to ensure gene-specific amplification.  $\beta$ -actin [265] was designed as an endogenous reference (i.e. housekeeping gene). cDNA from samples of adult *Daphnia* were used as controls. Primers used to detect *abcb1*, *abcc1/3*, *Abcc4*, and *Abcc5* [265] are shown in Table 14.

| Gene Name      | Oligo Forward Sequence | Oligo Reverse Sequence |
|----------------|------------------------|------------------------|
| <i>abcb1</i>   | GTATCCAGTGC GGAAGTGGC  | ACAGCGTATCGCTATTGCC    |
| <i>abcc1/3</i> | TAGCTCGCGCTCTACTGAGAA  | GATCGTCGGTCTCCAGATCG   |
| <i>Abcc4</i>   | CCCGATCCCTTTACGTTCGAT  | GGTGGCGTCCTACATGAGTGT  |
| <i>Abcc5</i>   | CAGTCCAGTCATCGAGAACGG  | TGACGCAACAGAGCTCGG     |
| <i>B-actin</i> | TTATGAAGGTTACGCCCTGCC  | GCTGTAACCGGTTTCAGTCAA  |

Table 15 Primer sequences of the genes used for real time protein chain reaction (RT-PCR)

### 5.2.5 Uptake of Ce and Er

Organisms were randomly collected (10 organisms from three of the six replicates containing each 30 daphnids) after 3, 7, 14, and 21 days from F0, F1 and F2. Ce

and Er concentration in daphnids' biomass followed [268]. Organisms were dried (65 °C) for 24 h and digested in aqua regia (HNO<sub>3</sub>/HCl =2:1, v/v) using a microwave oven (START D - Microwave Digestion System, Milestone S.r.l.) and analysed via ICP-MS as previously described in paragraph 5.2.1. Organisms were carefully rinsed with deionised water before the analytical procedure took place.

### **5.2.6 Statistical analysis**

Median effects concentrations were expressed as mean values and the relative standard deviation (95%) for both Ce and Er for the acute LC50s. Mortality data were normalized on negative controls with Abbott's formula  $((x_1 - x_0) / (100 - x_0) * 100)$  where  $x_1$  = treatment effect;  $x_0$  = negative control effect) [269]. Differences between treatment were assessed via one-way and two-way analysis of variance (ANOVA) to consider any difference between and within generations after the verification of normality and homoscedasticity.

Any difference in gene expression was checked via the Student t-test ( $\alpha$  = 0.05) considering populations before and after treatments. The *post-hoc* Tukey's test accounted for differences within groups setting the statistical significance at  $p < 0.05$ . Statistical analysis was carried out via SigmaPlot (Systat Software, San Jose, CA).

## **5.3 RESULTS AND DISCUSSION**

### **5.3.1 Chemical characterization of testing solutions**

Results from ICP-MS were summarized in Table 15 and indicated that Ce and Er were kept constant within 0.2 and 1.66 mg/L (i.e. 0.54 mg/L, mean value) and 0.2 and 0.97 mg/L (i.e. 0.43 mg/L, mean value), respectively. Measured concentrations used for concentration-response curves in acute tests were: 7.5, 124.5, 1228.5 and 10222.5 mg/L for Ce, and 10.5, 134.5, 1366.5, and 14568.5 mg/L for Er.

| Time (days) | Ce ( $\mu\text{g/L}$ ) | Er ( $\mu\text{g/L}$ ) |
|-------------|------------------------|------------------------|
| 3           | $1.28 \pm 0.17$        | $0.71 \pm 0.05$        |
| 7           | $0.34 \pm 0.08$        | $0.25 \pm 0.07$        |
| 14          | $0.24 \pm 0.10$        | $0.02 \pm 0.01$        |
| 21          | $0.20 \pm 0.03$        | $0.10 \pm 0.01$        |
| 24          | $1.66 \pm 0.06$        | $0.78 \pm 0.03$        |
| 28          | $0.43 \pm 0.02$        | $0.64 \pm 0.04$        |
| 35          | $0.41 \pm 0.02$        | $0.11 \pm 0.02$        |
| 42          | $0.31 \pm 0.03$        | $0.19 \pm 0.03$        |
| 45          | $0.69 \pm 0.05$        | $0.97 \pm 0.03$        |
| 49          | $0.36 \pm 0.07$        | $0.86 \pm 0.05$        |
| 56          | $0.27 \pm 0.07$        | $0.23 \pm 0.03$        |
| 63          | $0.27 \pm 0.05$        | $0.25 \pm 0.03$        |

Table 16 Ce and Er concentrations ( $\mu\text{g/L}$ ) during the exposure period corrected for background concentrations of Ce and Er in the control water.

### 5.3.2 Acute effects (48 h) of Ce and Er on *D. magna*

Acute LC50s for Ce and Er in *D. magna* were determined according to a 48 h static concentration-response toxicity test as reported in Figure 25. The LC50 ( $\pm 95\%$  confidence limit values) for Ce is 244.59 (81.94e934.26) mg/L ( $Y = -27.18 (\pm 9.08) + 14.03 (\pm 1.42) \ln(X)$ ;  $r^2 = 0.98$ ; standard error estimate = 7.629; normal distribution and constant variance).

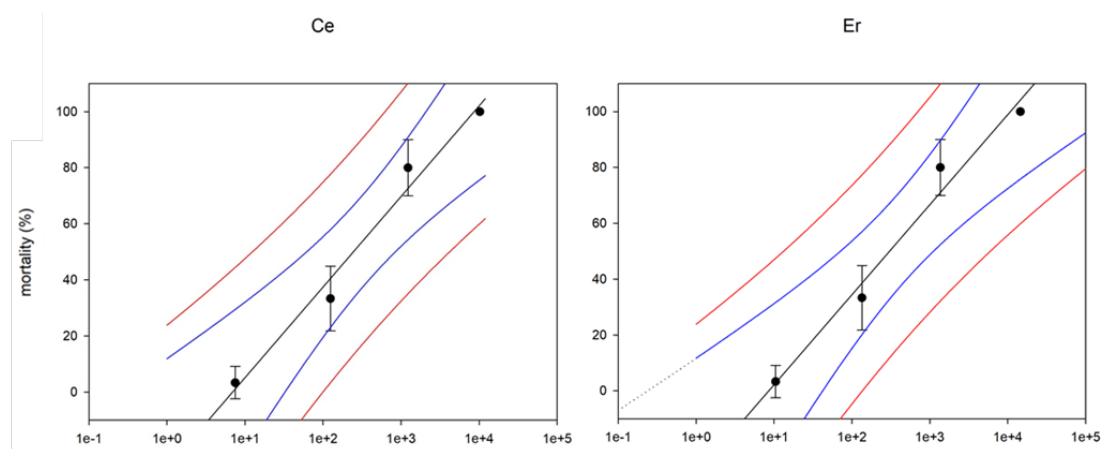


Figure 25 Concentration-response curves for Ce and Er after  $\ln$ -regression including 95% limit values regressions.

The LC50 for Ce determined in this paper is lower than [15] LC50 (26300 ± 3500 mg/L in artificial freshwater, and >50000 mg/L in natural lake freshwaters). In particular, they used as Ce source CeNO<sub>3</sub> 6H<sub>2</sub>O instead of CeCl<sub>3</sub> 7H<sub>2</sub>O, and the LC50 is based on nominal concentrations. The LC50 (±95% confidence limit values) for Er is 304.03 (94.18e1293.02) mg/L ( $Y = -30.06 (\pm 9.71) + 14.03 (\pm 1.47) \ln(X)$ ;  $r^2 = 0.98$ ; standard error estimate = 7.920; normal distribution and constant variance). Currently, no other LC50 data of Er on *D. magna* are available.

### **5.3.3 Growth rate, first brood appearance and offsprings production**

In Table 16, data about the organism's growth rate (gr), first brood (day- days of appearance after the test start), and the number of offspring per parental animal were summarized for both Ce and Er for F0, F1, and F2, including also the negative controls. About the growth rate, results evidenced constant values for negative controls (1.2-1.3 gr) along generations. In the case of Ce, values ranged from 1.2 (F0) and 1.6 (F1) to 1.3 (F2), suggesting slight growth stimulatory effects in F1. In the case of Er, values ranged from 1.0 (F0) and 1.7 (F1) to 1.5 (F2), indicating a greater growth stimulatory effect than Ce, especially in F1. The time required for the appearance of the first brood was very similar in all negative controls (8-9 days) as well as for Ce (7-10 days). Er produced a constant delay in the appearance of the first brood approximately doubling the negative control values (20-21 days) with no differences between generations (F0, F1 and F2). About the number of generated offspring per parental animal, values were constant for the negative controls (68-72 offspring). The amount of generated offspring was like negative controls for Ce in F0 and F1, while in F2 it was halved (only 36 offspring). Er showed an inhibitory effect in offspring generation in F0 and F2 (44 and 40 generated offspring, in that order), but the amount of generated offspring in F1 was like F1 negative control. These results suggested that the long-term chronic multigenerational exposure of *D. magna* to Ce produced no effects about organisms' growth rates and first brood emergence, but impaired offspring production in F2. Er exposure significantly affected both the first brood emergence and the amount of generated offspring in F0 and F2, but not in F1. For both Ce and Er, F1 generations showed slight stimulatory effects for growth rate and generated offspring similarly to [270] and [255], respectively. These effects completely disappeared in F2. Thus, in general, any maternal effect was clearly identified from F0 to F1 and from F1 to F2 for both Ce and Er.

| <b>Generations</b> | <b>Treatments</b> | <b>Growth rate (gr)</b> | <b>First brood (day)</b> | <b>Offspring per parental animal</b> |
|--------------------|-------------------|-------------------------|--------------------------|--------------------------------------|
| <b>F0</b>          | control           | 1.2                     | 9                        | 70                                   |
|                    | Ce                | 1.2                     | 10                       | 64                                   |
|                    | Er                | 1.0                     | 20                       | 44                                   |
| <b>F1</b>          | control           | 1.3                     | 8                        | 68                                   |
|                    | Ce                | 1.6                     | 8                        | 75                                   |
|                    | Er                | 1.7                     | 21                       | 64                                   |
| <b>F2</b>          | control           | 1.2                     | 8                        | 72                                   |
|                    | Ce                | 1.3                     | 7                        | 36                                   |
|                    | Er                | 1.5                     | 20                       | 40                                   |

*Table 17 Chronic toxicity effects on growth rate, day of first brood, and offspring produced for parental animal for both Ce and Er*

The Ce and Er cumulative mortality in F0, F1 and F2 on *D. magna* was summarized in Figure 26 after data normalization on negative controls (i.e. percentage of effect in negative controls was always  $\leq 10\%$ ). For Ce, dead organisms at the end of each generation tended to decrease, suggesting the presence of phenotypic adaptation mechanisms (i.e. detoxification). Also, F1 and F2 generations appeared earlier compared to the previous ones (i) F1 after 10 + 8 days; and ii) F2 after 10 + 8+7 days, as reported in Table 16, and similarly to negative controls. The maximum mortality was obtained for F0, F1 and F2 only at the end of each relative exposure period and up to 48%, 21% and 27%, in that order.

For Er, dead organisms slightly increased from F0 (40%) to F1 (45%), and decreased in F2, but in F2 the mortality was constant approximately for one week before the end of the exposure period (approximately 22%). The cumulative distribution curves of Er (Fig. 26) evidenced that compared to Ce, the new *D. magna* generations (F1 and F2) were delayed of 13 days (F1) and 12 days (F2) compared to negative controls and approximately 20 days to previous generations (F0 and F1, respectively) (Table 16).

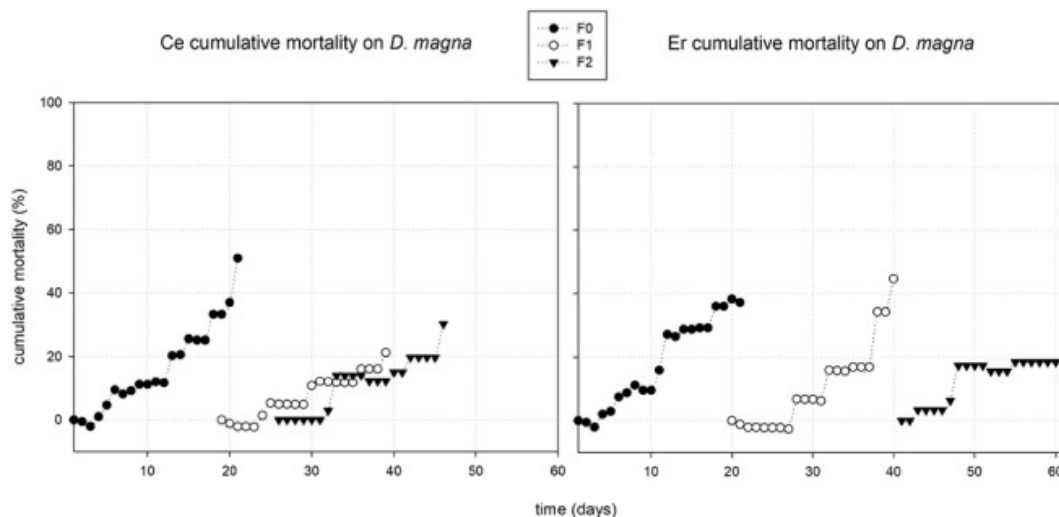


Figure 26 Ce and Er cumulative mortality in *D. magna* along generations (F0, F1 and F2) normalized to negative controls.

Thus, Er showed greater adverse effects compared to Ce. We can speculate about the exposure of *D. magna* to Er and the alteration of the consumption of lipid energy sources delaying reproduction (i.e., the lipid fraction is mainly involved in egg production and embryo development). As suggested by [260], the cellular energy allocation in *D. magna* is characterized by lipids (>50%), being a quite sensitive energy-reserve fraction able to change rapidly in response to stressing events. This hypothesis needs further investigations to be confirmed since the lipid fraction in the exposed daphnids was not assessed during this study.

### 5.3.4 Reactive oxygen species and enzymatic activity

ROS results were summarized in Figure 27 A for Ce and in Figure 27 B for Er after data normalization on negative controls including all generations. Statistical comparisons between effects due to contact time duration (3, 7, 14 and 21 days) and generations (F0, F1 and F2) were made available. For Ce (Fig. 27 A), no well-defined trends during the monitoring period were highlighted. At day 3, all generations presented values of ROS > 50% fluorescence, even if slightly decreasing from F0 to F1 ~ F2. At day 21, values substantially decreased even below 20% (F2) evidencing *D. magna* adaptation/detoxification abilities during Ce exposure. At day 14, ROS values increased up to values greater or comparable to

day 3, probably because organisms were collected soon after reproductive events. For Er (Fig. 27 B), ROS values were averagely greater than Ce, confirming that Er toxicity is greater than Ce as previously observed in paragraph 5.3.3 ROS values for F0 and F1 along the monitoring period (at day 3, 7, 14 and 21) presented a slight decrease (from values > 60% to values up to 40%, except for F2). ROS values at day 7 and 14 remained constant (F0 and F1) or significantly increased (F2, day 14) compared to previous scenarios (day 3 and day 7) just before *D. magna* reproductive events especially in F2 (day 20). At day 21, ROS values significantly decreased only for F2 (22%), while they still ranged up to 40% for F0 and F1, suggesting, like for Ce, potential adaptation/detoxification abilities.

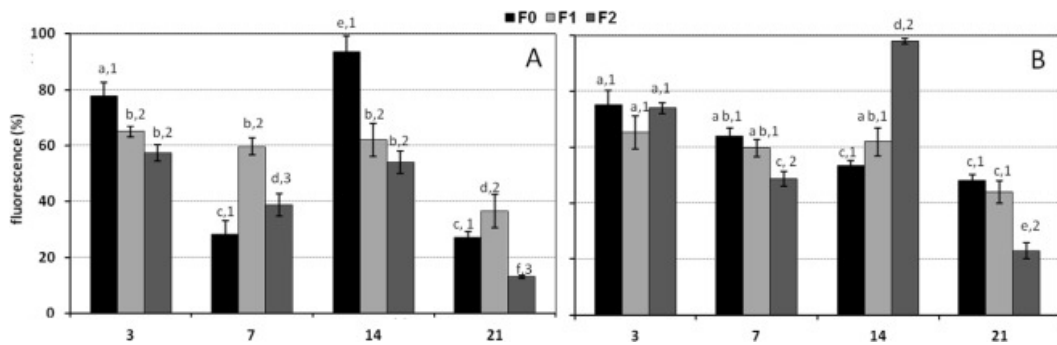


Figure 27 ROS production in *D. magna* exposed to Ce (panel A) and Er (panel B) along generations after normalization on negative controls. Results are presented as mean  $\pm$  SD ( $n = 3$ ). Letters (a-e) indicate significant differences between treatments (exposure times: 3, 7, 14 and 21 days), while numbers (1-3) significant differences between generations (F0, F1 and F2); the level of significance was set at  $\alpha \leq 0.05$  (ANOVA).

Antioxidant enzyme activity for CAT, SOD and GST were summarized in Figure 28. For Ce as reported in Fig. 28 A, CAT activity decreased during the exposure from day 3-21 for F0 and F1 and keeping constant relative values for F0 ( $177.8 \pm 10.1$  U/mg) and F1 ( $179.3 \pm 3.6$  U/mg) after day 3. In F2, CAT activity was constant during the exposure time ( $31.7 \pm 7.5$  U/mg). The average relative CAT activity per generation was always lower than the previous generation, approximately halving their values, suggesting decreased antioxidant abilities of *D. magna*. For Er, as reported in Fig. 28 B, CAT significantly decreased only at day 21 for F0 and F1, and in F2 values were lower than for Ce. For Ce as reported in Fig. 28 C, SOD

decreased from day 3-21 in all generations presenting at day 21 no significantly different concentrations between F0, F1 and F2. This suggests that each generation presented the same ability of superoxide dismutation. SOD activity seemed to be influenced mainly by exposure duration as showed by [271]. For Er (Fig. 28 D), SOD decreased in all generations from day 3 to day 21, but higher SOD relative values were found compared to Ce, suggesting that Er presented increased antioxidant capacities. Anyway, SOD levels at day 21 were not significantly different in F0, F1 and F2 evidencing the current ability of *D. magna* in managing the superoxide ( $O_2^-$ ) radicals.

GST activity for Ce (Fig. 28 E) was relatively low ranging between 13.6 and 57.2, 0e16.3, and 0.2e24.4 U/mg for F0, F1, and F2, in that order. This suggested that phase II metabolic pathways are scarcely involved in the detoxification process. GST activity for Er (Fig. 28 F) did not present a clear trend with the highest values in F1 ( $106.0 \pm 5.1$  U/mg) and F2 ( $106.0 \pm 6.3$  U/mg) at day 3, F0 at day 7 ( $160.2 \pm 3.2$  U/mg) and F2 at day 14 ( $94.2 \pm 5.3$  U/mg) in a way that seems to be independent from other events like reproduction (first brood) or the number of produced offsprings (Table 15). Thus, Er confirmed its higher toxicity than Ce, stimulating in *D. magna* the activation of phase II detoxification processes. Currently, the potential effects of high oxidizing levels between generations on the viability and growth of organisms remained substantially unexplored, due to the lack of correlations between existing data, and due to the fact that epigenetic endpoints were not taken into consideration. Falanga et al. [272] showed that effects on metabolomics across generations could be influenced by toxicant uptake and accumulation showing that the physiological state of the organism could influence the uptake and detoxification, sequestration, and elimination processes causing toxicity.

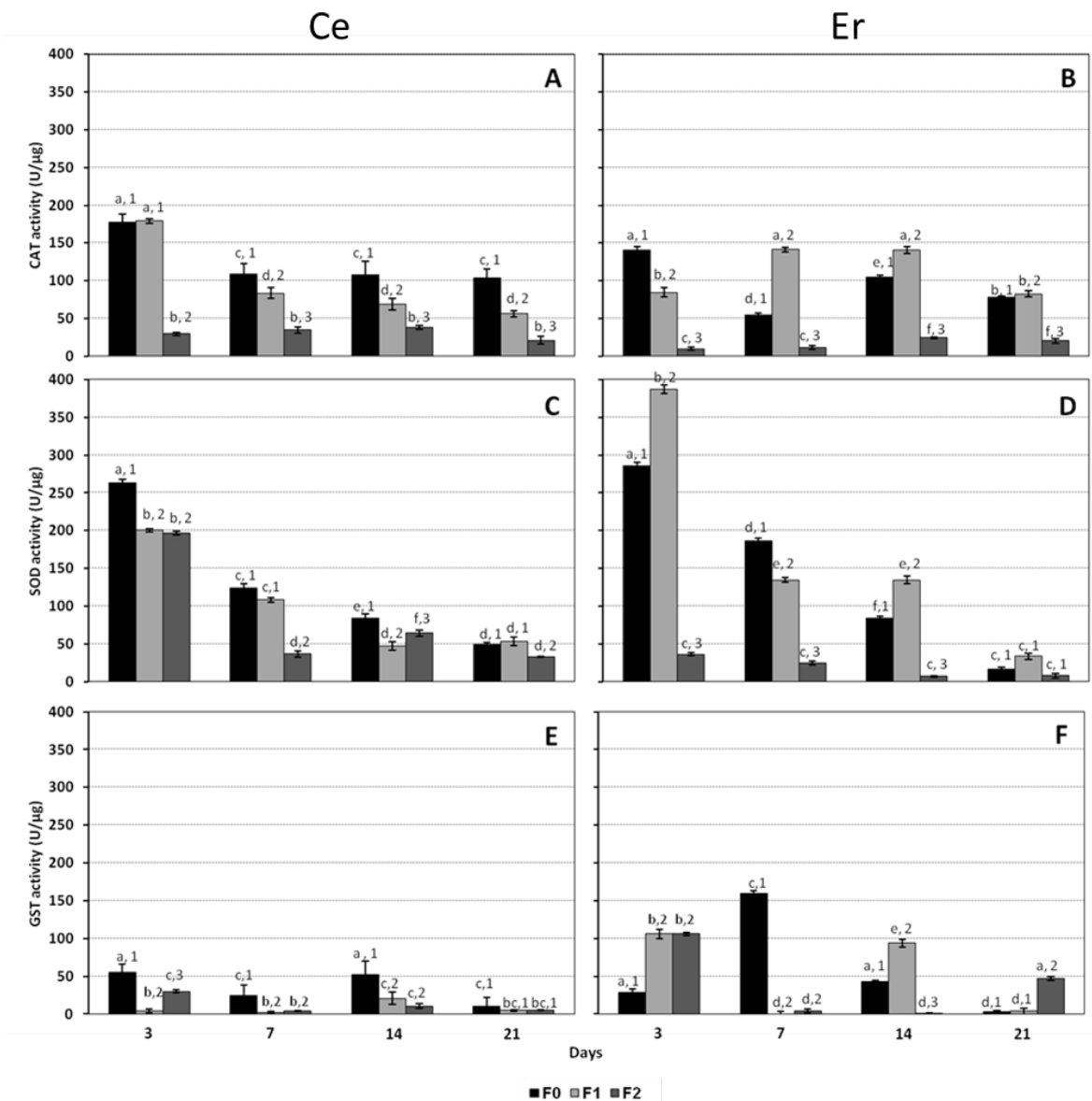


Figure 28 Antioxidant enzyme activities after normalization on negative controls; error bars represent standard deviations. Letters (a-f) indicate significant differences between exposure times (3, 7, 14 and 21 days), while numbers (1-3) between generations (F0, F1 and F2); the level of significance was set at  $\alpha=0.05$ ; CAT, SOD and GST were expressed as U/ $\mu\text{g}$  protein; A, C and E are referred to Ce and B, D and F to Er.

### 5.3.5 Gene expression

Results about the modification of ATP-binding cassette (ABC) gene expression in *D. magna* at day 3, 7, 14 and 21 were reported in Figure 29 (A, B, C and D) after treatment with Ce and in Fig. 29 (E, F, G and H) after exposure to Er. For Ce, in Fig. 29 A, the *abcb1* gene was upregulated in F0 on days 3 and 7, downregulated

on day 14 and then the expression level returned to normal at day 21. In F1, the gene was always downregulated. Finally, in F2, it was downregulated on days 3 and 7 and normal regulated on days 14 and 21.

In Fig. 29 B, the *abc1/3* gene was upregulated in F0 on days 3 and 7 and then the expression level returned to normal on days 14 and 21. At F1 generation, the gene was always downregulated. In F2, it was downregulated on days 3 and 7 and almost normal on day 14. The expression was normal regulated on day 21.

In Fig. 29 C, the *Abcc4* gene was. in F0 generation, upregulated on days 3 and 7, downregulated on day 14 and then the expression level returned to normal on day 21. In F1, the gene was always downregulated. In F2, it was downregulated on days 3 and 7 and almost normally regulated on days 14 and then the expression returned to background levels on day 21.

In Fig. 29 D, the *Abcc5* gene was upregulated on days 3 and 7 in F0 and downregulated on day 14 and 21. In F1, the gene was always downregulated. Finally, in F2, it was downregulated on days 3 and 7 and normal regulated on days 14 and 21.

For *Er*, in Fig. 29 E, the *abcb1* gene was upregulated on day 3 in F0. The expression was normal on day 7, downregulated on day 14 and then the expression level returned normal to day 21. At F1 generation, the gene was always downregulated. Finally, in F2, it was normal expressed on days 3 and 7 and downregulated on days 14 and 21.

In Fig. 29 F, the *abc1/3* gene was upregulated on day 3 in F0. The expression was normal on day 7, downregulated on day 14 and then it was upregulated at day 21. In F1, the gene was normally expressed on days 3 and 7, and downregulated on days 14 and 21. Finally, in F2, it was downregulated on days 3, 7 and 14, and normally regulated on days 21.

In Fig. 29 G, the *Abcc4* gene was upregulated on days 3 in F0 and downregulated on days 7 and 14, while on day 21 the gene was overexpressed. In F1, the gene was always downregulated. Finally, in F2, it was always normally regulated.

In Fig. 29 H, the *Abcc5* gene was upregulated on day 3 in F0, downregulated on days 7 and 14 and then the expression level upregulated again on day 21. In F1, the gene was always downregulated. Finally, it was always normally regulated in F2.

In general, there was a statistically significant alteration in treated daphnids ( $p < 0.05$ ) (Fig. 29). The treatment with Ce (Fig. 29 A, B, C and D) upregulated all genes in F0 on day 3. In the following

days the expression was reduced. Thus, expression levels were back to background levels on day 21. During F1, all genes downregulated, while during F2, they showed an initial downregulation that was normalized on day 21. In agreement with the bioaccumulation data, a greater expression of analysed genes was observed in F0 corresponding to a greater uptake of Ce. In contrast, F1 seemed to be very sensitive to the toxic effect of Ce showing an inhibition of the expression of all genes. In F2, the genes expression was normalized at day 21 when the uptake of Ce was reduced. In the case of Er (Fig. 29 E, F, G and H), F0 showed upregulation on day 3 of all genes which becomes comparable to control or downregulated on days 7 and 14. All genes were upregulated on day 21. The activity of Er during F0 was like that of Ce. F1 presented clear downregulation from day 3-21 except for *abcc1/3* that showed an expression comparable to control on days 3 and 7 followed by downregulation on days 14 and 21. During F2, it was observed downregulation for the *abcb1* and *abcc1/3* genes and an expression like the control for the *Abcc4* and *Abcc5* genes. These results indicated that initially, in F0, the daphniids activated the ABC transporter cassette to expel the foreign compound, but this activity was blocked during F1, similarly to Ce. F2 showed downregulation for *abcb1* and *abcc1/3* and a normal expression for *Abcc4* and *Abcc5*. Probably, there exist a different sensibility of daphniids to these toxicants along generations, suggesting that F1 could be the most sensitive. These results showed that Ce and Er can activate the ATP binding cassette indicating that organisms could reach an equilibrium between uptake and ejection along generations. Indeed, the membrane associated proteins belong to the superfamily of ABC transporters that are members of the MDR/TAP subfamily involved in multidrug resistance [273]. It was observed that toxicants can act in different ways as substrates and inhibitors of the cellular multixenobiotic resistance (MXR) system in *D. magna* [274]. The MXR is analogous to the multidrug resistance (MDR) in cancer cells or tissues against anticancer drugs limiting the efficiency of chemotherapy. It has been recently found that MXR-involved transporters are expressed in different stages of *D. magna* with high levels in neonates and adult life stages [265] and represents a defence-mechanism against environmental toxicants.

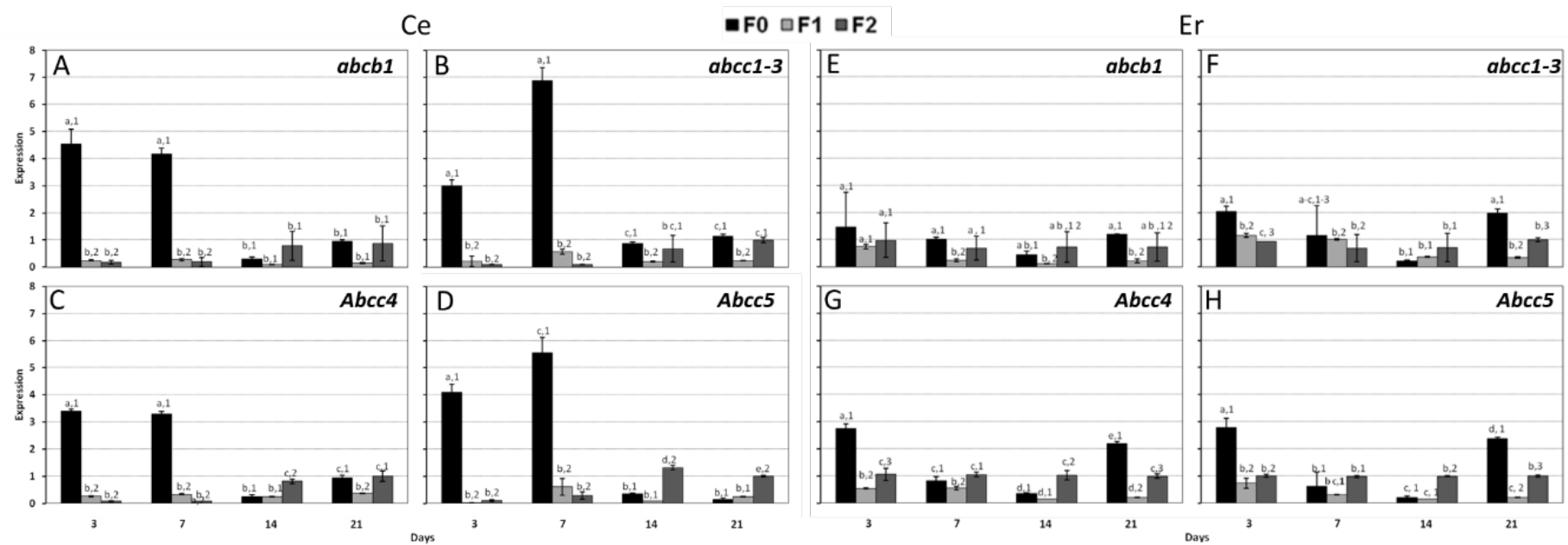


Figure 29 Real-time PCR analysis of the ATP-binding cassette (ABC) genes expression after treatment with Ce (A, B, C, and D) and Er (E, F, G and H) in *D. magna* F0, F1 and F2; gene expressions were evaluated with Student *t*-Test on control and treated daphnids; results are presented as mean  $\pm$  standard deviation ( $n = 3$ ) normalized to negative controls. Letters (a–e) indicate significant differences between contact times (3, 7, 14 and 21 days), while numbers (1–3) significant differences between generations (F0, F1 and F2); the level of significance was set at  $\alpha=0.05$ .

MXR is mediated by transport-membrane proteins belonging to the ATP binding cassette (ABC) protein family that identify chemical contaminants and pump them out of the cell keeping their levels in cells low. Similar activities are carried out by mammalian ABCB1 and ABCC proteins in higher organisms. Organisms with a strong MXR defence are less sensitive to toxic compounds because they cannot reach the respective site of action working as transporter substrates [274]. It was showed that MXR mechanisms are a part of the general response to stress, and Abcb1 and Abcc proteins have a role in the defence against xenobiotics transferring them out of the cells and keeping the intracellular concentration low[274]. If this activity is inhibited, the intracellular concentration of those compounds increased. As MXR activity affects both bioaccumulation and toxicity of chemicals, modulation of the activity may have ecotoxicological consequences. The activity of these proteins leads to a reduction in the intracellular concentration of various xenobiotics, thus reducing their toxicity. When the substrates are hydrophilic compounds with different moieties the activity of ABC transport is highlighted. Instead if the activity of the ABC proteins that keep xenobiotics out of cells is inhibited, the intracellular concentration of those compounds increases. Increasing levels of abcb1 and abcc1-3 to decrease the cytosolic concentrations of Ce and Er could reduce cell damage. The increase in ABC transporters expression under stress conditions has also been described by Navarro et al.[275]. MXR activity measurements in *D. magna* may provide valuable information about the effects of aquatic contaminants on this organism.

### 5.3.6 Uptake

Results about the uptake of Ce and Er were summarized in Figure 30 for F0, F1 and F2, including negative controls as well. In negative controls, the average Ce content per unit mass was of 20 ng/g, while the average concentration in exposed organisms (i.e. considering all generations) was averagely of 558 ng/g. According to Fig. 30, the Ce uptake showed a similar trend in F0, F1, and F2, presenting higher levels at the beginning of the exposure and a stabilization of the uptake concentration after day 14. At day 21, F0, F1 and F2 presented the following level of Ce:  $215 \pm 28$ , 331

$\pm 27$ , and  $290 \pm 43$  mg/g, in that order. These values decreased of 83%, 80%, and 59% compared to their relative value at day 3.

In negative controls, the average Er content per unit mass was of 41 ng/g, while the average concentration in exposed organisms (i.e. considering all generations) was averagely of 468 ng/g. Like for Ce, the Er uptake showed a similar trend in F0, F1, and F2, presenting higher levels at the beginning of the exposure, while its concentration started to significantly drop down after day 7, stabilizing after day 14 at values lower than day 3 of 82%, 72%, and 71% for F0 (312 ng/g), F1 (472 ng/g), and F2 (620 ng/g), in that order. Thus, both Ce and Er behaved similarly during the monitoring period (3, 7, 14, and 21 days), even though Ce was averagely uptaken more than Er. Uptake concentrations did not significantly correlate (analysis not reported here) with the parameters from Table 15, stating that the growth rate, the first brood emergence and the amount of offspring generated per parental animal are not affected by Ce and Er uptake. Similarly, uptake concentrations did not significantly correlate (analysis not reported here) with ROS concentrations, antioxidant enzyme activities and ABC gene expression. Such a result could be explained considering the mechanisms of self-purification operated by daphnids [276], which were able to excrete the amount of Ce in excess respect to the concentration beneficial for the organisms. The time required by Ce and Er to reach a stable uptake concentration in daphnids could be related their ability to excrete metals through faeces in a time longer compared to that required for metal assimilation [277]. The final content of Ce in *D. magna* samples was close to the concentrations stated as having micronutrient properties [278]. [279] reported that the maximum uptake of Ce onto *Spirulina platensis* alga occurred in less than one day

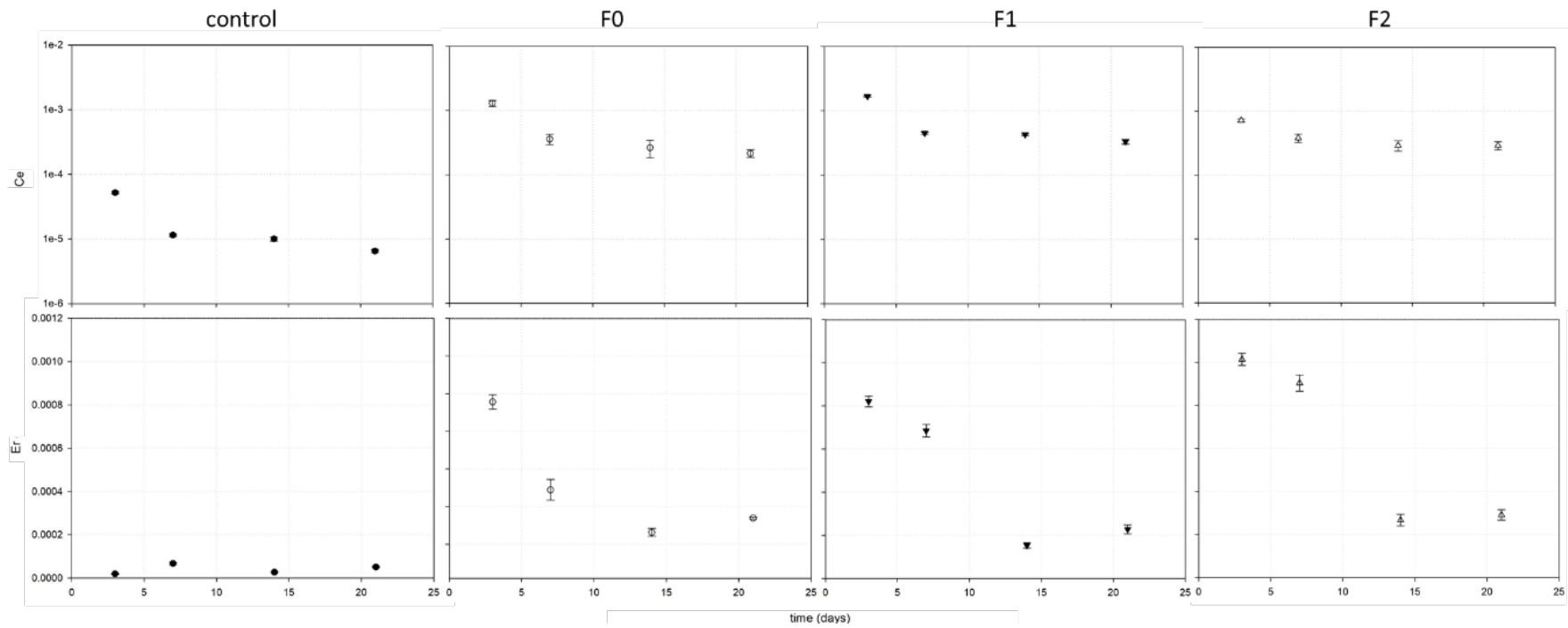


Figure 30 Ce and Er uptake ( $\mu\text{g/g}$ ) including negative controls considering F0, F1 and F2 exposure scenarios.

## 5.4 CONCLUSIONS

The long-term chronic multigenerational exposure (F0, F1 and F2) of *D. magna* to Ce and Er environmentally significant concentrations evidenced that:

- Organisms survival were reduced as their growth and reproduction compared to negative controls;
- Exposure decreased the enzymatic activity against oxidative stress (mainly ROS, SOD, and CAT) along F0, F1 and F2;
- ATP-binding cassette suggested that organisms could reach an equilibrium between uptake and ejection of both Ce and Er within three generations;
- Ce and Er behaved similarly during the monitoring period (3, 7, 14, and 21 days) with an uptake mean concentration of 558 and 468 ng/g, in that order;
- Any maternal effect was clearly identified from F0 to F1 and from F1 to F2 for both Ce and Er.

Multigenerational effects on physiological and biochemical responses were observed in *D. magna* with potential long-term repercussions. Further research is needed to strengthen the results about bioaccumulation (i.e. currently only Ce and Er uptake data are available) and to investigate the role of lipid content as an early warning marker to signal the exposure to stressing events. .

# CHAPTER 6

---

In this chapter, the results based on original contributions published in [11].

## 6.1 CERIUM AND LANTHANUM EFFECTS ON *RAPHIDOCELIS SUPCAPITATA* LONG-TERM MULTI-ENDPOINT EXPOSURE

Algae are primary producers and key organisms in the food chain allowing the potential biomagnification up to higher trophic levels of REEs with still unknown and unexpected effects on human health [10, 235, 280]. Some authors suggested that REEs could be uptaken and concentrated in chloroplasts, where the intracellular lanthanides could cross the internal membrane system until the replacement of magnesium in chlorophyll molecules [281-285]. Only a few microalgae species have been investigated mainly including *Chlorella vulgaris* and *Raphidocelis subcapitata* [280, 286-291]. The EC<sub>50</sub> of La was >10.1 mg/L for *Desmodesmus quadricauda* (50% inhibition after 22–23 days at 0.01 mg/L) and *Microcystis aeruginosa* [287], and >5.42 mg/L for *R. subcapitata* [20], and 51.72 (47.29–57.93) mg/L (i.e., nominal concentrations) [292], and 47.13 (45.30–51–56) mg/L (i.e., nominal concentrations) for *C. vulgaris* [292], and 4.38 (4.16–4.62) mg/L (i.e., nominal concentrations) for *Nitellopsis obtusa* [293]. The toxicity as EC<sub>50</sub> of Ce as Ce(NO<sub>3</sub>)<sub>3</sub> was from 3.15 to 6.32 mg/L (i.e., nominal concentrations) for *R. subcapitata* [20, 250]. Effects of Ce to *Desmodesmus quadricauda* at 0.001 mg/L evidenced biostimulation (16%) after 3 days [280], while in *Anabaena flosaquae*, after an initial biostimulation (16%, 3 days), showed inhibition (≈33%) at 5–10 mg/L after 17 days [288]. Most studies lacked environmentally relevant concentrations and REEs uptake [16, 294], like the main physiological mechanisms underlying REEs induced adaptation phenomena [249]. This research study investigated for the first time the effect of La and Ce considering a long-term exposure to *R. subcapitata* (i.e., 28 days renewal toxicity test). We investigated environmentally relevant concentrations looking at potential generational adaptations in microalgae supporting bioconcentration of La and Ce and hence their

possible transfer up to the food web. The multi-endpoint approach included the assessment of algal growth rate, determination of ROS, enzymatic activity, and uptake from exposure media.

## **6.2 MATERIAL AND METHODS**

### **6.2.1 Chemicals, testing solutions, and analytical characterization**

The experiments were carried out using commercially available chemicals: i) lanthanum(III) nitrate hexahydrate ( $\text{La}(\text{NO}_3)_3 \cdot 6\text{H}_2\text{O}$ , purity 97%); and ii) cerium(III) nitrate hexahydrate ( $\text{Ce}(\text{NO}_3)_3 \cdot 6\text{H}_2\text{O}$ , purity 97%) purchased from Sigma-Aldrich (Saint Louis, United States of America). Treatment solutions of La and Ce were prepared by adding REE solution (1000 mg/L) to artificial freshwater [241] at least 1 h before the exposure. The pH was measured with a pH-meter (Mettler Toledo Five Easy, Milan, Italy) prior to exposure and samples collection (day 3, 7, 14, 21, and 28). La and Ce concentrations were determined by inductively coupled plasma mass spectrometry (ICP-MS NexION 350 $\times$ , PerkinElmer, Inc., MA, USA). The limits of detection (LOD) and quantification (LOQ) were for La and Ce as follows: 0.0011 and 0.0010  $\mu\text{g/L}$  as LOD; and 0.0037 and 0.0033  $\mu\text{g/L}$  as LOQ. The calibration referred to the following standards: i) Lanthanum Standard for ICP (i.e., standard reference materials (SRM) from NIST  $\text{La}(\text{NO}_3)_3$  in  $\text{HNO}_3$  2–3% 1000 mg/L La Certipur®); Cerium Standard for ICP (i.e., SRM from NIST  $\text{Ce}(\text{NO}_3)_3$  in  $\text{HNO}_3$  2–3% 1000 mg/L Ce Certipur®). Analyses were carried out in triplicate on samples collected after day 7, 14, 21, and 28. About bioaccumulation experiments (i.e., explained in detail in the below sections), filters and organisms were dried at 65 °C for 24 h and digested in aqua regia ( $\text{HNO}_3/\text{HCl} = 1:3$ , v/v) using a microwave oven (START D, Microwave Digestion System, Milestone S.r.l.) and analysed via ICP-MS including the relative controls.

### **6.2.2 Cell culture conditions and *R. subcapitata* growth inhibition (GI) test**

Axenic cultures of *R. subcapitata* were maintained at the Hygiene Laboratory of the Department of Biology of the University of Naples Federico II in artificial freshwater ISO (2012) [241]. Preliminary algal growth inhibition tests (72 h) were performed according to ISO [241] in order to reflect the physiological status of algal cells [295]. Treatment solutions were prepared into each volumetric flask and organized in the following experimental design (i.e., nominal concentrations) to calculate the effective inhibition concentration at 10% (EC10) at pH = 7.8: i) from 0.7 mg/L to 5.5 mg/L for La; ii) from 1.0 mg/L to 8.4 mg/L for Ce. Algae were kept in a climatic growth chamber at constant temperature ( $24 \pm 2$  °C) and light conditions ( $100 \pm 10 \mu\text{E m}^{-2} \text{s}^{-1}$ ), and performing continuous shaking during maintenance and testing (50 rpm). After 72 h of exposure, the growth rate relative to the control was calculated by normalizing the final cell density of each replicate to control cultures (incubated in the absence of REEs).

### **6.2.3 A multi-endpoint experimental approach with *R. subcapitata***

Modified algal growth inhibition tests [241] were carried out for 28 days exposing microalgae to La and Ce into 250 mL volumetric flasks including four replicates and an inoculum of *R. subcapitata* of  $10^4$  cells/ mL. Exposure culturing media were spiked with La or Ce to obtain the relative EC10. All tested concentrations were analytically verified. Flasks were incubated for 28 days under the same conditions as the growth inhibition test. On day 3, 7, 14, 21, and 28, effects on microalgae were checked considering the optical density (OD) method (i.e., absorbance at 670 nm by Hach Lange DR5000 spectrophotometer). Algae were sampled after 7, 14, 21, and 28 days of exposure to analyse ROS production and the activation of antioxidant defence SOD and CAT, and to determine La and Ce concentrations bioaccumulated in the algal biomass. Solutions were partially renewed after each sampling period. Algae collection included two main aliquots: i) 100 mL of algae suspension were filtered ( $0.45 \mu\text{m}$  polycarbonate Millipore membrane under vacuum pressure) to check bioaccumulation (i.e., filters were rinsed six times with

ultrapure deionized water prior to acid digestion for chemical analysis); ii) 100 mL of algae suspension were centrifuged (1520g for 20 min, Beckman TJ-6, rotor 5-92, Milan, Italy) and the pellets were rinsed six times with ultra-pure deionized water prior to ROS, SOD, and CAT analysis. The remaining 50 mL of algae suspension were resuspended in freshly spiked La and Ce culturing media at the respective EC10 values at concentrations  $> 10^5$  cell/mL. A high-pressure homogenization method (French press cell, Thermo Electron Co., Waltham, MA, USA) was applied to the algal biomass at 78 atm to disrupt *R. subcapitata* cell wall. The extracts were suspended in potassium phosphate buffer solution (PBS 1 M at pH 7.4) and centrifuged for 20 min at 15,000g (4 °C). The supernatant was collected, and the protein concentration of each sample was measured using a spectrophotometer (Hach-Lange DR 5000) according to Bradfords method [263]. ROS content was quantified by the ability of free radicals to oxidize the non-fluorescent probe carboxy-H<sub>2</sub>DFFDA (Sigma Aldrich, Saint Louis, USA) to a fluorescent product that can be measured fluorometrically [296, 297]. SOD and CAT activities were carried out according to [298].

#### **6.2.4 Statistical analysis**

Median effects concentrations (EC50) and effective concentration at 10% inhibition (EC10) were expressed as mean values and the relative 95% confidence limit values for both La and Ce. Growth inhibition data were normalized on negative controls [241]. Differences between treatments were assessed via a two-way analysis of variance (ANOVA) after the verification of normality (Shapiro-Wilk (S-W) test) and homoscedasticity (Bartlett's (B) test). If samples are drawn from non-normal populations or do not have equal variances, the non-parametric method Kruskal-Wallis (K-W) ANOVA on ranks was taken into consideration. The *post-hoc* Tukeys test accounted for differences within groups setting the statistical significance at  $\alpha = 0.05$ . Pearson correlation coefficients ( $\alpha = 0.05$ ) were calculated between the values of biomarkers of stress and La and Ce bioconcentrated in microalgae. Statistical analysis was carried out using SigmaPlot (Systat Software, San Jose, CA) and GraphPad Prism (GraphPad, San Diego, CA, USA).

## 6.3 RESULTS AND DISCUSSION

### 6.3.1 72 h GI test

Data about 72 h GI were summarized after their normalization on negative controls in Figure 31. Measured concentrations used to calculate concentration-response curves were highlighted in Table 17. The pH values of solutions ranged between 7.60 and 8.00 (mean pH 7.80) all along the monitoring period.

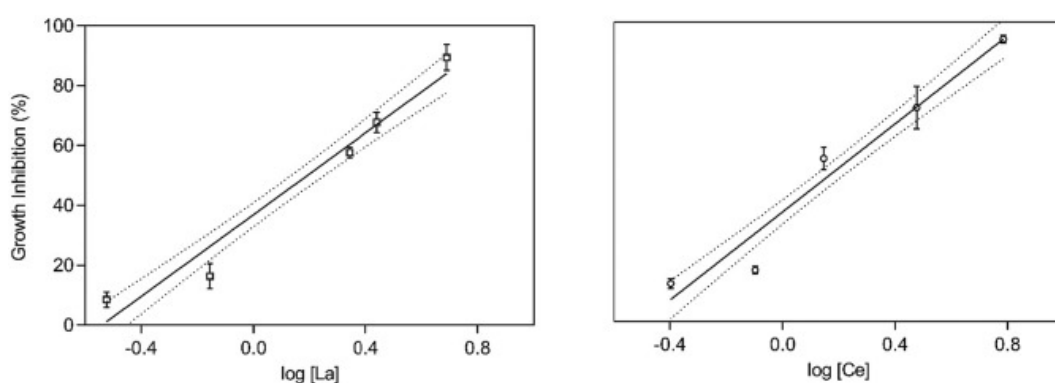


Figure 31 Concentration-response curves for La ( $Y = 68.72 * X + 37.09$ ,  $R^2 = 0.9555$   $std.err. = 6.976$ ) and Ce ( $Y = 75.34 * X + 35.38$   $R^2 = 0.9563$ ;  $std.err. = 8.350$ ) normalized to negative controls after semi-log regression, including 95% limit values ( $n = 4$ ).

| La      |             | Ce      |             |
|---------|-------------|---------|-------------|
| Nominal | Measured    | Nominal | Measured    |
| 0.7     | 0.30 ± 0.04 | 1.0     | 0.40 ± 0.04 |
| 1.4     | 0.70 ± 0.03 | 1.4     | 0.80 ± 0.02 |
| 2.2     | 2.20 ± 0.09 | 1.7     | 1.40 ± 0.08 |
| 2.8     | 2.80 ± 0.09 | 5.6     | 3.00 ± 0.05 |
| 5.5     | 4.90 ± 0.06 | 8.4     | 6.10 ± 0.07 |

Table 18 Nominal and measured (ICP-MS) La and Ce concentrations (mg/L) and the relative  $std.err.$  ( $n = 3$ ).

For La, the EC50 ( $\pm 95\%$  confidence limit values) and EC10 ( $\pm 95\%$  confidence limit values) were 1.6 (0.9–2.8) mg/L and 0.4 (0.2–0.8) mg/L, respectively ( $Y = 68.72 * X + 37.09$ ;  $R^2 = 0.95$ ; standard error ( $std.err.$ ) estimate = 6.98). For Ce, the EC50 ( $\pm 95\%$  confidence limit values) and EC10 ( $\pm 95\%$  confidence limit values) were 1.6

(0.9–2.8) mg/L and 0.5 (0.3–0.7) mg/L, respectively ( $Y = 75.34 * X + 35.38$ ;  $R^2 = 0.9563$ ;  $\text{std.err. estimate} = 7.2$ ). La and Ce showed comparable growth inhibitory effects, with EC50 values of approximately 1.5 mg/L, which is in line with previous findings [250, 252, 291]. As a consequence, for the 28 days long-term tests, testing media were spiked with 0.4 mg/L and 0.5 mg/L of La and Ce (i.e., EC10 values), respectively, simulating the exposure deriving from ore mine effluents [97].

### 6.3.2 Long-term exposure effects

Data about La and Ce cumulative growth inhibition after 3, 7, 14, 21, and 28 days were summarized in Figure 32 after data normalization on negative controls. Data were normally distributed (S-W) and presented equal variances (B test).

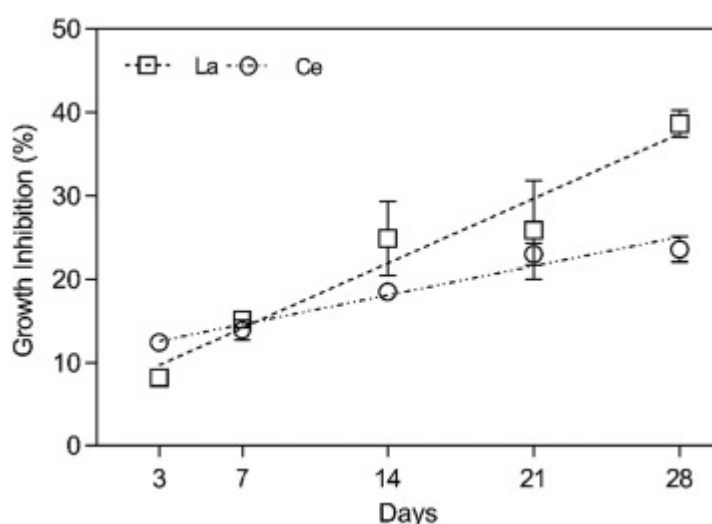


Figure 32 La (0.4 mg/L) and Ce (0.5 mg/L) cumulative growth inhibition of *R. subcapitata* after 3, 7, 14, 21, and 28 days of exposure normalized to negative controls ( $\pm \text{std.err.}$ ;  $n = 4$ ); La:  $Y = 0.4991 * X + 11.15$ ,  $R^2 = 0.7890$ ,  $\text{std.err.} = 2.307$ ; Ce:  $Y = 1.108 * X + 6.446$ ,  $R^2 = 0.7714$ ,  $\text{std.err.} = 5.773$

For La, GI increased three times from day 3 (8%) to day 14 (27%), being constant approximately for one week, then increased again at the end of the exposure period (38%). At the end of each week, the GI of Ce tended to slightly increase doubling from 12% (day 3) to 24% (day 28), thus suggesting an increased susceptibility along time. No significant differences (ANOVA,  $p > 0.05$ ) were observed after day 3, 7,

14, and 21 between La and Ce. A statistically significant difference ( $p < 0.05$ ) was found on day 28, where La was more toxic than Ce. The slow increase of toxic effects during the 28 days exposure period can suggest the presence of nutrient depletion phenomena rather than toxicity per se. It was reported that REEs could sequester essential nutrients such as phosphates producing death by starvation [299, 300]. This hypothesis needs further investigations to be confirmed since this effect could influence the EC50 of REEs, thus, potentially, environmental decision-making procedures. Results about ROS were summarized for La and Ce after data normalization on protein activity in Figure 33. Data were normally distributed (S-W), and presented equal variances (B test). Statistical comparisons between effects due to contact time duration (7, 14, 21 and 28 days) were included in the same figure (*post-hoc* Tukeys test).

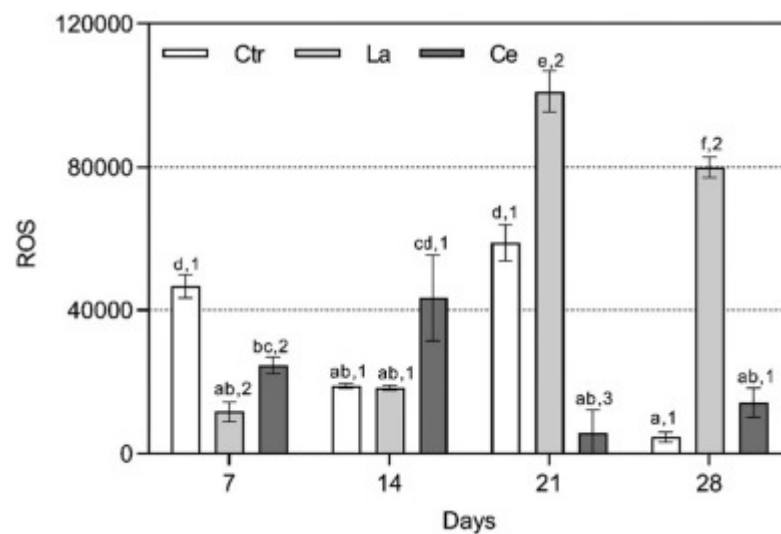


Figure 33 ROS production in *R. subcapitata* exposed to La and Ce lasting 28 days after normalization on protein content. Results are presented as mean  $\pm$  std.err. ( $n = 4$ ) in U/mg protein. Letters (a-f) indicate significant differences between exposure times (7, 14, 21, and 28) within treatments (La and Ce), while numbers (1–3) highlighted significant differences within exposure times (7, 14, 21, and 28) between treatments (La and Ce) ( $p < 0.05$ , Tukey's test).

For La, ROS production tended to increase during the 28 days exposure period and after day 14 was greater (days 21 and 28) than the negative control, evidencing the absence of adaptation/detoxification mechanisms. At day 7, La induced less ROS production, while at day 14 no statistical difference was found comparing the ROS

value from the control group. At days 21 and 28, ROS production drastically increased. Cerium exposure did not evidence any specific ROS trend with values substantially comparable between contact times. At 7, 21, and 28 days, Ce induced less, or comparable ROS levels compared to negative controls. Only at day 14, the microalgae exposed to Ce produced more ROS than the negative controls. Compared to La, *R. subcapitata* might follow a different detoxification strategy to contrast and/or clear the oxidative damage caused by ROS.

Data about CAT and SOD were summarized in Figure 34 (A and B, in that order) for both La and Ce after data normalization on protein content. Data were normally distributed (S-W), but they did not present equal variances (B test), so the K-W test was carried out. Generally, La and Ce had different effects on the activities of antioxidant enzymes at most of the considered scenarios compared to negative controls. The levels of CAT (Fig. 34A) and SOD (Fig. 34B) activities after La exposure were slightly enhanced after day 7 and remained constant approximately for the entire period of exposure from day 14 to day 28. CAT and SOD contents reached a maximum at day 14 with a value of 170 U/mg protein and 780 U/mg protein, respectively. About Ce exposure, the contents of CAT (Fig. 34A) and SOD (Fig. 34B) were at their minimum level. The highest CAT (400 U/mg protein) and SOD (2000 U/mg protein) activities appeared because of algal exposure to Ce after 14 days. At day 21 and 28, CAT activities were not significantly different ( $p > 0.05$ ).

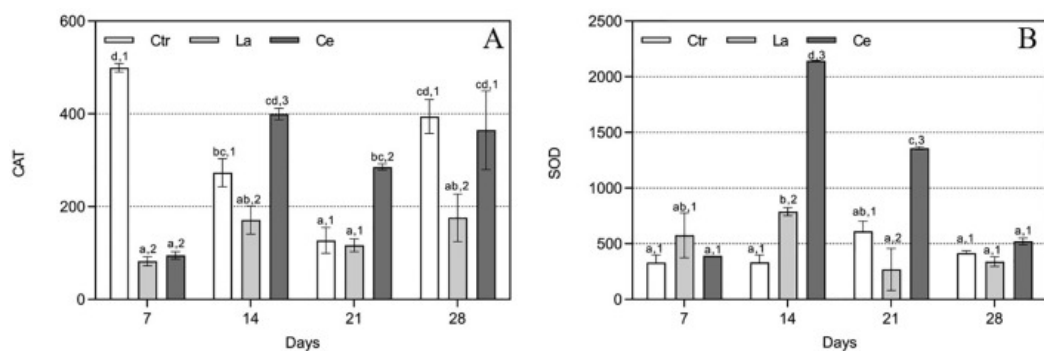


Figure 34 Antioxidant enzyme activities after normalization on protein content; CAT (A) and SOD (B) were expressed as U/mg protein. Results are presented as mean  $\pm$  std.err. ( $n = 4$ ). Letters (a–d) indicate significant differences between exposure times (7, 14, 21, and 28) within treatments (La and Ce), while numbers (1–3) highlighted significant differences within exposure times (7, 14, 21, and 28) between treatments (La and Ce) ( $p < 0.05$ , Tukey's test).

About SOD, at day 21 the activity significantly ( $p < 0.05$ ) decreased compared to day 14, reaching values in day 28 comparable to day 7 (i.e., being similar to negative control value too). Thus after 28 days of exposure, the levels of both CAT and SOD, being not significantly different from the respective negative controls, could suggest the reduction of oxidative stress via other detoxification mechanisms like for example phytochelatins (PCs) production [301] or bioconcentration. [301] observed that both calcium and lanthanum can influence the expression of PC synthase gene and cadmium absorption in *Lactuca sativa*. In particular, La(III) was able to enhance the mRNA level of LsPCS1 (i.e., phytochelatin synthase gene) and PCs accumulation. Other causes could be related to inactivation of enzymes by ROS, decrease in synthesis of enzyme, or change in the assembly of its subunits [302]. Comparatively, the activities of CAT and SOD in Ce exposure were higher than in La, suggesting that a lower antioxidative capacity was required to eliminate ROS generated by La-based treatments. Currently, little information about the mechanism of response to environmental stress in microalgae exposed to REEs is known. La and Ce treatments increased the oxidative stress and the activities of antioxidant enzymes (i.e., CAT and SOD) contributing to the elimination of ROS with peak activities at the intermediate monitoring periods (day 14 and 21). At the end of the exposure period (day 28), both La and Ce presented activity values similar or lower than the respective negative controls suggesting the potential development of tolerance to La and Ce due to the generational succession of *R. subcapitata* in 28 days (i.e., the culture was always kept in log-phase). This is something new compared to the existing knowledge about microalgae stress response also to other metals like cadmium, copper, chromium, and lead especially due to the extension of the exposure period from 15 days up to 28 days [303]. This is a challenging aspect for microalgae assemblages that could be further investigated considering suitable tolerance genes (i.e., rate of creation of tolerance genes by mutation, fitness cost of tolerance, and size of the population) on which the selection could act as already observed for other metals (e.g., copper from mining sites), but in macrophytes [304].

Results about La and Ce uptake in *R. subcapitata* were summarized in Figure 35 after their normalization to negative controls (i.e.,  $0.210 \pm 0.010$   $\mu\text{g La/g dry weight}$

(d.w.);  $0.368 \pm 0.030 \mu\text{g Ce/g d.w.}$ ). The average La content per unit mass was of  $2058 \mu\text{g/g d.w.}$  (i.e., mean of day 7, 14, 21, and 28 values) ranging from  $1442 \pm 459$ ,  $1684 \pm 347$ ,  $1947 \pm 296$ ,  $3157 \pm 265 \mu\text{g/g d.w.}$  at day 7, 14, 21, and 28. The amount of La in microalgae constantly increased from day 7 to day 28, substantially doubling its value in 21 days (day 28).

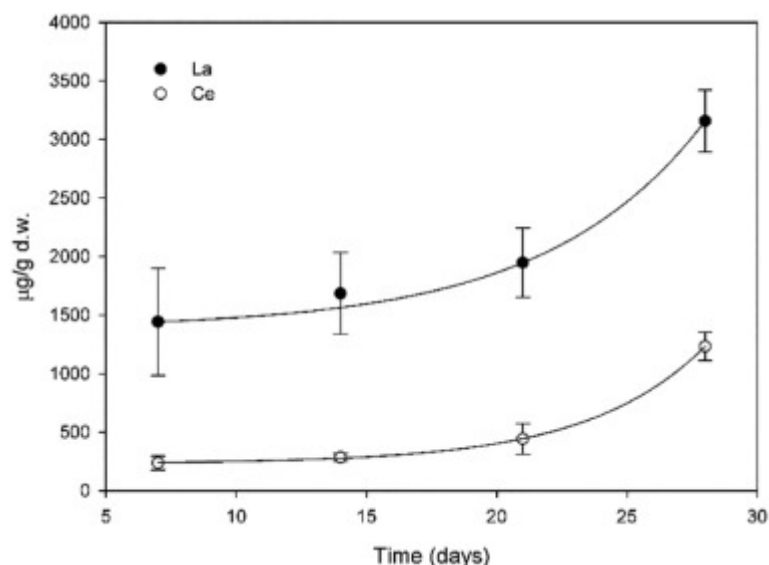


Figure 35 La and Ce uptake ( $\mu\text{g/g}$ ) in algal biomass at day 7, 14, 21, and 28 after normalization on negative controls; data are in  $\mu\text{g/g}$  ( $\pm\text{std.err.}$ ;  $n = 3$ ).

The average Ce content per unit mass in *R. subcapitata* was of  $353 \mu\text{g/g d.w.}$  ranging from  $237 \pm 59$ ,  $284 \pm 35$ ,  $442 \pm 131$ ,  $1232 \pm 120 \text{ d.w. } \mu\text{g/g}$  at day 7, 14, 21, and 28. Its content in microalgae slightly increased between day 7 and day 21 reaching the highest level in day 28. Cerium was able to bioconcentrate increasing its initial concentration (day 7) in microalgae by 5-fold in 21 days.

No significant Pearson correlations ( $p > 0.05$ ) between the biomarkers of stress and bioconcentrated La and Ce were found. The association between the induction of tolerance and bioconcentration could represent for La and Ce, and potentially for other REEs, the key for bioaccumulation and biomagnification through the food chain. [305] evidenced that freshwater zooplankton can bioconcentrate REEs from several environmental drivers including water column and bottom sediment, especially at higher dissolved organic carbon ratios and lower pH values, as also

confirmed in [20]. No information is currently available about trophic transfer of REEs from primary producers to primary consumers (i.e., zooplankton), but we can suspect that the potential convergence of tolerance acquisition and bioconcentration from water of La and Ce in *R. subcapitata* could strongly increase the potential biomagnification through the food chain, also with possible repercussion on food safety and human health.

## 6.4 CONCLUSIONS

This research focused on the effects of La and Ce as potential new emerging contaminants because of the alteration of their natural biogeochemical cycles. Populations of *R. subcapitata* were exposed to La and Ce serial concentrations (3 days) to define their concentration-response curves and the relative EC10. La and Ce EC10 values were used to spike the microalgae growth media for the 28 days long-term exposure to monitor their effects on growth inhibition, biomarkers of stress (ROS, SOD, and CAT), and the potential to bioconcentrate. La and Ce are able to slightly increase microalgae growth inhibition in 28 days (i.e., 38% and 28%, in that order), allowing them, at the same time, to bioconcentrate up 3157 and 1232  $\mu\text{g/g}$  dry weight, respectively. CAT and SOD presented relatively low activity levels, like for ROS in the case of Ce. ROS showed higher activities, but without any clear and specific correlations with toxicity data. Microalgae as primary producers showed to bioconcentrate La and Ce from spiked water, suggesting that further investigations on primary consumers (i.e., zooplankton) are necessary in order to verify their potential biomagnification through the food chain up to human beings. Further studies are also required to investigate the association between the induction of tolerance and bioconcentration in *R. subcapitata*.

# CHAPTER 7

---

In this chapter, part of the results was presented based on contribution under preparation titled:

**Siciliano A.**, Libralato G., Comparative toxicity of rare earth elements in *Phaeodactylum tricornutum* and *Aliivibrio fischeri*.

## **7.1 COMPARATIVE TOXICITY OF RARE EARTH ELEMENTS IN MARINE DIATOMS AND LUMINESCENT BACTERIA**

The increase concentration of REEs in aquatic systems have significant impacts in the organisms inhabiting these systems [306]. As emerging contaminants, there is still relatively little knowledge of the natural or anthropogenic cycles of REE in the environment. The content of REEs in seawater is controlled by factors relating to different input sources (e.g., terrestrial input from continental weathering, hydrothermal input) and scavenging processes related to depth, salinity, and oxygen levels [307, 308]. The distinctive character of the seawater REE distribution is largely controlled by the uniform trivalent behaviour of the elements (excepting Ce and Eu, which vary with oxygen levels) and estuarine and oceanic scavenging processes [309]. In contrast, anthropogenic, strongly chelated, anionic REE appear to have a conservative behaviour and a long environmental half-life [310-312]. REE anomalies due to anthropogenic activities were observed in seawaters in Plymouth Sound, UK [100], Ibaraki, Japan [101] and Western Philippine [99].

From the scarce literature on the REE toxicity to aquatic organisms, less data is available for marine organisms comparatively to freshwater ones [250, 306]. Considering the importance of marine and estuarine environments, which provide various resources and services, and that they are the final recipients of most REE continental inputs, it is crucial to study the potential impacts of these contaminants on inhabiting biota [306].

Considering the above mentioned, in this study the effects of Ce, Dy, Eu, La and Nd on the biochemical performance of the marine bacterium *Aliivibrio fischeri* and on the growth of the marine diatom *Phaeodactylum tricornutum* were investigated.

## **7.2 MATERIAL AND METHODS**

### **7.2.1 Chemicals, testing solutions, and analytical characterization**

The experiments were carried out using commercially available chemicals: i)  $\text{Ce}(\text{NO}_3)_3 \cdot 6\text{H}_2\text{O}$ , purity 97%;  $\text{Dy}(\text{NO}_3)_3 \cdot x\text{H}_2\text{O}$ , purity 99.9%;  $\text{Eu}(\text{NO}_3)_3 \cdot 5\text{H}_2\text{O}$ , purity 99.9%;  $\text{La}(\text{NO}_3)_3 \cdot 6\text{H}_2\text{O}$ , purity 97% and  $\text{Nd}(\text{NO}_3)_3 \cdot 6\text{H}_2\text{O}$ , purity 99.9% purchased from Sigma-Aldrich (Saint Louis, United States of America). Treatment solutions of REEs were prepared by adding REEs' solution (1000 mg/L) to artificial seawater [313] at least 1 h before the exposure. The pH was measured with a pH-meter (Mettler Toledo Five Easy, Milan, Italy) prior to exposure. REE concentrations were determined by inductively coupled plasma mass spectrometry (ICP-MS NexION 350×, PerkinElmer, Inc., MA, USA).

### **7.2.2 *P. tricornutum* bioassay**

Axenic cultures of *P. tricornutum* microalgae were cultured at Hygiene Laboratory, Department of Biology at the University of Naples Federico II in artificial seawater medium [313]. Algal growth inhibition test (72 h) was performed according to ISO [313] by using multiwell plates. Inoculum of exponentially growing microalgae were exposed to solutions spiked with REEs for 72 h at  $22 \pm 1$  °C under continuous light of 6,700 lux and with continuous shaking at 50 rpm.

Three replicates for control and each sample were prepared. After a 72-h exposure, spectrophotometric measurement of samples at 670 nm (DR 5000 sc, Hach) was performed to determine algal cell density. The growth rate relative to control was calculated by normalizing the final cell density of each replicate by that of the control culture.

### **7.2.3 *A. fischeri* bioassay**

The acute bioluminescence test with *A. fischeri* (NRRLB-11177) was carried out in accordance with the ISO 11348-3 [314]. The inhibition of bioluminescence in the

presence of the REEs solutions was measured after 30 min of exposure. The toxic effect values are given by the ratio of the decrease in bacterial light output emitted by the bacterium in the sample compared to the control. To provide the relevant osmotic pressure for the test organisms, the salinity concentration of the stock solution was adjusted by 2% for NaCl. The temperature during exposure was 15 °C according to the Microtox standard procedure.

#### **7.2.4 Statistical analysis**

Median effect concentrations (EC50), EC5 and EC10 were calculated as mean values and relative 95% confidence limit values [74], for *P. tricornutum* and *A. fischeri*. Differences between treatments were assessed via one-way analysis of variance (ANOVA) after the verification of normality (Shapiro-Wilk's test) and homoscedasticity (Levene's test). The *post-hoc* Tukey's test accounted for differences within groups setting the statistical significance at  $p < 0.05$ . Statistical analysis was carried out via SigmaPlot (Systat Software, San Jose, CA).

### **7.3 RESULTS AND DISCUSSION**

Measured concentrations used to calculate concentration-response curves were highlighted in Table 18. The analytical/nominal ratios mostly ranged from 0.7 to 1.2; thus, nominal concentration values were considered as reliable for concentration-related trends. These results agree with previously studies [114, 240] and confirmed the plausible closeness of nominal REE concentrations vs. analytical determination [240].

|                       | Nominal<br>(mg/L) | Measured<br>(mg/L) |      |      |      |      |
|-----------------------|-------------------|--------------------|------|------|------|------|
|                       |                   | Ce                 | Dy   | Eu   | La   | Nd   |
| <i>A. fischeri</i>    | 0.6               | 0.63               | 0.56 | 0.80 | 0.70 | 0.55 |
|                       | 0.8               | 1.07               | 0.57 | 1.06 | 0.84 | 0.85 |
|                       | 1.2               | 1.12               | 1.40 | 1.59 | 1.24 | 1.42 |
|                       | 1.5               | 1.64               | 1.55 | 1.69 | 1.44 | 1.57 |
|                       | 2.5               | 2.19               | 2.74 | 2.95 | 2.03 | 2.84 |
|                       | 5                 | 5.04               | 6.20 | 5.82 | 6.00 | 6.05 |
| <i>P. tricornutum</i> | 0.3               | 0.30               | 0.30 | 0.30 | 0.30 | 0.30 |
|                       | 0.6               | 0.63               | 0.56 | 0.81 | 0.70 | 0.55 |
|                       | 1.2               | 1.13               | 1.40 | 1.59 | 1.24 | 1.42 |
|                       | 2.5               | 2.19               | 2.74 | 2.95 | 2.03 | 2.84 |
|                       | 5                 | 5.04               | 6.21 | 5.82 | 6.00 | 6.05 |

Table 19 Nominal and measured (ICP-MS) Ce, Dy, Eu, La and Nd concentrations (mg/L).

In Figure 36, the results of luminescence inhibition of *A. fischeri* were reported for Ce, Dy, Eu, La and Nd. A linear regression model was considered to fit data concentration-response relationships. All equations and the relative standard errors were included in Fig. 36. These equations allowed the determination of EC50, EC10, and EC5 that were summarized in Table 19.

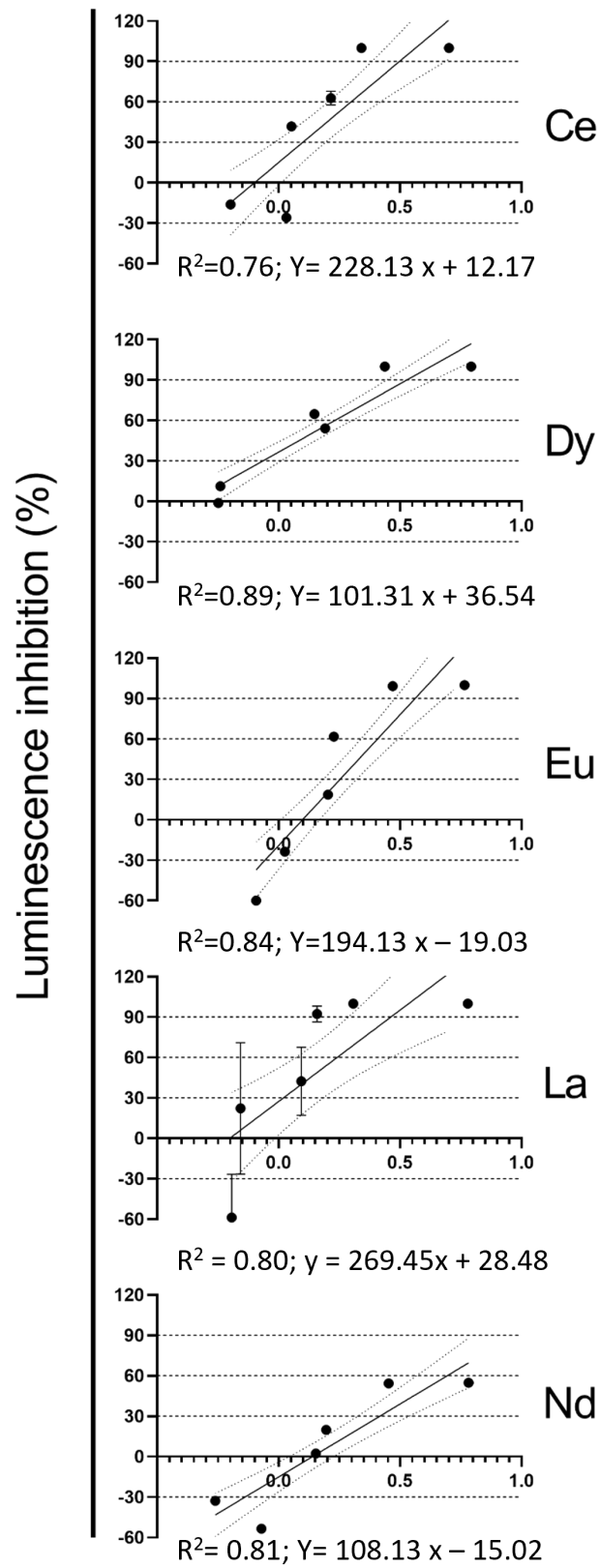


Figure 36 Concentration-response relationship of Ce, Dy, Eu, La and Nd exposed to *A. fischeri*; concentrations in the x-axis are expressed as mg/L.

|           | EC5                   | EC10                  | EC20                   | EC50                   |
|-----------|-----------------------|-----------------------|------------------------|------------------------|
| <b>Ce</b> | 0.93<br>(0.44 – 1.83) | 0.99<br>(0.47 – 1.92) | 1.08<br>(0.52 – 2.11)  | 1.46<br>(0.71 – 2.82)  |
| <b>Dy</b> | 0.49<br>(0.35 - 0.71) | 0.55<br>(0.39 - 0.81) | 0.69<br>(0.48 - 1.03)  | 1.36<br>(0.91 - 2.15)  |
| <b>Eu</b> | 1.33<br>(0.92 - 2.41) | 1.41<br>(0.97 - 2.61) | 1.59<br>(1.06 - 3.05)  | 2.27<br>(1.42 - 4.85)  |
| <b>La</b> | 0.82<br>(0.43-1.55)   | 0.85<br>(0.44-1.62)   | 0.93<br>(0.48-1.76)    | 1.20<br>(0.63-2.28)    |
| <b>Nd</b> | 1.53<br>(0.65 - 8.50) | 1.70<br>(0.70 - 9.98) | 2.11<br>(0.83 - 13.73) | 3.99<br>(1.33 - 35.81) |

Table 20 EC5, EC10, and EC50 values for Ce, Dy, Eu; La and Nd on *A. fischeri*; values are in mg/L; n.a. = not available; REEs = rare earth elements; EC = effective concentration; average EC values are provided  $\pm 95\%$  confidence limit values in brackets ( $n = 3$ ).

Considering the Ce exposure, stimulation effects were detected at low concentration. The effects ranged between  $-16\%$  (0.63 mg/L) and  $100\%$  (5.040 mg/L) ( $R^2=0.76$ ;  $Y= 228.13 x + 12.17$ ). For Ce, the EC50 value was 1.46 (0.71 – 2.82) mg/L (Tab.18), this value was much lower than the  $EC_{50} > 6$  mg/L calculated by [250, 315]. No toxic effects ( $EC_{50} > 100$  mg/L) were observed for *A. fischeri* in Ce exposure by [97]. This discrepancy could be explained by the different nature of the lanthanides tested (nitrates in the current study and chlorides in the work of [250, 315]).

For Dy ( $R^2=0.89$ ;  $Y= 101.31 x + 36.54$ ), a slight stimulatory effect was detected at 0.56 mg / L and 100% inhibition was achieved at 2.7 mg / L. Dy EC50 was 1.36 mg/L (0.91 - 2.15) mg/L. This value could not be compared with those previous reports in which Dy was excluded.

About *A. fischeri* exposure the effects varied between  $-60\%$  at 0.8 mg/L and  $100\%$  at 5.8 mg/L (Fig. 36). For Eu EC50 was 2.27 (1.42 - 4.85) mg/L and no results of previous literature studies have been found.

La showed strong biostimulation at the concentration of 0.7 mg / L but starting from 0.8 mg / L inhibition was noted that reached the  $100\%$  at 6 mg / L. The EC50 of La

was 1.20 (0.63-2.28) mg / L (Table 18) and this value was very different to those previously evaluated [315].

Nd exposure showed stimulation at the first three concentrations (0.55, 0.85 and 1.42 mg/L, less marked than in the Eu. The EC50 for Nd was 3.99 (1.33 - 35.81) mg / L (Table 18) and very close to that previously evaluated in [315], in which the Ec50 at 30 minutes for Nd was 6.87 mg / L, a value that fell within range of confidence interval of this study.

For all REE tested there was a biostimulatory effect at the lowest concentrations and an inhibitory effect at the highest concentrations. This biphasic response to exposure to increasing amounts of a substance was already described in the scientific literature and namely known as hormesis [135, 316, 317].

The rapid increase of inhibitory effects, in terms of bioluminescence, after exposure to REE could be due to interactions between the elements and bacterial outer membrane, resulting in disturbances in the cellular transport of metal ions[318].

Based on the calculated EC50 values (Tab. 19) the following toxicity relationship can be established: La >Dy> Ce > Eu > Nd.

In Figure 36, the results about the growth inhibition of *P.tricornutum* were reported for Ce, Dy, Eu, La and Nd. All equations and the relative standard errors were provided in fig. 36 and the determination of EC50, EC10, and EC5 were summarized in Table 19.

As a general overview of the obtained results, the algal growth always evidenced inhibitory effects at the tested concentrations for all the investigated REEs, except for Dy and La which, similarly, displayed biostimulation effect at the two lowest tested concentrations.

Cell density data of *P. tricornutum* cultures exposed to different concentrations of Ce showed strong deceleration of growth (88% of effect) under the highest concentration in comparison with the remaining conditions (Fig.37).

Considering the cell density of the *P. tricornutum* cultures exposed to the different levels of Dy, it was possible to observe that the two lowest concentrations of this element induced a higher number of cells per unit of volume of culture (Fig. 37)compared to control group, resulting in negative values of growth inhibition. At the basis of this increase in cell density was probably the increasing number of

divisions per day and reduced doubling time, resulting in an increasing trend in specific growth rate, although neither of these parameters was statistically significant. In contrast, clear inhibition of growth was observed for the concentrations, with the average values close to 15% for 1.4 mg/L, 30% for 2.7 mg/L and 74% for the higher dose (6.2 mg/L). Eu displays clear toxicity at higher doses (2.9 and 5.8 mg/L), with the average values of 45% and 71%, respectively. Exposure to the other concentrations slightly increased the inhibition (Fig. 37).

*P. tricornutum* cells exposed to La concentrations of 0.3–0.7 mg/L showed greater growth than control group after 72h. Inhibition was observed after 72 h at the other concentrations (Fig.37). About the Nd exposure, the growth of *P. tricornutum* cultures was reduced at all concentrations and showed strong decelerations of growth (45- 60% of effects) at 2.8 and 6.0 mg/L (Fig.37). The remaining conditions reported inhibitory effect within 5% and 30%. To the best of our knowledge, this is the first study that reported data on REE toxicity towards the bioindicator *P. tricornutum*. For this reason, it was possible to compare the results obtained only with studies on other seaweed such as *Skeletonema costatum*.

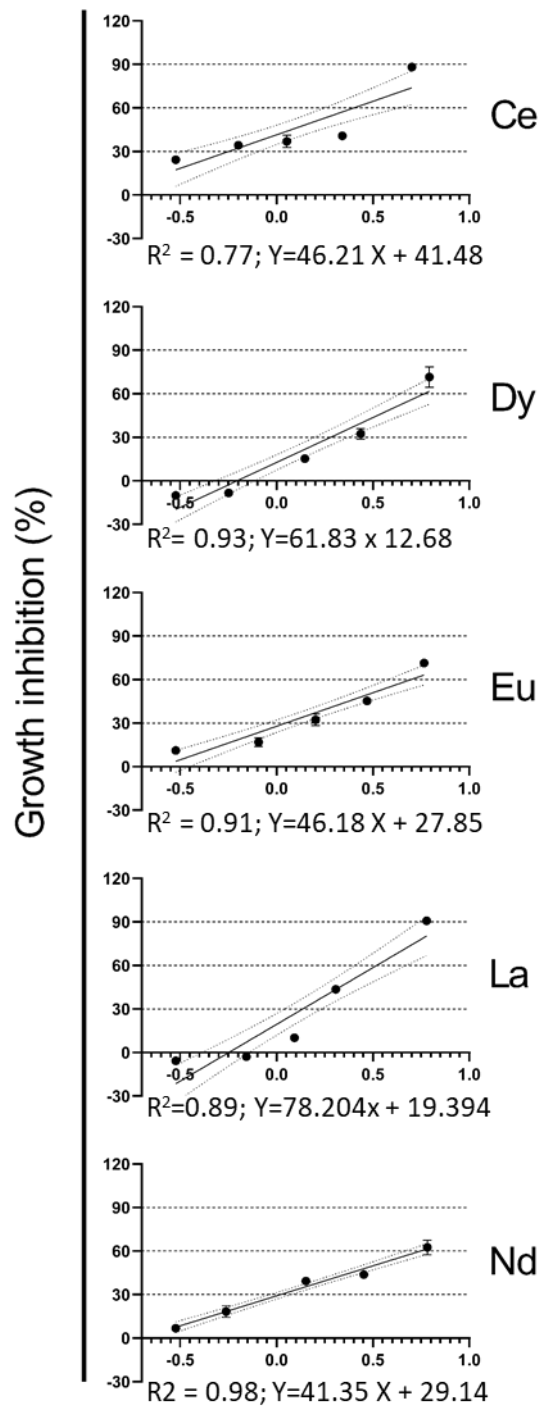


Figure 37 Concentration-response relationship of Ce, Dy, Eu, La and Nd exposed to *P. tricornutum*; concentrations in the x-axis are expressed as mg/L.

|    | EC5                   | EC10                  | EC20                  | EC50                  |
|----|-----------------------|-----------------------|-----------------------|-----------------------|
| Ce | 0.16<br>(0.04 - 0.78) | 0.21<br>(0.05 - 1.01) | 0.34<br>(0.08 - 1.68) | 1.53<br>(0.32 - 7.75) |
| Dy | 0.75<br>(0.31 - 1.81) | 0.90<br>(0.38 - 2.18) | 1.31<br>(0.55 - 3.16) | 4.01<br>(1.67 - 9.70) |
| Eu | 0.32<br>(0.11 - 0.84) | 0.41<br>(0.15 - 1.07) | 0.68<br>(0.25 - 1.74) | 3.02<br>(1.16 - 7.41) |
| La | 0.65<br>(0.24-1.89)   | 0.76<br>(0.28-2.19)   | 1.02<br>(0.37-2.97)   | 2.46<br>(0.87-7.34)   |
| Nd | 0.26<br>(0.17 - 0.40) | 0.34<br>(0.23 - 0.53) | 0.60<br>(0.39 - 0.92) | 3.19<br>(2.09 - 4.88) |

Table 21 EC5, EC10, and EC50 values for Ce, Dy, Eu, La and Nd on *P. tricornutum*; values are in mg/L; n.a. = not available; REEs = rare earth elements; EC = effective concentration; average EC values are provided  $\pm 95\%$  confidence limit values in brackets ( $n = 3$ ).

The EC50 ( $\pm 95\%$  confidence limit values) for Ce was 1.53 (0.32 - 7.75) mg/L ( $R^2 = 0.77$ ;  $Y=46.21 X + 41.48$ ; normal distribution and constant variance). The EC50 for Ce determined in this study was lower than [291] *S. costatum* EC50 (4.2 mg/L) but comparable considering the confidence limit values and the use in [291] of nominal concentrations

The EC50 ( $\pm 95\%$  confidence limit values) for Dy 4.01 (1.67 - 9.70) mg/L ( $R^2 = 0.93$ ;  $Y=61.83 x 12.68$ ; normal distribution and constant variance), this value was stackable with *S. costatum* EC50 (4.6 mg/L) of the previous study cited [291].

The EC50 ( $\pm 95\%$  confidence limit values) obtained for Eu was 3.02 (1.16 - 7.41) mg/L, for La was 2.46 (0.87-7.34) mg/La and Nd was 3.19 (2.09 - 4.88) mg/L similar to those reported in previous study [291], which corresponded to 4.42 mg/L, 4.84 mg/L, and 4.42 mg/L for Eu, La and Nd respectively.

The results demonstrated that the tested REEs had similar toxic effects to *P. tricornutum* and *S. costatum*. Algae are ecologically important organisms in the aquatic food chain and are frequently used in environmental studies to assess the relative toxicity of various chemicals; one of the most important functions is that algae contribute substantially to the total primary ecosystem production in most aquatic habitats. Due to their short response times, algae often provide one of the first signs of ecosystem impacts, thus allowing corrective regulatory and management actions to be taken before other unwanted impacts occur.

Based on the calculated EC50 values (Tab. 20) the following toxicity relationship was established: Ce>La>Eu>Nd>Dy.

## 7.4 CONCLUSIONS

A comparative investigation on HREE-associated toxicity in bacterium *A. fischeri* and diatom *P. tricornutum* provided evidence for similar effects of individual REEs, namely Ce, Dy, Eu, La and Gd postulating therefore the same toxicity effects on single-celled organisms. Different REEs had different toxicities on higher level living organisms, suggesting that higher level organisms evolved more sensitive toxic reaction to lanthanides which poses the question as to which cells or tissues of higher order organisms are affected by the lanthanides. The REE tested showed EC50 values between 1.20 mg/L and 4.99 mg/L which were considered relevant from an environmental risk assessment perspective.

Further investigations on REEs are warranted in other unicellular species in order to determine whether these elements could show predictable patterns in bioavailability, bioaccumulation and ecotoxicity, as well as studies addressing their combined effect.

# GENERAL CONCLUSIONS

---

Increased anthropogenic levels of REEs and toxicity on different organisms of both terrestrial and marine environments near industrial facilities were investigated to evaluate the influence and the occurrence of REEs in soil and sediment on a global level.

Industrial areas were rich in various REEs, derived from the related anthropogenic activities and accumulating in the local natural resources (like soils and sediments). In Taranto, Gardanne and Augusta-Priolo areas different levels on REEs were found. The concentration of total REEs in soils was from 2.7 up to 251.8 mg/Kg. The concentration of LREEs was higher than HREEs and Ce was the most abundant, followed by La and Nd. In Pozzuoli area, the concentration of total REEs in soils was 68.5 to 247.2 mg/Kg and Sc was the most abundant, followed by Ce and La.

Although, application of REEs could stimulate and promote biological growth and development at low concentrations, relatively high concentrations of REEs (~ 200 mg/Kg) may cause serious adverse effects on both plants and organisms at physiological and cellular levels.

Field evaluations indicated that REEs can impair soil/sediment organisms. Field trials contributed to better understanding the effects of REEs on non-target organisms in the ecosystem. Due to different levels of REEs in soils and sediments and the different toxicity, the study are still unable to attribute them as unique factors of toxicity.

Anyway, considering that REEs are present in complex environmental matrices, more studies must be performed to unveil their “matrix” effect.

Laboratory results showed that REEs can be a threat to aquatic organism including both freshwater and seawater ones. Acidic conditions increased the toxicity of the selected REEs (namely Ce, Gd, La and Nd) by increasing the amount of free trivalent ions. The sensitivity of freshwater organisms and the inherent toxicity increased with increasing atomic number in the lanthanides. Marine species

exhibited a different sensitivity to REEs, suggesting to investigate more in detail concentration-response effects.

The considered biological models responded to REEs oxidative injury activating various enzymatic and non-enzymatic antioxidants, but no specific correlation was found. Besides, the capacity to bioconcentrate REEs from spiked water suggested that further investigations are necessary in order to verify REEs potential biomagnification through the food chain up to human beings in a one-health perspective.

There is still an important gap in the knowledge of REEs toxicity, especially in threshold level concentrations related to the heavier elements and the extrapolation of the present results should be very careful because of the different exposure scenarios in other areas where REEs can be present due to direct (i.e., use as growth promoter in agricultural amendments) or indirect (i.e, industrial activity) presence. Future studies should consider the influence of physicochemical properties of natural resources to determine REE toxicity and further elucidate the specific role of changing redox conditions and factors controlling the release REEs dynamics of toxicity.

Overall, data on individual elements should be produced to determine predictable patterns in bioavailability, bioaccumulation and ecotoxicity, as well as studies addressing their combined effect.

In the context of above mentioned results, the following specific points are foreseen in the near future:

- Regulatory standards are required to establish the safe threshold concentrations of REEs for soil, sediment, water and living organisms.
- New public policies and the development of more effective treatment technologies, i.e. waste management strategy, are expected to manage the future adverse impacts of REE in environmental systems.

## REFERENCES

---

1. IUPAC, *Nomenclature of inorganic chemistry. Recommendations 2005*. 2005, Connelly NG et al., editors. .
2. Pereira, H.A., et al., *A multivariate approach at the thermodynamic properties of rare earth elements*. *Thermochimica Acta*, 2019. **678**: p. 178315.
3. Ramos, S.J., et al., *Rare earth elements in the soil environment*. *Current Pollution Reports*, 2016. **2**(1): p. 28-50.
4. Robinson, W., H. Bastron, and K. Murata, *Biogeochemistry of the rare-earth elements with particular reference to hickory trees*. *Geochimica et Cosmochimica Acta*, 1958. **14**(1-2): p. 55-67.
5. Balaram, V., *Rare earth elements: A review of applications, occurrence, exploration, analysis, recycling, and environmental impact*. *Geoscience Frontiers*, 2019. **10**(4): p. 1285-1303.
6. Gwenzi, W., et al., *Sources, behaviour, and environmental and human health risks of high-technology rare earth elements as emerging contaminants*. *Science of the Total Environment*, 2018. **636**: p. 299-313.
7. Gravina, M., et al., *Heavy rare earth elements affect *Sphaerechinus granularis* sea urchin early life stages by multiple toxicity endpoints*. *Bulletin of environmental contamination and toxicology*, 2018. **100**(5): p. 641-646.
8. Pagano, G., et al., *Human exposures to rare earth elements: Present knowledge and research prospects*. *Environmental research*, 2019. **171**: p. 493-500.
9. Tommasi, F., et al., *Review of rare earth elements as fertilizers and feed additives: a knowledge gap analysis*. *Archives of Environmental Contamination and Toxicology*, 2020: p. 1-10.
10. Thomas, P.J., et al., *Rare earth elements (REEs): effects on germination and growth of selected crop and native plant species*. *Chemosphere*, 2014. **96**: p. 57-66.

11. Siciliano, A., et al., *Long-term multi-endpoint exposure of the microalga *Raphidocelis subcapitata* to lanthanum and cerium*. Science of The Total Environment, 2021: p. 148229.
12. Kotelnikova, A., et al., *Toxicity assay of lanthanum and cerium in solutions and soil*. Ecotoxicology and environmental safety, 2019. **167**: p. 20-28.
13. Carpenter, D., et al., *Uptake and effects of six rare earth elements (REEs) on selected native and crop species growing in contaminated soils*. PLoS One, 2015. **10**(6): p. e0129936.
14. Adeel, M., et al., *Cryptic footprints of rare earth elements on natural resources and living organisms*. Environment international, 2019. **127**: p. 785-800.
15. Blinova, I., et al., *Evaluation of the potential hazard of lanthanides to freshwater microcrustaceans*. Science of the total environment, 2018. **642**: p. 1100-1107.
16. Blinova, I., et al., *Potential hazard of lanthanides and lanthanide-based nanoparticles to aquatic ecosystems: data gaps, challenges and future research needs derived from bibliometric analysis*. Nanomaterials, 2020. **10**(2): p. 328.
17. Herrmann, H., et al., *Aquatic ecotoxicity of lanthanum—A review and an attempt to derive water and sediment quality criteria*. Ecotoxicology and Environmental Safety, 2016. **124**: p. 213-238.
18. Oral, R., et al., *Cytogenetic and developmental toxicity of cerium and lanthanum to sea urchin embryos*. Chemosphere, 2010. **81**(2): p. 194-198.
19. Romero-Freire, A., et al., *Assessment of the toxic effects of mixtures of three lanthanides (Ce, Gd, Lu) to aquatic biota*. Science of the Total Environment, 2019. **661**: p. 276-284.
20. Siciliano, A., et al., *Cerium, gadolinium, lanthanum, and neodymium effects in simplified acid mine discharges to *Raphidocelis subcapitata*, *Lepidium sativum*, and *Vicia faba**. Science of The Total Environment, 2021. **787**: p. 147527.

21. Valcheva-Traykova, M., L. Saso, and I. Kostova, *Involvement of lanthanides in the free radicals homeostasis*. Current topics in medicinal chemistry, 2014. **14**(22): p. 2508-2519.
22. Wei, B., et al., *Rare earth elements in human hair from a mining area of China*. Ecotoxicology and environmental safety, 2013. **96**: p. 118-123.
23. Hao, Z., et al., *Levels of rare earth elements, heavy metals and uranium in a population living in Baiyun Obo, Inner Mongolia, China: A pilot study*. Chemosphere, 2015. **128**: p. 161-170.
24. Pagano, G., et al., *Rare earth elements in human and animal health: state of art and research priorities*. Environmental research, 2015. **142**: p. 215-220.
25. Thyssen, P. and K. Binnemans, *Accommodation of the rare earths in the periodic table: A historical analysis*, in *Handbook on the Physics and Chemistry of Rare Earths*. 2011, Elsevier. p. 1-93.
26. 中田亮一, *Stable isotopic and speciation studies on neo-rare earth element geochemistry and paleoenvironmental analysis*. 2013, 広島大学.
27. Lin, R., Y. Soong, and E.J. Granite, *Evaluation of trace elements in US coals using the USGS COALQUAL database version 3.0. Part I: Rare earth elements and yttrium (REY)*. International Journal of Coal Geology, 2018. **192**: p. 1-13.
28. Ober, J., *Mineral commodity Summaries 2017, Mineral Commodity Summaries*. US Geological Survey Reston, 2017.
29. Chakhmouradian, A.R. and F. Wall, *Rare earth elements: minerals, mines, magnets (and more)*. Elements, 2012. **8**(5): p. 333-340.
30. Jordens, A., Y.P. Cheng, and K.E. Waters, *A review of the beneficiation of rare earth element bearing minerals*. Minerals Engineering, 2013. **41**: p. 97-114.
31. Gupta, C.K. and N. Krishnamurthy, *Extractive metallurgy of rare earths*. International Materials Reviews, 1992. **37**(1): p. 197-248.
32. Haxel, G., *Rare earth elements: critical resources for high technology*. Vol. 87. 2002: US Department of the Interior, US Geological Survey.
33. Voncken, J.H.L., *The rare earth elements: an introduction*. 2016: Springer.

34. Pang, X., D. Li, and A. Peng, *Application of rare-earth elements in the agriculture of China and its environmental behavior in soil*. Environmental Science and Pollution Research, 2002. **9**(2): p. 143-148.
35. Gambogi, J., *US Geological Survey, Mineral Commodity Summaries, January 2021*. 2021, tech. rep.
36. Fortier, S.M., et al., *Draft critical mineral list—Summary of methodology and background information—US Geological Survey technical input document in response to Secretarial Order No. 3359*. 2018, US Geological Survey.
37. Wedepohl, K.H., *The composition of the continental crust*. Geochimica et cosmochimica Acta, 1995. **59**(7): p. 1217-1232.
38. Migaszewski, Z.M. and A. Gajuszka, *The characteristics, occurrence, and geochemical behavior of rare earth elements in the environment: a review*. Critical reviews in environmental science and technology, 2015. **45**(5): p. 429-471.
39. Silva, J.H., *Nanostructuring Gd<sub>5</sub> (Si, Ge) 4 Multifunctional Materials*. 2017, Universidade do Porto (Portugal).
40. Komeda, T., K. Katoh, and M. Yamashita, *Single Molecule Magnet for Quantum Information Process*. Molecular Technology, Volume 3: Materials Innovation, 2019.
41. Wahyudi, T., *Reviewing the properties of rare earth element-bearing minerals, rare earth elements and cerium oxide compound*. Indonesian Mining Journal, 2015. **18**(2): p. 92-108.
42. Tommasi, F., et al., *Review of rare earth elements as fertilizers and feed additives: a knowledge gap analysis*. Archives of Environmental Contamination and Toxicology, 2021. **81**(4): p. 531-540.
43. Cardoso, C.E., et al., *Recovery of rare earth elements by carbon-based nanomaterials—a review*. Nanomaterials, 2019. **9**(6): p. 814.
44. Hurst, C.A., *China's Ace in the Hole Rare Earth Elements*. 2010, FOREIGN MILITARY STUDIES OFFICE (ARMY) FORT LEAVENWORTH KS.
45. Roskill, *Rare earths global industry, markets and outlook*. 2015.

46. Wee, J.-H. and K.-Y. Lee, *Overview of the effects of rare-earth elements used as additive materials in molten carbonate fuel cell systems*. Journal of materials science, 2006. **41**(12): p. 3585-3592.
47. Omodara, L., et al., *Recycling and substitution of light rare earth elements, cerium, lanthanum, neodymium, and praseodymium from end-of-life applications-A review*. Journal of Cleaner Production, 2019. **236**: p. 117573.
48. Zhao, Z., et al., *Recovery of rare earth elements from spent fluid catalytic cracking catalysts using leaching and solvent extraction techniques*. Hydrometallurgy, 2017. **167**: p. 183-188.
49. Choudhary, V.R., et al., *Oxidative conversion of methane to CO and H<sub>2</sub> over Pt or Pd containing alkaline and rare earth oxide catalysts*. Fuel, 1998. **77**(13): p. 1477-1481.
50. Brykin, A., A. Artemov, and K. Kolegov, *Analysis of the market of rare-earth elements (REEs) and REE catalysts*. Catalysis in industry, 2014. **6**(1): p. 1-7.
51. Xu, J.J., et al., *Synthesis of perovskite-based porous La<sub>0.75</sub>Sr<sub>0.25</sub>MnO<sub>3</sub> nanotubes as a highly efficient electrocatalyst for rechargeable lithium–oxygen batteries*. Angewandte Chemie International Edition, 2013. **52**(14): p. 3887-3890.
52. Tavakkoli, H. and M. Yazdanbakhsh, *Fabrication of two perovskite-type oxide nanoparticles as the new adsorbents in efficient removal of a pesticide from aqueous solutions: Kinetic, thermodynamic, and adsorption studies*. Microporous and mesoporous materials, 2013. **176**: p. 86-94.
53. Onozuka, K., et al., *Perovskite-type La<sub>2</sub>Ti<sub>2</sub>O<sub>7</sub> mesoporous photocatalyst*. Journal of Solid State Chemistry, 2012. **192**: p. 87-92.
54. Luo, W., et al., *Efficient removal of organic pollutants with magnetic nanoscaled BiFeO<sub>3</sub> as a reusable heterogeneous Fenton-like catalyst*. Environmental science & technology, 2010. **44**(5): p. 1786-1791.
55. Wang, N., et al., *Ligand-induced drastic enhancement of catalytic activity of nano-BiFeO<sub>3</sub> for oxidative degradation of bisphenol A*. ACS Catalysis, 2011. **1**(10): p. 1193-1202.

56. Chen, X., et al., *Synergy effect between adsorption and heterogeneous photo-Fenton-like catalysis on LaFeO<sub>3</sub>/lignin-biochar composites for high efficiency degradation of ofloxacin under visible light*. Separation and Purification Technology, 2022. **280**: p. 119751.
57. Zhou, S., et al., *Synergistic photocatalytic and Fenton-like degradation of MO by nanocatalyst La<sub>0.7</sub>Sr<sub>0.3</sub>Mn<sub>0.85</sub>Fe<sub>0.15</sub>O<sub>3</sub>*. Journal of Nanoparticle Research, 2021. **23**(9): p. 1-18.
58. Fouad, K., et al., *Optimization of catalytic wet peroxide oxidation of carbofuran by Ti-LaFeO<sub>3</sub> dual photocatalyst*. Environmental Technology & Innovation, 2021. **23**: p. 101778.
59. del Álamo, A.C., et al., *Fenton-like catalyst based on a reticulated porous perovskite material: activity and stability for the on-site removal of pharmaceutical micropollutants in a hospital wastewater*. Chemical Engineering Journal, 2020. **401**: p. 126113.
60. Nie, Y., et al., *Enhanced Fenton-like degradation of refractory organic compounds by surface complex formation of LaFeO<sub>3</sub> and H<sub>2</sub>O<sub>2</sub>*. Journal of hazardous materials, 2015. **294**: p. 195-200.
61. Hammouda, S.B., et al., *Reactivity of novel Ceria–Perovskite composites CeO<sub>2</sub>-LaMO<sub>3</sub> (MCu, Fe) in the catalytic wet peroxidative oxidation of the new emergent pollutant ‘Bisphenol F’: Characterization, kinetic and mechanism studies*. Applied Catalysis B: Environmental, 2017. **218**: p. 119-136.
62. Xie, H., J. Zeng, and G. Zhou, *CeCu composite oxide for chlorophenol effective removal by heterogeneous catalytic wet peroxide oxidation*. Environmental Science and Pollution Research, 2020. **27**(1): p. 846-860.
63. Xu, L. and J. Wang, *Degradation of 2, 4, 6-trichlorophenol using magnetic nanoscaled Fe<sub>3</sub>O<sub>4</sub>/CeO<sub>2</sub> composite as a heterogeneous Fenton-like catalyst*. Separation and Purification Technology, 2015. **149**: p. 255-264.
64. Zhang, N., et al., *Effects of Ce doping on the Fenton-like reactivity of Cu-based catalyst to the fluconazole*. Chemical Engineering Journal, 2020. **395**: p. 124897.

65. Ji, P., et al., *Ce<sup>3+</sup>-centric organic pollutant elimination by CeO<sub>2</sub> in the presence of H<sub>2</sub>O<sub>2</sub>*. *ChemCatChem*, 2010. **2**(12): p. 1552-1554.
66. Zhang, N., et al., *Ceria accelerated nanoscale zerovalent iron assisted heterogenous Fenton oxidation of tetracycline*. *Chemical Engineering Journal*, 2019. **369**: p. 588-599.
67. Zhang, N., et al., *Critical role of oxygen vacancies in heterogeneous Fenton oxidation over ceria-based catalysts*. *Journal of colloid and interface science*, 2020. **558**: p. 163-172.
68. Bünzli, J.-C.G. and S.V. Eliseeva, *Lanthanide NIR luminescence for telecommunications, bioanalyses and solar energy conversion*. *Journal of Rare Earths*, 2010. **28**(6): p. 824-842.
69. Luo, Y., et al., *Molecular Magnetic Resonance Imaging with Contrast Agents for Assessment of Inflammatory Bowel Disease: A Systematic Review*. *Contrast Media & Molecular Imaging*, 2020. **2020**.
70. Inoue, K., et al., *Impact on gadolinium anomaly in river waters in Tokyo related to the increased number of MRI devices in use*. *Marine pollution bulletin*, 2020. **154**: p. 111148.
71. Raval, M., et al., *Yttrium-90 radioembolization of hepatic metastases from colorectal cancer*. *Frontiers in oncology*, 2014. **4**: p. 120.
72. White, J., et al., *Yttrium-90 transarterial radioembolization for chemotherapy-refractory intrahepatic cholangiocarcinoma: a prospective, observational study*. *Journal of Vascular and Interventional Radiology*, 2019. **30**(8): p. 1185-1192.
73. Rustad, J.R., *Peak nothing: Recent trends in mineral resource production*. *Environmental science & technology*, 2012. **46**(3): p. 1903-1906.
74. Galdiero, E., et al., *Cerium and erbium effects on Daphnia magna generations: A multiple endpoints approach*. *Environmental Pollution*, 2019. **254**: p. 112985.
75. Naccarato, A., et al., *Agrochemical treatments as a source of heavy metals and rare earth elements in agricultural soils and bioaccumulation in ground beetles*. *Science of The Total Environment*, 2020. **749**: p. 141438.

76. Pagano, G., et al., *Health effects and toxicity mechanisms of rare earth elements—Knowledge gaps and research prospects*. Ecotoxicology and environmental safety, 2015. **115**: p. 40-48.
77. Wang, C., et al., *Comparative studies on the concentration of rare earth elements and heavy metals in the atmospheric particulate matter in Beijing, China, and in Delft, the Netherlands*. Environment International, 2001. **26**(5-6): p. 309-313.
78. Wang, Z., et al., *Accumulation of rare earth elements in corn after agricultural application*. Journal of Environmental Quality, 2001. **30**(1): p. 37-45.
79. Ferrat, M., et al., *Improved provenance tracing of Asian dust sources using rare earth elements and selected trace elements for palaeomonsoon studies on the eastern Tibetan Plateau*. Geochimica et Cosmochimica Acta, 2011. **75**(21): p. 6374-6399.
80. Abbott, A.N., et al., *The sedimentary flux of dissolved rare earth elements to the ocean*. Geochimica et Cosmochimica Acta, 2015. **154**: p. 186-200.
81. Chen, J., et al., *Diagenetic uptake of rare earth elements by bioapatite, with an example from Lower Triassic conodonts of South China*. Earth-science reviews, 2015. **149**: p. 181-202.
82. Chen, J., et al., *Rare earths exposure and male infertility: the injury mechanism study of rare earths on male mice and human sperm*. Environmental Science and Pollution Research, 2015. **22**(3): p. 2076-2086.
83. Yang, X., et al., *Rare earth elements of aeolian deposits in Northern China and their implications for determining the provenance of dust storms in Beijing*. Geomorphology, 2007. **87**(4): p. 365-377.
84. Kulaksız, S. and M. Bau, *Anthropogenic gadolinium as a microcontaminant in tap water used as drinking water in urban areas and megacities*. Applied Geochemistry, 2011. **26**(11): p. 1877-1885.
85. Kulaksız, S. and M. Bau, *Rare earth elements in the Rhine River, Germany: first case of anthropogenic lanthanum as a dissolved microcontaminant in the hydrosphere*. Environment International, 2011. **37**(5): p. 973-979.

86. Tepe, N., M. Romero, and M. Bau, *High-technology metals as emerging contaminants: Strong increase of anthropogenic gadolinium levels in tap water of Berlin, Germany, from 2009 to 2012*. Applied geochemistry, 2014. **45**: p. 191-197.
87. Lindner, U., et al., *Analysis of gadolinium-based contrast agents in tap water with a new hydrophilic interaction chromatography (ZIC-cHILIC) hyphenated with inductively coupled plasma mass spectrometry*. Analytical and bioanalytical chemistry, 2015. **407**(9): p. 2415-2422.
88. Merschel, G., et al., *Tracing and tracking wastewater-derived substances in freshwater lakes and reservoirs: Anthropogenic gadolinium and geogenic REEs in Lake Paranoá, Brasilia*. Comptes Rendus Geoscience, 2015. **347**(5-6): p. 284-293.
89. Jiang, D.G., et al., *A survey of 16 rare earth elements in the major foods in China*. Biomedical and Environmental Sciences, 2012. **25**(3): p. 267-271.
90. Li, C., et al., *Recycling rare earth elements from industrial wastewater with flowerlike nano-Mg (OH) 2*. ACS applied materials & interfaces, 2013. **5**(19): p. 9719-9725.
91. Li, X., et al., *A human health risk assessment of rare earth elements in soil and vegetables from a mining area in Fujian Province, Southeast China*. Chemosphere, 2013. **93**(6): p. 1240-1246.
92. Gwenz, W., et al., *Sources and Health Risks of Rare Earth Elements in Waters*, in *Water Pollution and Remediation: Heavy Metals*. 2021, Springer. p. 1-36.
93. Uchida, S., et al., *Concentrations of REEs, Th and U in river waters collected in Japan*. Journal of alloys and compounds, 2006. **408**: p. 525-528.
94. Salminen, R., et al., *FOREGS Geochemical Atlas of Europe, Part 1—Background Information, Methodology, and Maps*. Geological Survey of Finland, Espoo, 690 p. 2016.
95. Miao, L., et al., *Geochemistry and biogeochemistry of rare earth elements in a surface environment (soil and plant) in South China*. Environmental Geology, 2008. **56**(2): p. 225-235.

96. Markert, B., *The pattern of distribution of lanthanide elements in soils and plants*. *Phytochemistry*, 1987. **26**(12): p. 3167-3170.
97. Verplanck, P.L., et al., *Rare earth element partitioning between hydrous ferric oxides and acid mine water during iron oxidation*. *Applied Geochemistry*, 2004. **19**(8): p. 1339-1354.
98. Zhao, F., et al., *The geochemistry of rare earth elements (REE) in acid mine drainage from the Sitai coal mine, Shanxi Province, North China*. *International Journal of Coal Geology*, 2007. **70**(1-3): p. 184-192.
99. Goldstein, S.J. and S.B. Jacobsen, *Rare earth elements in river waters*. *Earth and Planetary Science Letters*, 1988. **89**(1): p. 35-47.
100. Karadaş, C., D. Kara, and A. Fisher, *Determination of rare earth elements in seawater by inductively coupled plasma mass spectrometry with off-line column preconcentration using 2, 6-diacetylpyridine functionalized Amberlite XAD-4*. *Analytica chimica acta*, 2011. **689**(2): p. 184-189.
101. Zhu, Y., *Determination of rare earth elements in seawater samples by inductively coupled plasma tandem quadrupole mass spectrometry after coprecipitation with magnesium hydroxide*. *Talanta*, 2020. **209**: p. 120536.
102. Ojiambo, S.B., et al., *Strontium isotopes and rare earth elements as tracers of groundwater–lake water interactions, Lake Naivasha, Kenya*. *Applied Geochemistry*, 2003. **18**(11): p. 1789-1805.
103. Möller, P., A. Knappe, and P. Dulski, *Seasonal variations of rare earths and yttrium distribution in the lowland Havel River, Germany, by agricultural fertilization and effluents of sewage treatment plants*. *Applied geochemistry*, 2014. **41**: p. 62-72.
104. Cao, S., et al., *Health benefit from decreasing exposure to heavy metals and metalloid after strict pollution control measures near a typical river basin area in China*. *Chemosphere*, 2017. **184**: p. 866-878.
105. Shan, X.-q., J. Lian, and B. Wen, *Effect of organic acids on adsorption and desorption of rare earth elements*. *Chemosphere*, 2002. **47**(7): p. 701-710.
106. Johannesson, K.H., et al., *Rare earth element concentrations and speciation in organic-rich blackwaters of the Great Dismal Swamp, Virginia, USA*. *Chemical Geology*, 2004. **209**(3-4): p. 271-294.

107. Piper, D.Z. and M. Bau, *Normalized rare earth elements in water, sediments, and wine: identifying sources and environmental redox conditions*. American Journal of Analytical Chemistry, 2013. **2013**.
108. Wilke, C., et al., *Speciation of the trivalent f-elements Eu (III) and Cm (III) in digestive media*. Journal of inorganic biochemistry, 2017. **175**: p. 248-258.
109. AA, D., *1941Influence of cerium, lanthanum and samarium on development of peas*. C R Acad Sci URSS. **32**: p. 669-670.
110. Jha, A.M. and A.C. Singh, *Clastogenicity of lanthanides—induction of micronuclei in root tips of Vicia faba*. Mutation Research/Genetic Toxicology, 1994. **322**(3): p. 169-172.
111. Jha, A.M. and A.C. Singh, *Clastogenicity of lanthanides: induction of chromosomal aberration in bone marrow cells of mice in vivo*. Mutation Research/Genetic Toxicology, 1995. **341**(3): p. 193-197.
112. Hu, X., et al., *Bioaccumulation of lanthanum and cerium and their effects on the growth of wheat (Triticum aestivum L.) seedlings*. Chemosphere, 2002. **48**(6): p. 621-629.
113. Xiong, S.-L., et al., *Interactive effects of lanthanum and cadmium on plant growth and mineral element uptake in crisped-leaf mustard under hydroponic conditions*. Journal of plant nutrition, 2006. **29**(10): p. 1889-1902.
114. Oral, R., et al., *Heavy rare earth elements affect early life stages in Paracentrotus lividus and Arbacia lixula sea urchins*. Environmental research, 2017. **154**: p. 240-246.
115. Zhang, H., et al., *Ecotoxicological assessment of lanthanum with Caenorhabditis elegans in liquid medium*. Metallomics, 2010. **2**(12): p. 806-810.
116. Zhang, Z., et al., *Effects of rare earth elements La and Yb on the morphological and functional development of zebrafish embryos*. Journal of Environmental Sciences, 2012. **24**(2): p. 209-213.

117. Kawagoe, M., et al., *Acute effects on the lung and the liver of oral administration of cerium chloride on adult, neonatal and fetal mice*. Journal of Trace Elements in Medicine and Biology, 2008. **22**(1): p. 59-65.
118. He, X., et al., *Neurotoxicological evaluation of long-term lanthanum chloride exposure in rats*. Toxicological Sciences, 2008. **103**(2): p. 354-361.
119. Hardas, S.S., et al., *Brain distribution and toxicological evaluation of a systemically delivered engineered nanoscale ceria*. Toxicological Sciences, 2010. **116**(2): p. 562-576.
120. Huang, P., et al., *Effects of lanthanum, cerium, and neodymium on the nuclei and mitochondria of hepatocytes: accumulation and oxidative damage*. Environmental Toxicology and Pharmacology, 2011. **31**(1): p. 25-32.
121. Nalabotu, S.K., et al., *Intratracheal instillation of cerium oxide nanoparticles induces hepatic toxicity in male Sprague-Dawley rats*. International journal of nanomedicine, 2011. **6**: p. 2327.
122. Zhao, H., et al., *Oxidative stress in the kidney injury of mice following exposure to lanthanides trichloride*. Chemosphere, 2013. **93**(6): p. 875-884.
123. Zhao, H., et al., *Liver injury and its molecular mechanisms in mice caused by exposure to cerium chloride*. Archives of environmental contamination and toxicology, 2012. **62**(1): p. 154-164.
124. Aalapati, S., et al., *Toxicity and bio-accumulation of inhaled cerium oxide nanoparticles in CD1 mice*. Nanotoxicology, 2014. **8**(7): p. 786-798.
125. Cheng, J., et al., *Gene expression profile in chronic mouse liver injury caused by long-term exposure to CeCl<sub>3</sub>*. Environmental toxicology, 2014. **29**(7): p. 837-846.
126. Hong, J., et al., *Pulmonary toxicity in mice following exposure to cerium chloride*. Biological trace element research, 2014. **159**(1): p. 269-277.
127. Trifuoggi, M., et al., *Comparative toxicity of seven rare earth elements in sea urchin early life stages*. Environmental Science and Pollution Research, 2017. **24**(25): p. 20803-20810.
128. Mattson, M.P., *Hormesis defined*. Ageing research reviews, 2008. **7**(1): p. 1-7.

129. Fashui, H., W. Ling, and L. Chao, *Study of lanthanum on seed germination and growth of rice*. Biological trace element research, 2003. **94**(3): p. 273-286.
130. Wang, C., et al., *Toxicological effects involved in risk assessment of rare earth lanthanum on roots of Vicia faba L. seedlings*. Journal of environmental sciences, 2011. **23**(10): p. 1721-1728.
131. Ma, J.J., Y.J. Ren, and L.Y. Yan, *Effects of spray application of lanthanum and cerium on yield and quality of Chinese cabbage (Brassica chinensis L) based on different seasons*. Biological trace element research, 2014. **160**(3): p. 427-432.
132. Salgado, O.G.G., et al., *Cerium alleviates drought-induced stress in Phaseolus vulgaris*. Journal of Rare Earths, 2020. **38**(3): p. 324-331.
133. de Oliveira, C., et al., *Bioaccumulation and effects of lanthanum on growth and mitotic index in soybean plants*. Ecotoxicology and environmental safety, 2015. **122**: p. 136-144.
134. Liu, D., S. Zheng, and X. Wang, *Lanthanum regulates the reactive oxygen species in the roots of rice seedlings*. Scientific reports, 2016. **6**(1): p. 1-7.
135. Sun, H., et al., *Regular time-dependent cross-phenomena induced by hormesis: A case study of binary antibacterial mixtures to Aliivibrio fischeri*. Ecotoxicology and environmental safety, 2020. **187**: p. 109823.
136. Técher, D., et al., *Not merely noxious? Time-dependent hormesis and differential toxic effects systematically induced by rare earth elements in Escherichia coli*. Environmental Science and Pollution Research, 2020. **27**(5): p. 5640-5649.
137. Jenkins, W., et al., *Fibroblast response to lanthanoid metal ion stimulation: potential contribution to fibrotic tissue injury*. Biological trace element research, 2011. **144**(1): p. 621-635.
138. Liu, D., et al., *The dual-effects of LaCl<sub>3</sub> on the proliferation, osteogenic differentiation, and mineralization of MC3T3-E1 cells*. Biological trace element research, 2012. **150**(1): p. 433-440.

139. Hirst, S.M., et al., *Bio-distribution and in vivo antioxidant effects of cerium oxide nanoparticles in mice*. Environmental toxicology, 2013. **28**(2): p. 107-118.
140. García-Jiménez, A., et al., *Lanthanum affects bell pepper seedling quality depending on the genotype and time of exposure by differentially modifying plant height, stem diameter and concentrations of chlorophylls, sugars, amino acids, and proteins*. Frontiers in plant science, 2017. **8**: p. 308.
141. Elbasan, F., et al., *Rare-earth element scandium improves stomatal regulation and enhances salt and drought stress tolerance by up-regulating antioxidant responses of Oryza sativa*. Plant Physiology and Biochemistry, 2020. **152**: p. 157-169.
142. Yin, H., et al., *Effect of the Rare Earth Element Lanthanum (La) on the Growth and Development of Citrus Rootstock Seedlings*. Plants, 2021. **10**(7): p. 1388.
143. d'Aquino, L., et al., *Effect of some rare earth elements on the growth and lanthanide accumulation in different Trichoderma strains*. Soil Biology and Biochemistry, 2009. **41**(12): p. 2406-2413.
144. Trifuoggi, M., et al., *Topsoil and urban dust pollution and toxicity in Taranto (southern Italy) industrial area and in a residential district*. Environmental monitoring and assessment, 2019. **191**(1): p. 1-12.
145. Oral, R., et al., *Soil pollution and toxicity in an area affected by emissions from a bauxite processing plant and a power plant in Gardanne (southern France)*. Ecotoxicology and environmental safety, 2019. **170**: p. 55-61.
146. Šmuc, N.R., et al., *Geochemical characteristics of rare earth elements (REEs) in the paddy soil and rice (Oryza sativa L.) system of Kočani Field, Republic of Macedonia*. Geoderma, 2012. **183**: p. 1-11.
147. Petronio, B.M., et al., *Spatial and temporal heavy metal concentration (Cu, Pb, Zn, Hg, Fe, Mn, Hg) in sediments of the mar piccolo in Taranto (Ionian Sea, Italy)*. Water, Air, & Soil Pollution, 2012. **223**(2): p. 863-875.
148. Cernigliaro, A., et al., *The epidemiological surveillance in the programme of public health intervention in the national priority contaminated sites of*

- Sicily Region (Southern Italy): update of mortality, hospitalization, and cancer incidence.* *Epidemiologia e prevenzione*, 2019. **43**(2-3): p. 132-143.
149. Chen, Y., *Promising application of rare earths in steel and non-ferrous metals.* *Rare Earth Inf*, 2005. **5**: p. 34-35.
150. Comba, P., et al., *Environment and health in Taranto, southern Italy: epidemiological studies and public health recommendations.* *Epidemiologia e prevenzione*, 2012. **36**(6): p. 305-320.
151. Soleo, L., et al., *Health risk assessment of exposure to metals in the workers of the steel foundry and in the general population of Taranto (Italy).* *Giornale italiano di medicina del lavoro ed ergonomia*, 2012. **34**(4): p. 381-391.
152. Mataloni, F., et al., *A cohort study on mortality and morbidity in the area of Taranto, Southern Italy.* *Epidemiologia e prevenzione*, 2012. **36**(5): p. 237-252.
153. Cardellicchio, N., et al., *The Mar Piccolo of Taranto: an interesting marine ecosystem for the environmental problems studies.* *Environmental Science and Pollution Research*, 2016. **23**(13): p. 12495-12501.
154. Costa, E., et al., *Ecotoxicological effects of sediments from Mar Piccolo, South Italy: toxicity testing with organisms from different trophic levels.* *Environmental Science and Pollution Research*, 2016. **23**(13): p. 12755-12769.
155. Di Leo, A., et al., *Mobilization of trace metals and PCBs from contaminated marine sediments of the Mar Piccolo in Taranto during simulated resuspension experiment.* *Environmental Science and Pollution Research*, 2016. **23**(13): p. 12777-12790.
156. Moschino, V. and L. Da Ros, *Biochemical and lysosomal biomarkers in the mussel *Mytilus galloprovincialis* from the Mar Piccolo of Taranto (Ionian Sea, Southern Italy).* *Environmental Science and Pollution Research*, 2016. **23**(13): p. 12770-12776.
157. Narracci, M., M. Acquaviva, and R. Cavallo, *Mar Piccolo of Taranto: *Vibrio* biodiversity in ecotoxicology approach.* *Environmental Science and Pollution Research*, 2014. **21**(3): p. 2378-2385.

158. Liberti, L., et al., *Air pollution from a large steel factory: polycyclic aromatic hydrocarbon emissions from coke-oven batteries*. Journal of the Air & Waste Management Association, 2006. **56**(3): p. 255-260.
159. Jia, G., et al., *A radiological survey and the impact of the elevated concentrations of <sup>210</sup>Pb and <sup>210</sup>Po released from the iron-and steel-making plant ILVA Taranto (Italy) on the environment and the public*. Environmental Science: Processes & Impacts, 2013. **15**(3): p. 677-689.
160. Kanarbik, L., et al., *Environmental effects of soil contamination by shale fuel oils*. Environmental Science and Pollution Research, 2014. **21**(19): p. 11320-11330.
161. Ren, X., et al., *Sorption, transport and biodegradation—an insight into bioavailability of persistent organic pollutants in soil*. Science of the total environment, 2018. **610**: p. 1154-1163.
162. Xu, G., et al., *Research and application of non-traditional chemical stabilizers on bauxite residue (red sand) dust control, a review*. Science of the total environment, 2018. **616**: p. 1552-1565.
163. Xue, S., et al., *A review of the characterization and revegetation of bauxite residues (Red mud)*. Environmental Science and Pollution Research, 2016. **23**(2): p. 1120-1132.
164. Trieff, N., et al., *Effluent from bauxite factory induces developmental and reproductive damage in sea urchins*. Archives of Environmental Contamination and Toxicology, 1995. **28**(2): p. 173-177.
165. His, E., et al., *Sublethal and lethal toxicity of aluminum industry effluents to early developmental stages of the *Crassostrea gigas* oyster*. Archives of Environmental Contamination and Toxicology, 1996. **30**(3): p. 335-339.
166. Dauvin, J.-C., *Towards an impact assessment of bauxite red mud waste on the knowledge of the structure and functions of bathyal ecosystems: The example of the Cassidaigne canyon (north-western Mediterranean Sea)*. Marine Pollution Bulletin, 2010. **60**(2): p. 197-206.
167. Howe, P.L., et al., *Toxicity of raw and neutralized bauxite refinery residue liquors to the freshwater cladoceran *Ceriodaphnia dubia* and the marine*

- amphipod Paracalliope australis*. Environmental toxicology and chemistry, 2011. **30**(12): p. 2817-2824.
168. Klebercz, O., et al., *Ecotoxicity of fluvial sediments downstream of the Ajka red mud spill, Hungary*. Journal of Environmental Monitoring, 2012. **14**(8): p. 2063-2071.
169. Mišík, M., et al., *Red mud a byproduct of aluminum production contains soluble vanadium that causes genotoxic and cytotoxic effects in higher plants*. Science of the total environment, 2014. **493**: p. 883-890.
170. Olszewska, J.P., et al., *Assessing the legacy of red mud pollution in a shallow freshwater lake: arsenic accumulation and speciation in macrophytes*. Environmental science & technology, 2016. **50**(17): p. 9044-9052.
171. Higgins, D., T. Curtin, and R. Courtney, *Effectiveness of a constructed wetland for treating alkaline bauxite residue leachate: a 1-year field study*. Environmental Science and Pollution Research, 2017. **24**(9): p. 8516-8524.
172. Haberl, J., et al., *Quantification of main and trace metal components in the fly ash of waste-to-energy plants located in Germany and Switzerland: an overview and comparison of concentration fluctuations within and between several plants with particular focus on valuable metals*. Waste Management, 2018. **75**: p. 361-371.
173. Raja, R., et al., *Impairment of soil health due to fly ash-fugitive dust deposition from coal-fired thermal power plants*. Environmental monitoring and assessment, 2015. **187**(11): p. 1-18.
174. Twardowska, I. and K. Schramm, *Occurrence of persistent organic pollutants (PAHs, PCDD and PCDF) in fly ash generated in coal-fired thermal and power plants in Silesia, Poland*. Central European journal of public health, 2000. **8**: p. 6-8.
175. Ruwei, W., et al., *Levels and patterns of polycyclic aromatic hydrocarbons in coal-fired power plant bottom ash and fly ash from Huainan, China*. Archives of environmental contamination and toxicology, 2013. **65**(2): p. 193-202.

176. Freire, M., H. Lopes, and L.A. Tarelho, *Critical aspects of biomass ashes utilization in soils: Composition, leachability, PAH and PCDD/F*. Waste Management, 2015. **46**: p. 304-315.
177. Wikström, E., et al., *Key parameters for de novo formation of polychlorinated dibenzo-p-dioxins and dibenzofurans*. Environmental science & technology, 2003. **37**(9): p. 1962-1970.
178. Santoro, M., et al., *Congenital anomalies in contaminated sites: A Multisite Study in Italy*. International journal of environmental research and public health, 2017. **14**(3): p. 292.
179. Huebner, W.W., et al., *Mortality updates (1970–1997) of two refinery/petrochemical plant cohorts at Baton Rouge, Louisiana, and Baytown, Texas*. Journal of occupational and environmental medicine, 2004. **46**(12): p. 1229-1245.
180. Campo, G., *Occupational diseases in the petrochemical sector: types and temporal trends*. Giornale italiano di medicina del lavoro ed ergonomia, 2013. **35**(4): p. 288-290.
181. Pirastu, R., et al., *Mortality results in SENTIERI Project*. Epidemiologia e prevenzione, 2011. **35**(5-6 Suppl 4): p. 29-152.
182. Di Leonardo, R., et al., *Highly contaminated areas as sources of pollution for adjoining ecosystems: The case of Augusta Bay (Central Mediterranean)*. Marine pollution bulletin, 2014. **89**(1-2): p. 417-426.
183. De Domenico, E., et al., *Biological responses of juvenile European sea bass (Dicentrarchus labrax) exposed to contaminated sediments*. Ecotoxicology and environmental safety, 2013. **97**: p. 114-123.
184. González, V., et al., *Assessing the impact of organic and inorganic amendments on the toxicity and bioavailability of a metal-contaminated soil to the earthworm Eisenia andrei*. Environmental Science and Pollution Research, 2013. **20**(11): p. 8162-8171.
185. Copat, C., et al., *Trace Element Bioaccumulation in Stone Curlew (Burhinus oedicephalus, Linnaeus, 1758): A Case Study from Sicily (Italy)*. International journal of molecular sciences, 2020. **21**(13): p. 4597.

186. Hentati, O., et al., *Toxicity assessment for petroleum-contaminated soil using terrestrial invertebrates and plant bioassays*. Environmental monitoring and assessment, 2013. **185**(4): p. 2989-2998.
187. Escarré, J., et al., *Heavy metal concentration survey in soils and plants of the Les Malines mining district (Southern France): implications for soil restoration*. Water, Air, & Soil Pollution, 2011. **216**(1): p. 485-504.
188. Woszczyk, M., W. Spsychalski, and L. Boluspaeva, *Trace metal (Cd, Cu, Pb, Zn) fractionation in urban-industrial soils of Ust-Kamenogorsk (Oskemen), Kazakhstan—implications for the assessment of environmental quality*. Environmental Monitoring and Assessment, 2018. **190**(6): p. 1-16.
189. USEPA, U.S.E.P.A., *Method 3050B: acid digestion of sediments, sludges, and soils, revision 2*. Washington, DC. 1996.
190. ISO, I.O.f.S., *UNI EN ISO 16171 in Sludge, treated biowaste and soil - Determination of elements using inductively coupled plasma mass spectrometry (ICP-MS)*. 2016.
191. INTERNATIONAL, A., *ASTM E2172: 1-11: standard guide for conducting a laboratory soil toxicity test with the nematode *Caenorhabditis elegans**. 2014, ASTM International West Conshohocken.
192. Puglia, A., *Relazione sui dati ambientali dell'area di Taranto*. 2016.
193. Gentner, D.R., et al., *Elucidating secondary organic aerosol from diesel and gasoline vehicles through detailed characterization of organic carbon emissions*. Proceedings of the National Academy of Sciences, 2012. **109**(45): p. 18318-18323.
194. Cassee, F.R., et al., *Exposure, health and ecological effects review of engineered nanoscale cerium and cerium oxide associated with its use as a fuel additive*. Critical reviews in toxicology, 2011. **41**(3): p. 213-229.
195. Dale, J.G., et al., *Transformation of cerium oxide nanoparticles from a diesel fuel additive during combustion in a diesel engine*. Environmental science & technology, 2017. **51**(4): p. 1973-1980.
196. Kumar, M.V., A.V. Babu, and P.R. Kumar, *Influence of metal-based cerium oxide nanoparticle additive on performance, combustion, and emissions*

- with biodiesel in diesel engine*. Environmental Science and Pollution Research, 2019. **26**(8): p. 7651-7664.
197. Oral, R., et al., *Sediment pollution and toxicity in a formerly industrialized bay in central mediterranean (POZZUOLI, Italy)*. Fresenius Environmental Bulletin, 2020. **29**(10): p. 9498-9510.
  198. Oliveri, E., et al., *Carbonate stromatolites from a Messinian hypersaline setting in the Caltanissetta Basin, Sicily: petrographic evidence of microbial activity and related stable isotope and rare earth element signatures*. Sedimentology, 2010. **57**(1): p. 142-161.
  199. Bau, M. and P. Dulski, *Anthropogenic origin of positive gadolinium anomalies in river waters*. Earth and Planetary Science Letters, 1996. **143**(1-4): p. 245-255.
  200. Zhang, J. and Y. Nozaki, *Rare earth elements and yttrium in seawater: ICP-MS determinations in the East Caroline, Coral Sea, and South Fiji basins of the western South Pacific Ocean*. Geochimica et Cosmochimica Acta, 1996. **60**(23): p. 4631-4644.
  201. Jeandel, C., D. Thouron, and M. Fieux, *Concentrations and isotopic compositions of neodymium in the eastern Indian Ocean and Indonesian straits*. Geochimica et Cosmochimica Acta, 1998. **62**(15): p. 2597-2607.
  202. Alibo, D.S. and Y. Nozaki, *Dissolved rare earth elements in the South China Sea: Geochemical characterization of the water masses*. Journal of Geophysical Research: Oceans, 2000. **105**(C12): p. 28771-28783.
  203. Censi, P., et al., *Yttrium and REE signature recognized in Central Mediterranean Sea (ODP Site 963) during the MIS 6–MIS 5 transition*. Palaeogeography, Palaeoclimatology, Palaeoecology, 2010. **292**(1-2): p. 201-210.
  204. Haley, B.A., G.P. Klinkhammer, and J. McManus, *Rare earth elements in pore waters of marine sediments*. Geochimica et Cosmochimica Acta, 2004. **68**(6): p. 1265-1279.
  205. Liu, Y.-G., M. Miah, and R. Schmitt, *Cerium: a chemical tracer for paleo-oceanic redox conditions*. Geochimica et Cosmochimica Acta, 1988. **52**(6): p. 1361-1371.

206. Olmez, I., et al., *Rare earth elements in sediments off southern California: a new anthropogenic indicator*. Environmental science & technology, 1991. **25**(2): p. 310-316.
207. Long, E.R., *Calculation and uses of mean sediment quality guideline quotients: a critical review*. Environmental science & technology, 2006. **40**(6): p. 1726-1736.
208. De Vivo, B. and A. Lima, *Characterization and remediation of a brownfield site: the Bagnoli case in Italy*, in *Environmental Geochemistry*. 2008, Elsevier. p. 355-385.
209. Albanese, S., et al., *Geochemical baselines and risk assessment of the Bagnoli brownfield site coastal sea sediments (Naples, Italy)*. Journal of Geochemical Exploration, 2010. **105**(1-2): p. 19-33.
210. Romano, E., et al., *The impact of the Bagnoli industrial site (Naples, Italy) on sea-bottom environment. Chemical and textural features of sediments and the related response of benthic foraminifera*. Marine Pollution Bulletin, 2009. **59**(8-12): p. 245-256.
211. Qu, C., et al., *Polycyclic aromatic hydrocarbons in the sediments of the Gulfs of Naples and Salerno, Southern Italy: Status, sources and ecological risk*. Ecotoxicology and environmental safety, 2018. **161**: p. 156-163.
212. Damiani, V., et al., *A case study: bay of Pozzuoli (Gulf of Naples, Italy)*, in *Ecological Effects of In Situ Sediment Contaminants*. 1987, Springer. p. 201-211.
213. Trifuoggi, M., et al., *Distribution and enrichment of trace metals in surface marine sediments in the Gulf of Pozzuoli and off the coast of the brownfield metallurgical site of Ilva of Bagnoli (Campania, Italy)*. Marine pollution bulletin, 2017. **124**(1): p. 502-511.
214. Arienzo, M., et al., *Characterization and source apportionment of polycyclic aromatic hydrocarbons (pahs) in the sediments of gulf of Pozzuoli (Campania, Italy)*. Marine Pollution Bulletin, 2017. **124**(1): p. 480-487.

215. *Italian Parliament. Law 9 December 1998 n. 426. New interventions in the environmental field. Official Gazette of the Italian Republic n. 291 of 14 December 1998 (in Italian)*
- 1998.
216. *Italian Parliament. Law 23 December 2000 n. 388. Provisions for the preparation of the annual and multiannual State budget (2001 finance law). Official Gazette of the Italian Republic n. 302 Ordinary Supplement n. 219 of 29 Decem (in Italian). 2000.*
217. Pagano, G., et al., *Sea urchin bioassays in toxicity testing: II. Sediment evaluation*. *Expert Opin Environ Biol* 6, 2017. **1**: p. 2.
218. ISO, I.S.O., *10253:2016 Water quality -- Marine Algal Growth Inhibition Test with Skeletonema sp. and Phaeodactylum tricornutum*. 2016.
219. King, J.F., et al., *Aqueous acid and alkaline extraction of rare earth elements from coal combustion ash*. *International Journal of Coal Geology*, 2018. **195**: p. 75-83.
220. Franus, W., M.M. Wiatros-Motyka, and M. Wdowin, *Coal fly ash as a resource for rare earth elements*. *Environmental Science and Pollution Research*, 2015. **22**(12): p. 9464-9474.
221. Romaña, L.-A., et al., *Use of Radioactive Tracing Techniques to Identify Participate Deposits and Biological Effects of Urban Effluents Discharges from Sewage Outfalls*. *Water Science and Technology*, 1992. **25**(12): p. 115-122.
222. Pagano, G., et al., *Chapter 5 - DEVELOPMENTAL, CYTOGENETIC AND BIOCHEMICAL EFFECTS OF SPIKED OR ENVIRONMENTALLY POLLUTED SEDIMENTS IN SEA URCHIN BIOASSAYS*, in *Biomarkers in Marine Organisms*, P. Garrigues, et al., Editors. 2001, Elsevier Science: Amsterdam. p. 85-129.
223. Nieto, J.M., et al., *Acid mine drainage pollution in the Tinto and Odiel rivers (Iberian Pyrite Belt, SW Spain) and bioavailability of the transported metals to the Huelva Estuary*. *Environment International*, 2007. **33**(4): p. 445-455.

224. Olías, M., et al., *Evaluation of the dissolved contaminant load transported by the Tinto and Odiel rivers (South West Spain)*. Applied Geochemistry, 2006. **21**(10): p. 1733-1749.
225. Cravotta III, C.A., *Dissolved metals and associated constituents in abandoned coal-mine discharges, Pennsylvania, USA. Part 1: Constituent quantities and correlations*. Applied Geochemistry, 2008. **23**(2): p. 166-202.
226. Merten, D., et al., *Rare earth element patterns: a tool for understanding processes in remediation of acid mine drainage*. Geochemistry, 2005. **65**: p. 97-114.
227. Da Silva, E.F., et al., *Mineralogy and geochemistry of trace metals and REE in volcanic massive sulfide host rocks, stream sediments, stream waters and acid mine drainage from the Lousal mine area (Iberian Pyrite Belt, Portugal)*. Applied geochemistry, 2009. **24**(3): p. 383-401.
228. Sahoo, P., et al., *Geochemical characteristics of coal mine discharge vis-à-vis behavior of rare earth elements at Jaintia Hills coalfield, northeastern India*. Journal of Geochemical Exploration, 2012. **112**: p. 235-243.
229. Rim, K.T., K.H. Koo, and J.S. Park, *Toxicological evaluations of rare earths and their health impacts to workers: a literature review*. Safety and health at work, 2013. **4**(1): p. 12-26.
230. Stewart, B.W., et al., *Rare earth element resources in coal mine drainage and treatment precipitates in the Appalachian Basin, USA*. International Journal of Coal Geology, 2017. **169**: p. 28-39.
231. Sun, G., et al., *Rare earth elements in street dust and associated health risk in a municipal industrial base of central China*. Environmental geochemistry and health, 2017. **39**(6): p. 1469-1486.
232. Gonzalez-Gil, G., et al., *Leaching and accumulation of trace elements in sulfate reducing granular sludge under concomitant thermophilic and low pH conditions*. Bioresource technology, 2012. **126**: p. 238-246.
233. Li, H.-R., et al., *Acid Rain Increases Impact of Rice Blast on Crop Health via Inhibition of Resistance Enzymes*. Plants, 2020. **9**(7): p. 881.

234. Xia, B., et al., *Analysis of the combined effects of lanthanum and acid rain, and their mechanisms, on nitrate reductase transcription in plants*. Ecotoxicology and environmental safety, 2017. **138**: p. 170-178.
235. Bott, T.L., et al., *Abandoned coal mine drainage and its remediation: impacts on stream ecosystem structure and function*. Ecological applications, 2012. **22**(8): p. 2144-2163.
236. Kraus, J.M. and J.P. Pomeranz, *Cross-ecosystem linkages and trace metals at the land-water interface*, in *Contaminants and Ecological Subsidies*. 2020, Springer. p. 91-109.
237. Haferburg, G., et al., *Biosorption of metal and salt tolerant microbial isolates from a former uranium mining area. Their impact on changes in rare earth element patterns in acid mine drainage*. Journal of basic microbiology, 2007. **47**(6): p. 474-484.
238. Romero, F.M., et al., *Acid drainage at the inactive Santa Lucia mine, western Cuba: Natural attenuation of arsenic, barium and lead, and geochemical behavior of rare earth elements*. Applied Geochemistry, 2010. **25**(5): p. 716-727.
239. Inaba, T., et al., *Estimation of cumulative cadmium intake causing Itai-itai disease*. Toxicology letters, 2005. **159**(2): p. 192-201.
240. Pagano, G., et al., *Comparative toxicities of selected rare earth elements: Sea urchin embryogenesis and fertilization damage with redox and cytogenetic effects*. Environmental research, 2016. **147**: p. 453-460.
241. ISO, I.S.O., *8692:2012 water quality - fresh water algal growth inhibition test with unicellular green algae*. 2012.
242. ISO, I.O.S., *11269-1:2012 soil quality - determination of the effects of pollutants on soil flora - part 1: method for the measurement of inhibition of root growth*. 2012.
243. Libralato, G., et al., *Phytotoxicity of ionic, micro-and nano-sized iron in three plant species*. Ecotoxicology and environmental safety, 2016. **123**: p. 81-88.
244. ISO, I.O.S., *29200 soil quality—assessment of genotoxic effects on higher plants—Vicia faba micronucleus test*. 2013.

245. Schindelin, J., et al., *The ImageJ ecosystem: An open platform for biomedical image analysis*. *Molecular reproduction and development*, 2015. **82**(7-8): p. 518-529.
246. Rodea-Palomares, I., et al., *An insight into the mechanisms of nanoceria toxicity in aquatic photosynthetic organisms*. *Aquatic toxicology*, 2012. **122**: p. 133-143.
247. Aharchaou, I., et al., *Lanthanum and cerium toxicity to the freshwater green alga *Chlorella fusca*: applicability of the Biotic Ligand Model*. *Environmental toxicology and chemistry*, 2020. **39**(5): p. 996-1005.
248. Liang, C. and W. Wang, *Antioxidant response of soybean seedlings to joint stress of lanthanum and acid rain*. *Environmental Science and Pollution Research*, 2013. **20**(11): p. 8182-8191.
249. Wang, L., et al., *Combined effects of lanthanum (III) chloride and acid rain on photosynthetic parameters in rice*. *Chemosphere*, 2014. **112**: p. 355-361.
250. González, V., et al., *Lanthanide ecotoxicity: First attempt to measure environmental risk for aquatic organisms*. *Environmental pollution*, 2015. **199**: p. 139-147.
251. Malhotra, N., et al., *An updated review of toxicity effect of the rare earth elements (REEs) on aquatic organisms*. *Animals*, 2020. **10**(9): p. 1663.
252. Joonas, E., et al., *Potency of (doped) rare earth oxide particles and their constituent metals to inhibit algal growth and induce direct toxic effects*. *Science of the Total Environment*, 2017. **593**: p. 478-486.
253. Stauber, J. and M. Binet, *Canning River Phoslock field trials—Ecotoxicity testing final report*, in *CSIRO & the WA Waters and Rivers Commission. Report No: ET 317R*. 2000.
254. Wang, Y.-L., et al., *Reduction of hyperhydricity in the culture of *Lepidium meyenii* shoots by the addition of rare earth elements*. *Plant Growth Regulation*, 2007. **52**(2): p. 151-159.
255. Blaise, C., et al., *Ecotoxicity responses of the freshwater cnidarian *Hydra attenuata* to 11 rare earth elements*. *Ecotoxicology and environmental safety*, 2018. **163**: p. 486-491.

256. Sneller, F., et al., *Maximum permissible concentrations and negligible concentrations for rare earth elements (REEs)*. 2000.
257. ISO, E., *Water quality—Determination of the inhibition of the mobility of *Daphnia magna* Straus (Cladocera, Crustacea)—Acute toxicity test*. EN ISO, 2012. **6341**: p. 1996.
258. OECD, *Daphnia magna Reproduction Test*, in *OECD Guidelines for the Testing of Chemicals, Section 2: Effects on Biotic Systems*view. 2012.
259. Galdiero, E., et al., *Integrated analysis of the ecotoxicological and genotoxic effects of the antimicrobial peptide melittin on *Daphnia magna* and *Pseudokirchneriella subcapitata**. Environ. Pollut., 2015. **203**: p. 145-152.
260. Maselli, V., et al., *Multigenerational effects and DNA alterations of QDs-Indolicidin on *Daphnia magna**. Environmental Pollution, 2017. **224**: p. 597-605.
261. Rueden, C.T., et al., *ImageJ2: ImageJ for the next generation of scientific image data*. 2017. **18**(1): p. 529.
262. Lampert, W. and I.J.F.E. Trubetskova, *Juvenile growth rate as a measure of fitness in *Daphnia**. 1996: p. 631-635.
263. Bradford, M.M., *A rapid and sensitive method for the quantitation of microgram quantities of protein utilizing the principle of protein-dye binding*. Analytical biochemistry, 1976. **72**(1-2): p. 248-254.
264. Galdiero, E., et al., *An integrated study on antimicrobial activity and ecotoxicity of quantum dots and quantum dots coated with the antimicrobial peptide indolicidin*. International journal of nanomedicine, 2016. **11**: p. 4199-4211.
265. Campos, B., et al., *First evidence for toxic defense based on the multixenobiotic resistance (MXR) mechanism in *Daphnia magna**. Aquatic toxicology, 2014. **148**: p. 139-151.
266. De Marco, N., et al., *Eukaryotic initiation factor eIF6 modulates the expression of Kermit 2/XGIPC in IGF- regulated eye development*. Developmental Biology, 2017. **427**(1): p. 148-154.

267. Tussellino, M., et al., *Chlorpyrifos exposure affects fgf8, sox9, and bmp4 expression required for cranial neural crest morphogenesis and chondrogenesis in Xenopus laevis embryos*. Environmental and Molecular Mutagenesis, 2016. **57**(8): p. 630-640.
268. Rauch, S. and G.M. Morrison, *Platinum uptake by the freshwater isopod Asellus Aquaticus in urban rivers*. Science of The Total Environment, 1999. **235**(1): p. 261-268.
269. Finney, D.J., *Probit analysis*. 1971.
270. Zhang, C., et al., *Effects of rare earth elements on growth and metabolism of medicinal plants*. Acta Pharmaceutica Sinica B, 2013. **3**(1): p. 20-24.
271. Song, Y., M. Chen, and J. Zhou, *Effects of three pesticides on superoxide dismutase and glutathione-S-transferase activities and reproduction of Daphnia magna*. Archives of Environmental Protection, 2017.
272. Falanga, A., et al., *Metabolomic and oxidative effects of quantum dots-indolicidin on three generations of Daphnia magna*. Aquatic Toxicology, 2018. **198**: p. 158-164.
273. Yakusheva, E. and D. Titov, *Structure and function of multidrug resistance protein I*. Biochemistry (Moscow), 2018. **83**(8): p. 907-929.
274. Jordão, R., et al., *Induction of multixenobiotic defense mechanisms in resistant Daphnia magna clones as a general cellular response to stress*. Aquatic Toxicology, 2016. **175**: p. 132-143.
275. Navarro, A., et al., *Abcb and Abcc transporter homologs are expressed and active in larvae and adults of zebra mussel and induced by chemical stress*. Aquatic toxicology, 2012. **122**: p. 144-152.
276. Adam, N., et al., *The uptake and elimination of ZnO and CuO nanoparticles in Daphnia magna under chronic exposure scenarios*. Water research, 2015. **68**: p. 249-261.
277. Yu, R.-Q. and W.-X. Wang, *Biokinetics of cadmium, selenium, and zinc in freshwater alga Scenedesmus obliquus under different phosphorus and nitrogen conditions and metal transfer to Daphnia magna*. Environmental Pollution, 2004. **129**(3): p. 443-456.

278. Ramírez-Olvera, S.M., et al., *Cerium enhances germination and shoot growth, and alters mineral nutrient concentration in rice*. PLoS One, 2018. **13**(3): p. e0194691.
279. Sadovsky, D., et al., *Biosorption potential of cerium ions using Spirulina biomass*. Journal of rare earths, 2016. **34**(6): p. 644-652.
280. Goecke, F., V. Zachleder, and M. Vítová, *Rare earth elements and algae: physiological effects, biorefinery and recycling*, in *Algal Biorefineries*. 2015, Springer. p. 339-363.
281. Kang, L., Z. Shen, and C. Jin, *Neodymium cations Nd 3+ were transported to the interior of Euglena gracilis* 277. Chinese Science Bulletin, 2000. **45**(7): p. 585-592.
282. Shen, H., et al., *Investigation of metal ion accumulation in Euglena gracilis by fluorescence methods*. Nuclear Instruments and Methods in Physics Research Section B: Beam Interactions with Materials and Atoms, 2002. **189**(1-4): p. 506-510.
283. Guo, P., et al., *Study of metal bioaccumulation by nuclear microprobe analysis of algae fossils and living algae cells*. Nuclear Instruments and Methods in Physics Research Section B: Beam Interactions with Materials and Atoms, 2000. **161**: p. 801-807.
284. Ren, Q., et al., *Cytochemical behavior of rare earth ions in Euglena gracilis studied by XAFS*. Journal of radioanalytical and nuclear chemistry, 2007. **272**(2): p. 359-362.
285. Ren, M., et al., *Sub-100-nm STIM imaging and PIXE quantification of rare earth elements in algae cells*. X-Ray spectrom special issue. In: F. Goecke et al, 2013.
286. Hu, Q., et al., *Effects of Sm and Y on growth of Chlorella ellipsoidea*. Agro Environ. Prot.(Chin.), 2001. **20**: p. 398-404.
287. Jin, X., et al., *Effects of lanthanum (III) and EDTA on the growth and competition of Microcystis aeruginosa and Scenedesmus quadricauda*. Limnologica, 2009. **39**(1): p. 86-93.

288. Yingjun, W., et al., *Effects of cerium on growth and physiological characteristics of Anabaena flosaquae*. Journal of Rare Earths, 2012. **30**(12): p. 1287-1292.
289. Fuma, S., et al., *Effects of dysprosium on the species-defined microbial microcosm*. Bulletin of environmental contamination and toxicology, 2005. **74**(2): p. 263-272.
290. Evseeva, T., et al., *Comparative estimation of  $^{232}\text{Th}$  and stable Ce (III) toxicity and detoxification pathways in freshwater alga *Chlorella vulgaris**. Chemosphere, 2010. **81**(10): p. 1320-1327.
291. Tai, P., et al., *Biological toxicity of lanthanide elements on algae*. Chemosphere, 2010. **80**(9): p. 1031-1035.
292. Bergsten-Torralba, L., et al., *Toxicity of three rare earth elements, and their combinations to algae, microcrustaceans, and fungi*. Ecotoxicology and Environmental Safety, 2020. **201**: p. 110795.
293. Manusadzianas, L., et al., *Ecotoxicity Responses of the Macrophyte Algae *Nitellopsis obtusa* and Freshwater Crustacean *Thamnocephalus platyurus* to 12 Rare Earth Elements*. Sustainability, 2020. **12**(17): p. 7130.
294. Miazek, K., et al., *Effect of metals, metalloids and metallic nanoparticles on microalgae growth and industrial product biosynthesis: a review*. International Journal of Molecular Sciences, 2015. **16**(10): p. 23929-23969.
295. Piovár, J., et al., *Influence of long-term exposure to copper on the lichen photobiont *Trebouxia erici* and the free-living algae *Scenedesmus quadricauda**. Plant growth regulation, 2011. **63**(1): p. 81-88.
296. Almeida, A.C., et al., *Oxidative stress in the algae *Chlamydomonas reinhardtii* exposed to biocides*. Aquatic toxicology, 2017. **189**: p. 50-59.
297. Almeida, A.C., et al., *Oxidative stress potential of the herbicides bifenox and metribuzin in the microalgae *Chlamydomonas reinhardtii**. Aquatic Toxicology, 2019. **210**: p. 117-128.
298. Galdiero, E., et al., *An integrated study on antimicrobial activity and ecotoxicity of quantum dots and quantum dots coated with the antimicrobial peptide indolicidin*. International journal of nanomedicine, 2016. **11**: p. 4199.

299. Yuan, X.-Z., et al., *Phosphorus fixation in lake sediments using LaCl<sub>3</sub>-modified clays*. *ecological engineering*, 2009. **35**(11): p. 1599-1602.
300. Lürling, M. and F. van Oosterhout, *Case study on the efficacy of a lanthanum-enriched clay (Phoslock®) in controlling eutrophication in Lake Het Groene Eiland (The Netherlands)*. *Hydrobiologia*, 2013. **710**(1): p. 253-263.
301. He, Z., et al., *Different effects of calcium and lanthanum on the expression of phytochelatin synthase gene and cadmium absorption in Lactuca sativa*. *Plant Science*, 2005. **168**(2): p. 309-318.
302. Cheng, J., et al., *The effect of cadmium on the growth and antioxidant response for freshwater algae Chlorella vulgaris*. *SpringerPlus*, 2016. **5**(1): p. 1-8.
303. Danouche, M., et al., *Heavy metals phycoremediation using tolerant green microalgae: Enzymatic and non-enzymatic antioxidant systems for the management of oxidative stress*. *Journal of Environmental Chemical Engineering*, 2020. **8**(5): p. 104460.
304. Macnair, M.R., *The genetics of metal tolerance in vascular plants*. *New phytologist*, 1993. **124**(4): p. 541-559.
305. MacMillan, G.A., et al., *Environmental drivers of rare earth element bioaccumulation in freshwater zooplankton*. *Environmental science & technology*, 2018. **53**(3): p. 1650-1660.
306. Freitas, R., et al., *Toxicological effects of the rare earth element neodymium in Mytilus galloprovincialis*. *Chemosphere*, 2020. **244**: p. 125457.
307. Greaves, M., H. Elderfield, and E. Sholkovitz, *Aeolian sources of rare earth elements to the Western Pacific Ocean*. *Marine Chemistry*, 1999. **68**(1-2): p. 31-38.
308. Nozaki, Y., *Rare Earth Elements and their Isotopes in the Ocean*, in *Encyclopedia of Ocean Sciences*, J.H. Steele, Editor. 2001, Academic Press: Oxford. p. 2354-2366.
309. Nothdurft, L.D., G.E. Webb, and B.S. Kamber, *Rare earth element geochemistry of Late Devonian reefal carbonates, Canning Basin, Western*

- Australia: confirmation of a seawater REE proxy in ancient limestones. Geochimica et Cosmochimica Acta*, 2004. **68**(2): p. 263-283.
310. Kulaksız, S. and M. Bau, *Anthropogenic dissolved and colloid/nanoparticle-bound samarium, lanthanum and gadolinium in the Rhine River and the impending destruction of the natural rare earth element distribution in rivers. Earth and Planetary Science Letters*, 2013. **362**: p. 43-50.
311. Kulaksız, S. and M. Bau, *Contrasting behaviour of anthropogenic gadolinium and natural rare earth elements in estuaries and the gadolinium input into the North Sea. Earth and Planetary Science Letters*, 2007. **260**(1-2): p. 361-371.
312. Lawrence, M.G., C. Ort, and J. Keller, *Detection of anthropogenic gadolinium in treated wastewater in South East Queensland, Australia. Water research*, 2009. **43**(14): p. 3534-3540.
313. ISO, I.S.O., *10253:2016 Water quality -- Marine Al gal Growth Inhibition Test with Skeletonema sp. and Phaeodactylum tricorutum*. 2016.
314. ISO, I., *11348-3. Water quality-Determination of the inhibitory effect of water samples on the light emission of Vibrio fischeri (Luminescent bacteria test)-Part 3: Method using freeze-dried bacteria. International Organization for Standardization, London, UK*, 2007.
315. Kurvet, I., et al., *Toxicity of nine (doped) rare earth metal oxides and respective individual metals to aquatic microorganisms Vibrio fischeri and Tetrahymena thermophila. Materials*, 2017. **10**(7): p. 754.
316. Calabrese, E.J. and L.A. Baldwin, *Hormesis: the dose-response revolution. Annual review of pharmacology and toxicology*, 2003. **43**(1): p. 175-197.
317. Mattson, M.P. and E.J. Calabrese, *A revolution in biology, toxicology and medicine*. 2010: Springer.
318. Evans, C.H., *Biochemistry of the Lanthanides. Vol. 8*. 2013: Springer Science & Business Media.